

POLITECNICO DI MILANO

Scuola di Ingegneria Industriale e dell'Informazione

Corso di Laurea Magistrale in
Ingegneria Biomedica



**CONTINUOUS MAMMALIAN CELL CULTURES
CHARACTERIZATION AND OPTIMIZATION OF TWO
PERFUSION SYSTEMS**

Relatore: Prof. Massimo MORBIDELLI

Correlatore: Daniel KARST

Autore:

Elisa SERRA matr. 799440

Anno Accademico 2013/2014

TABLE OF CONTENTS

ACKNOWLEDGEMENTS	iii
LIST OF FIGURES.....	iv
LIST OF TABLES.....	viii
LIST OF ABBREVIATIONS	ix
ABSTRACT	1
SOMMARIO	5
INTRODUCTION	10
1.1 CELL CULTURE	11
1.1.1 Batch	11
1.1.2 Fed-batch.....	12
1.1.3 Continuous culture	13
1.1.4 Process parameters	15
1.2 MAMMALIAN CELL PERFUSION CULTURE	16
1.2.1 Kinetics of perfusion cultures.....	16
1.2.2 Cell retention device.....	17
1.2.3 Objectives in a perfusion culture	20
1.3 CHARACTERISATION AND OPERATING CONDITIONS OF A PERFUSION CELL CULTURE	21
1.3.1 Hydrodynamic stress	21
1.3.2 Fouling	22
1.3.3 Mass transfer	23
1.4 COMPARISON ATF AND TFF	24
1.5 AIM OF THE PROJECT	26
MATERIALS AND METHODS.....	27
2.1 PERFUSION BIOREACTOR DESIGN	27
2.1.1 Bioreactor	27
2.2 CHARACTERISATION	29
2.2.1 External loop flow rate	29
2.2.2 Hydrodynamic shear stress.....	30
2.2.3 k_La measurement	32

2.3 CELL CULTURE	34
2.3.1 Cell line	34
2.3.2 Medium and feed.....	34
2.3.3 Expansion	35
2.4 SPIN TUBE EXPERIMENTS.....	36
2.4.1 Setting a constant harvest/bleed ratio	36
2.4.2 Different cell densities and percentage of feed.....	37
2.5 BIOREACTOR RUNS.....	39
2.5.1 Bioreactor preparation	39
2.5.2 Seed reactor	40
2.5.3 Comparison ATF and TFF	41
2.6 OFFLINE MEASUREMENTS AND ANALYTICS.....	44
2.7 SPECIFIC CALCULATION	49
RESULTS AND DISCUSSION.....	50
3.1 CHARACTERISATION	50
3.1.1 External loop flow rate	50
3.1.2 Hydrodynamic stress	51
3.1.3 k_La characterisation	55
3.2 EXPANSION	56
3.3 SPIN TUBE EXPERIMENTS.....	57
3.3.1 Constant harvest/bleed ratio	57
3.3.2 Different cell density and percentage of feed	61
3.4 BIOREACTOR RUNS.....	65
3.4.1 Preliminary run: media composition	65
3.4.2 Seed reactor	66
3.4.3 Comparison of ATF and TFF applying manual bleed	68
3.4.4 Comparison of TFF and TFF applying manual bleed	72
3.4.5 Online measurements	79
CONCLUSIONS AND OUTLOOKS	82
REFERENCES	84

ACKNOWLEDGEMENTS

I am grateful to Prof. Dr. Morbidelli for giving me the possibility to be part of such a great group.

I would like to thank the whole Morbidelli group and in particular the Biocells group. A special thank goes to Daniel for introducing me to the world of the cell culture and for supervising me patiently during these months. Additionally I would like to thank Thomas for sharing a bit of his knowledge and I would like to express my gratitude to Dr. Miroslav Soos for being my supervisor at ETH.

Thanks to my office mates, the Woko guys and my Italian friends for their support and for always pushing me on the right way.

Finally, I would like to express my gratitude to my family that in these years allowed me studying, supporting me in all my choices.

LIST OF FIGURES

Figure 1 - Sketch of the TFF (left) and ATF (right) setups compared in the project. In the TFF a bearglass centrifugal pump creates a one way flow in the hollow fiber, in the ATF the diaphragm pump generates an alternative flow in the cartridge. The harvest on the permeate site of the hollow fiber was withdrawn by a peristaltic pump.	2
Figure 2 - A) Shear stress in the ATF system as function of the flow rate, determined without hollow fiber (green square), with the “short” hollow fiber (empty circle) and with the “long” one (green triangle) attached. B) Shear stress in the TFF system, as a function of the flow rate, calculated without hollow fiber (blue triangle), with the “short” hollow fiber (empty circle) and with the “long” one (blue square).	3
Figure 3 - Viable cell density (A), viability (B), reactor titer (C) and retention (D), as a function of time, in the TFF (green) equipped with the flow sensor and the biomass sensor and in the ATF (blue).	4
Figura 1 – Rappresentazione schematica dei due sistemi a perfusione, a sinistra il TFF e a destra l’ ATF, studiati. Nel TFF una pompa centrifuga crea un flusso monodirezionale all’interno dell’ <i>hollow fiber</i> , nell’ATF una pompa a diaframma crea un flusso alternato.....	6
Figura 2 – A) Sforzo di taglio in un sistema equipaggiato con l’ATF, in funzione della portata, determinato senza <i>hollow fiber</i> (quadrato verde), con la “short” <i>hollow fiber</i> (cerchio vuoto) e con la “long” <i>hollow fiber</i> (triangolo verde). B) Sforzo di taglio nel sistema equipaggiato con la TFF, in funzione della portata, determinato senza <i>hollow fiber</i> (triangolo blu), con la “short” <i>hollow fiber</i> (cerchio vuoto) e con la “long” <i>hollow fiber</i> (quadrato blu).....	7
Figura 3 - Densità cellulare (A) ,vitalità (B), concentrazione del prodotto nel reattore (C) e ritenzione (D) ,in funzione del tempo, nel TFF con il sensore di flusso e di biomassa (verde) e nella ATF (blu).....	9
Figure 4 - Batch stirred bioreactor.....	11
Figure 5 - Mammalian cell growth in a batch reactor as a function of time.....	12
Figure 6 - Fed batch stirred bioreactor characterised by an inlet stream that permits to feed one or more nutrients during the culture.	13
Figure 7 - Perfusion system equipped with a feed line that permits to add continuously nutrients and a bleed line that allows taking out the by products and the death cells. A cell retention device separates the supernatant containing the product from the cell suspension.	14
Figure 8 - Typical viable cell densities, as a function of time, obtainable in a batch (blue), fed-batch (red) and perfusion (black) cell culture.	15
Figure 9 - Schematic representation of a perfused bioreactor equipped with a tangential flow hollow fiber. A pump returns the concentrated stream to the reactor and one creates a trans-membrane pressure that allows the removal of supernatant from the hollow fiber. ..	19

Figure 10 - Perfused bioreactor equipped with an alternative tangential filter. A diaphragm pump controlled by a vacuum creates a two ways flow inside the cartridge.	20
Figure 11 - Cell lysis due to the deformation into the membrane pores of diameter D_p induced by the transmembrane pressure (TMP) [20].	22
Figure 12 - Cell density and viability, as a function of time, in the ATF system (left) and	25
Figure 13 - Sketch of the ATF setup, equipped with the “short” hollow fiber connected to a diaphragm pump that creates an alternating flow in the cartridge.....	28
Figure 14 - Sketch of the TTF setup equipped with the “short” hollow fiber connected to a bearingless centrifugal pump creating a one-way flow in the cartridge.....	29
Figure 15 - Sketch of the experimental k_{La} determination. N_2 is first purged to zero the DO, followed by the subsequent supply of pure air. The change of oxygen concentration is monitored over time.	33
Figure 16 - Expansion procedure from thawing (WD00) to inoculation (WD07). The containers in which cells were suspended and the respective cell densities and incubator settings are reported.....	35
Figure 17 - Sketch of the experimental procedure: subsequently to the bleeding, the cells are spun down and the supernatant is removed (harvest). Finally the cells are resuspended in fresh media (feed).	37
Figure 18 - DoE of viable cell density and feed fraction in the base medium. Six conditions were investigated: $30 * 10^6$ cells/ml – 5%, $30 * 10^6$ cells/ml – 25%, $70 * 10^6$ cells/ml – 5%, $70 * 10^6$ cells/ml – 25%, $50 * 10^6$ cells/ml – 5% and $50 * 10^6$ cells/ml – 15%.....	38
Figure 19 - Sketch representing the adaptive bleeding strategy. Twice a day, the viable cell density was measured and the respective amount of cell suspension to bleed $5 * 10^6$ cells/ml below the set point was withdrawn.	38
Figure 20 - Control system used in the bioreactor to keep constant the working volume. The harvest flow rate is set to 1 RV/day and the bleeding is performed manually or automatically according to the cell density. The feed pump is controlled by the weight of the balance.	42
Figure 21 - Fraction of production medium (purple) and production medium supplemented with 10% of feed (green) used with 20, 40 and $60 * 10^6$ cells/ml.....	43
Figure 22 - A) Liquid flow measured with the “long” hollow fiber in the TFF setup, running the centrifugal pump at 50, 1100, 1500, 2000, 2500 and 3000 rpm. B) Flow rate, as function of the rotational speed, measured without (black square), with the “short” (open circle) and the “long” (black triangle)	51
Figure 23 - A) Structural factor ($S(q)$), as a function of the scattering multiple (q), measured in a batch culture at 30 rpm (closed square), 170 rpm (opened left triangle) and 350 rpm (closed right triangle). B) Evaluation of the fractal dimension (d_f) from the power law of $S(q)$ plotted as a function of $q Rg$ measured in a batch culture at 30 rpm (closed square), 170 rpm (opened left triangle) and 350 rpm (closed right triangle).	52
Figure 24 – Evolving shear stress, as a function of time, measured with the PMMA method in the ATF system without the hollow fiber module in the external loop.....	52

Figure 25 – A) Shear stress in the ATF system, as a function of the flow rate, calculated without (green square), with the “short” (empty circle) and with the “long” (green triangle) hollow fiber module attached. B) Shear stress in the TFF system, as a function of the flow rate, calculated without (blue triangle), with the “short” (empty circle) and with the “long” (blue square) hollow fiber attached.	54
Figure 26 - Shear stress, as a function of the Reynolds impeller, calculated in a batch system stirring and stirring and sparging constantly at 20 l/min.	55
Figure 27 - A) DO, as a function of time, measured in the TFF system equipped with the “short” hollow fiber. B) $\ln CL * -CL$, as a function of time, measured in the ATF and TFF setups with the external loop.	56
Figure 28 - A) Viable cell density profile during the expansion procedure from day 0 (thawing) until day 7 (inoculation). B) Amount of volume in which the cells are suspended and respective containers in which they are stored (1 spin tubes, 3 spin tubes, 2 roller bottles and 1 reactor).	57
Figure 29 - Viable cell density, as a function of time, in the five spin tubes investigated: batch (pink), 5% bleed (purple), 10% bleed (orange), 25% bleed (red) and 50% bleed (blue).....	58
Figure 30 - Glucose (A) and lactate (B) concentration, as a function of time, in the five spin tubes investigated: batch (pink), 5% bleed (purple), 10% bleed (orange), 25% bleed (red) and 50% bleed (blue).	58
Figure 31 – Viability, as a function of time, in the five spin tubes investigated: batch (pink), 5% bleed (purple), 10% bleed (orange), 25% bleed (red) and 50% bleed (blue)...	59
Figure 32 - Specific growth rate, as a function of time, in the five spin tubes investigated: batch (pink), 5% bleed (purple), 10% bleed (orange), 25% bleed (red) and 50% bleed (blue).....	60
Figure 33 – Tite (A) and specific productivity (B), as a function of time, in the five spin tubes investigated: batch (pink), 5% bleed (purple), 10% bleed (orange), 25% bleed (red) and 50% bleed (blue).	61
Figure 34 - Viable cell density (A) and viability (B), as a function of time, in the six spin tubes: $30 * 10^6$ cells and 5% of feed (pink circle), $30 * 10^6$ cells and 25% of feed (purple circle), $50 * 10^6$ cells and 15% of feed (orange triangle), $50 * 10^6$ cells and 5% of feed (red square), $70 * 10^6$ cells and 25% of feed (blue circle), $70 * 10^6$ cells and 5% of feed (green triangle).....	62
Figure 35 – Glucose (A) and lactate (B) concentration, as a function of time, in the six spin tubes: $30 * 10^6$ cells and 5% of feed (pink circle), $30 * 10^6$ cells and 25% of feed (purple circle), $50 * 10^6$ cells and 15% of feed (orange triangle), $50 * 10^6$ cells and 5% of feed (red square), $70 * 10^6$ cells and 25% of feed (blue circle), $70 * 10^6$ cells and 5% of feed (green triangle).....	62
Figure 36 – Growth rate, as a function of time, in the six spin tubes: $30 * 10^6$ cells and 5% of feed (pink circle), $30 * 10^6$ cells and 25% of feed (purple circle), $50 * 10^6$ cells and 15% of feed (orange triangle), $50 * 10^6$ cells and 5% of feed (red square), $70 * 10^6$ cells and 25% of feed (blue circle), $70 * 10^6$ cells and 5% of feed (green triangle).	63

Figure 37 – A) Titer, as a function of time, in the six spin tubes: 30×10^6 cells and 5% of feed (pink circle), 30×10^6 cells and 25% of feed (purple circle), 50×10^6 cells and 15% of feed (orange triangle), 50×10^6 cells and 5% of feed (red square), 70×10^6 cells and 25% of feed (blue circle), 70×10^6 cells and 5% of feed (green triangle). B) Titer as a function of the feed fraction and viable cell density.	64
Figure 38 - Viable cell density (A) and glucose concentration (B) as a function of time. .	65
Figure 39 - Amino acids concentrations as a function of time. Highlighted in green the asparagine, in blue the tyrosine and in yellow the cysteine.	66
Figure 40 – Viable cell density (A) and perfusion rate (B), as a function of time.	67
Figure 41 – Glucose concentration in the seed bioreactor as a function of time.....	68
Figure 42 - Viable cell density (A) and viability (B) as a function of time in the TFF (green square) and	69
Figure 43 – Harvest (blue), bleed (pink) and perfusion (purple) rate, as a function of time, in the TFF (A) and ATF (B) reactors.	70
Figure 44 – A) Glucose concentration, as a function of time, in the feed (dark green) and in TFF (green) and ATF (bleu) reactors. B) Lactate concentration, as a function of time, in TFF (green) and ATF (bleu) reactors.	71
Figure 45 – A) Titer in the ATF reactor (blue circle) and in the harvest (light blue square) as a function of time. B) Titer in the TFF reactor (light green square) and in the harvest (green circle) as a function	72
Figure 46 - Viable cell density (A) and viability (B), as a function of time, in the TFF (green square) and ATF (bleu circle) reactors.....	73
Figure 47 – Harvest (bleu), bleed (pink) and perfusion (purple) rate, as a function of time, in the TFF (A) and ATF (B) reactors.	74
Figure 48 - A) Glucose concentration, as a function of time, in the feed (dark green) and in TFF (green) and ATF (bleu) reactors. B) Lactate concentration, as a function of time, in TFF (green) and ATF (bleu) reactors.	75
Figure 49 – A) Titer in the ATF reactor equipped with an online biomass sensor (light blue square) and in the harvest (blue circle) as a function of time. B) Titer in the TFF reactor equipped with an online biomass sensor (light green square) and in the harvest (green circle) as a function of time. C) Retention of the product in the ATF setup. D) Retention of the product in the TFF setup equipped with the biomass sensor.....	76
Figure 50 – Glyforms measured in the two experiments at the same day	78
Figure 51 – Glycoforms in the ATF setup equipped with the biomass sensor at working	78
Figure 52 - A) Fraction of oxygen sparged in the ATF (bleu) and TFF (green), without biomass sensor, as a function of time. B) pCO_2 measured in the ATF reactor equipped with the biomass sensor. C) pH measured in the ATF (bleu) and TFF (green) without biomass sensor as a function of time. D) Weight of the TFF reactor without biomass sensor during the experiment.	80
Figure 53 – Viable cell density, as function of time, measured using the online biomass sensor	81

LIST OF TABLES

Table 1 - Main characteristics of the “short” and “long” hollow fiber.....	27
Table 2 - Rotational speeds of the bearingless centrifugal pump used to study the flow rate with no hollow fiber and with both the “short” as well as the “long”.....	30
Table 3 - Conditions investigated during the analysis of the maximum shear stress in a reference batch setup and in both TFF and ATF setups without as well as with “short” and “long” hollow fiber.....	32
Table 4 - Fraction of the perfusion, harvest and bleeding used in the 6 spin tubes.....	36
Table 5 – Velocities and Reynolds numbers calculated in the “short” and “long” hollow fiber setting a flow rate equal to 0.5 l/min, 1 l/min and 1.5 l/min.....	53
Table 6 - k_{La} values calculated with the dynamic method in the TFF system and in the ATF without the external loop and with the “short” hollow fiber.....	56
Table 7 – Osmolality of the medium with 5%, 15% and 25% fraction of feed.....	64
Table 8 – Mean viable cell density (VCD), perfusion and bleed rate, reactor and harvest titer, ammonia concentration measured in the ATF without biomass sensor and TFF with biomass sensor at 20×10^6 cells/ml, 40×10^6 cells/ml and 60×10^6 cells/ml.....	77
Table 9 – Mean specific growth rate (μ), mean specific consumption of glucose (qGLC), mean specific production of lactate (qLAC), mean specific production of antibodies (qmAb) in the ATF without biomass sensor and TFF with biomass sensor at 20×10^6 cells/ml, 40×10^6 cells/ml and 60×10^6 cells/ml.....	77

LIST OF ABBREVIATIONS

2-AA	2-Anathralamide
Ab	Antibody
ATF	Alternating Tangential Flow
CCC	critical coagulation concentration
CFD	Computational Fluid Dynamics
CHO	Chinese Hamster Ovary
CMP	Cell per ml
CO ₂	carbon dioxide
CSPR	Cell Specific Perfusion Rate
DMSO	Dimethylsulfoxide
DO	Dissolved Oxygen
DoE	Design of Experiments
FDA	Food and Drug Administration
Frac_O ₂	Fraction of O ₂
GIDH	Glutamate Dehydrogenase
GLC	Glucose
H ₂ O	Water
HCl	Hydrochloric acid
HF	Hollow Fiber
HILIC	Hydrophobic interaction chromatography
HPLC	High Performance Liquid Chromatography
ID	Inner Diameter
Ig	Immunoglobulin

IgG	Immunoglobulin G
L	Length
LAC	Lactate
mAb	monoclonal antibody
MALDI-TOF	Time-Of-Flight Mass-Spectroscopy
N ₂	Azote
Na	Sodium
NADPH	Nicotinamide Adenine Dinucleotide Phosphate
NaOH	Sodium Hydroxide
NSD	Nucleotide sugar donor
O ₂	Oxygen
OD	Outer Diameter
OTR	Oxygen Transfer Rate
PID	Proportional Integral Derivative
PMMA	Polymethyl Methacrylate
RPM	Round Per Minute
FR	Flow Rate
RV	Reactor Volume
SALS	Small Angle Light Scattering
SEM	Scanning Electron Microscope
ST	Spin Tube
TFF	Tangential Flow Filtration
TMP	Transmembrane pressure

UV	Ultraviolet
VCD	Viable Cell Density
vvm	Volumw per Volume per Minute
WCB	Working Cell Bank
WD	Working Day

Glycosylation nomenclature

M6	Man ₆ GlcNAc ₂
M5	Man ₅ GlcNAc ₂
FA1	GlcNAcMan ₅ GlcNAc ₂ Fuc
FA2G0	GlcNAc ₂ Man ₅ GlcNAc ₂ Fuc
FA2G1	GalGlcNAc ₂ Man ₅ GlcNAc ₂ Fuc
FA2G2	Gal ₂ GlcNAc ₂ Man ₅ GlcNAc ₂ Fuc
FA2G2S1	SiaGal ₂ GlcNAc ₂ Man ₅ GlcNAc ₂ Fuc
FA2G2S2	Sia ₂ Gal ₂ GlcNAc ₂ Man ₅ GlcNAc ₂ Fuc

Amino acids nomenclature

ALA	Alanine
ARG	Arginine
ASN	Asparagine
ASP	Aspartic acid
CYS	Cysteine
GLN	Glutamine
GLU	Glutamic acid
GLY	Glycine
HIS	Histidine
ILE	Isoleucine
LEU	Leucine
LYS	Lysine
MET	Methionine
PHE	Phenylalanine
PRO	Proline
SER	Serine
THR	Threonine
TRP	Tryptophan
TYR	Tyrosine
VAL	Valine

ABSTRACT

Since their introduction on the market in 1986, antibodies have gained interest representing 30% of nowadays total biopharmaceutical production. The required complex post-translational modifications are in general not achievable with bacteria or yeast, so the majority of the antibodies is produced by mammalian cells. For this reason in the last decades the interest on mammalian cell cultures has increased. Traditionally the fed batch systems are used to produce antibodies. In the fed batch mode one or more nutrients are fed in the reactor in response to their depletion. Such cultivation lasts approximately two weeks with a maximum cell density around 20×10^6 cells/ml. After this time the process is stopped and the product is harvested. During 2000s new media formulations and cell lines have permitted to reach higher cell densities and higher titers. As consequence of these progresses, industries started to focus on perfusion cultures. In the perfusion system a constant environment favourable for cells is obtained through the continuous addition of nutrients and removal of by-products. To minimize cell loss, the perfusion system is equipped with a cell retention device allowing to take out the product during the run while recycling the cells back in the reactor. The cell retention devices can exploit either the difference in density (i.e. gravity settler, centrifuges and acoustic settler) or in size (i.e. spin filter and hollow fiber). Compared to the fed batch system the perfusion mode allows prolonged and steady healthy culture at higher cell densities with a constant quality of the product. Because the product is removed during the culture, the perfusion system is also suitable for the production of unstable proteins.

In this project two different perfusion systems have been compared: the Tangential Flow Filter (TFF) and the Alternating Tangential Flow Filter (ATF) (Figure 1). Both systems employ a hollow fiber which is a cylindrical cartridge constituted by multiple cylindrical porous fibers in which the suspension flows tangentially. In the TFF the hollow fiber is connected to the reactor by a double port and the flow recirculates in one direction, whereas in the ATF it is connected by a single port and the cell suspension is alternatively pumped forth and back to the reactor by a diaphragm pump. According to the vendor, the diaphragm pump should induce lower shear stress compared to the one created by the

centrifugal or peristaltic pump used in the TFF setup. Moreover, the two ways flow inside the hollow fiber is thought to prevent filter fouling and the change in transmembrane pressure should create a back flush cleaning the pores of the fibers.

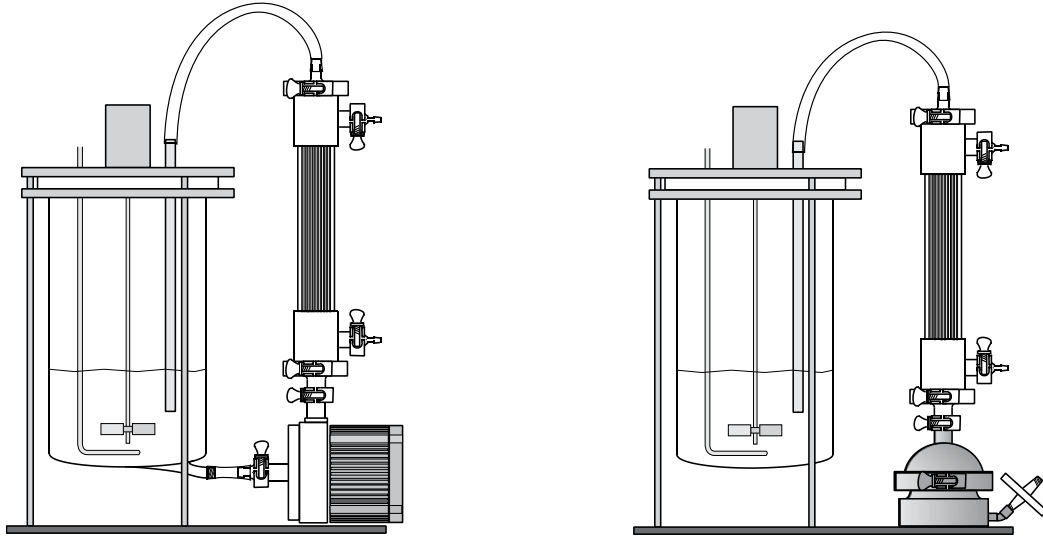


Figure 1 - Sketch of the TFF (left) and ATF (right) setups compared in the project. In the TFF a bearglass centrifugal pump creates a one way flow in the hollow fiber, in the ATF the diaphragm pump generates an alternative flow in the cartridge. The harvest on the permeate site of the hollow fiber was withdrawn by a peristaltic pump.

The designed reactor setups were thoroughly characterized in terms of maximum shear stress and oxygen transfer rate. It was found that the oxygen transfer rate is not influenced by the setup and is sufficient to provide enough oxygen to the cells. Instead, the shear stress study revealed significantly lower stress values induced by the diaphragm pump compared to the centrifugal pump (Figure 2). In both setups the shear stress induced was depended on the type of hollow fiber mounted in the external loop. The “long” hollow fiber, 60 cm in length and a total area of 1300 cm², creates higher shear stress than the “short” one characterised by a length of 25 cm and a total area of 1570 cm². In any case, with the operating parameters used in the cell culture (i.e. gas flow rate of 20 l/h and rotational speed of the impeller set to 400 rpm), in both systems the maximum shear stress was lower than the threshold of 50 Pa, knowing to negatively affect viable cell density.

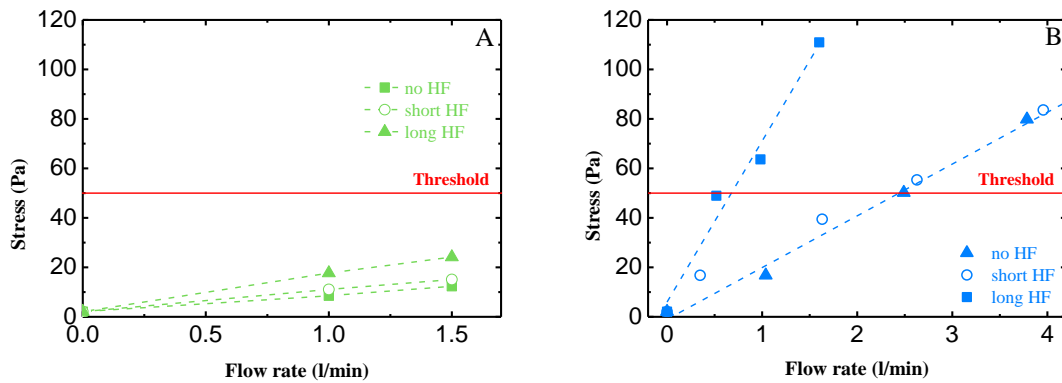


Figure 2 - A) Shear stress in the ATF system as function of the flow rate, determined without hollow fiber (green square), with the “short” hollow fiber (empty circle) and with the “long” one (green triangle) attached. B) Shear stress in the TFF system, as a function of the flow rate, calculated without hollow fiber (blue triangle), with the “short” hollow fiber (empty circle) and with the “long” one (blue square).

Prior to the bioreactor runs, spin tube experiments were conducted, to investigate the effect of the bleed rate on the perfusion culture and to test different media compositions in order to maintain constant viable cell density at various set points. The spin tube experiments showed that an adaptive bleeding should be used to keep the cell density constant during time and that with more than 25×10^6 cells/ml the base medium is not sufficient but it has to be supplemented with concentrated feed and glucose. Subsequently, the two reactor setups were compared performing two cell cultures. Three different consecutive viable cell density set points were kept for one week with a viability mostly higher than 90% (Figure 3B). Starting at 20×10^6 cells/ml, cells were grown to 60×10^6 cells/ml, followed by a set point of 40×10^6 cells/ml (Figure 3A). The set points were maintained by changing the media composition and were kept constant adjusting the bleeding. In the first run a manual bleeding was performed, meaning that the cell density was measured and the corresponding amount of volume to bleed 2×10^6 cells/ml below the set point was withdrawn. In the ATF setup it was possible to reach and keep the three steady states while in the TFF at 60×10^6 cells/ml the system crashed because the flow in the external loop stopped. Therefore, in a second run a clamp-on flow sensor was added in the TFF setup in order to online monitor the flow rate in the external loop and keeping it constant by adjusting the rotational speed of the centrifugal pump. Moreover, to automatize the process an online biomass sensor was mounted in both reactors and an automatic bleeding was

performed according to the viable cell density measured online. The use of the flow sensor avoided the blockage of the hollow fiber and enabled the achievement of the three steady states in the TFF (Figure 3A). Moreover, the biomass sensor allowed the flattening of the cell density profile since the cell suspension was removed in an automatic manner every time that the cell density exceeded the set point. The analysis of the product concentration showed that a constant cell density determines a constant production (Figure 3C). No difference in the quality of the product was observed between the two systems, meaning that it is not influenced by the setup. However, even if in term of quality the two systems behaved similarly, the retention of the product inside the reactor equipped with the TFF was significantly higher than the one in the ATF (Figure 3D). So, the dynamics of the ATF characterised by the alternating flow decreased the fouling. In conclusion, in both systems a viable culture at three steady states was accomplished. Nevertheless, due to the lower retention, the ATF should be preferred for the production of therapeutic proteins.

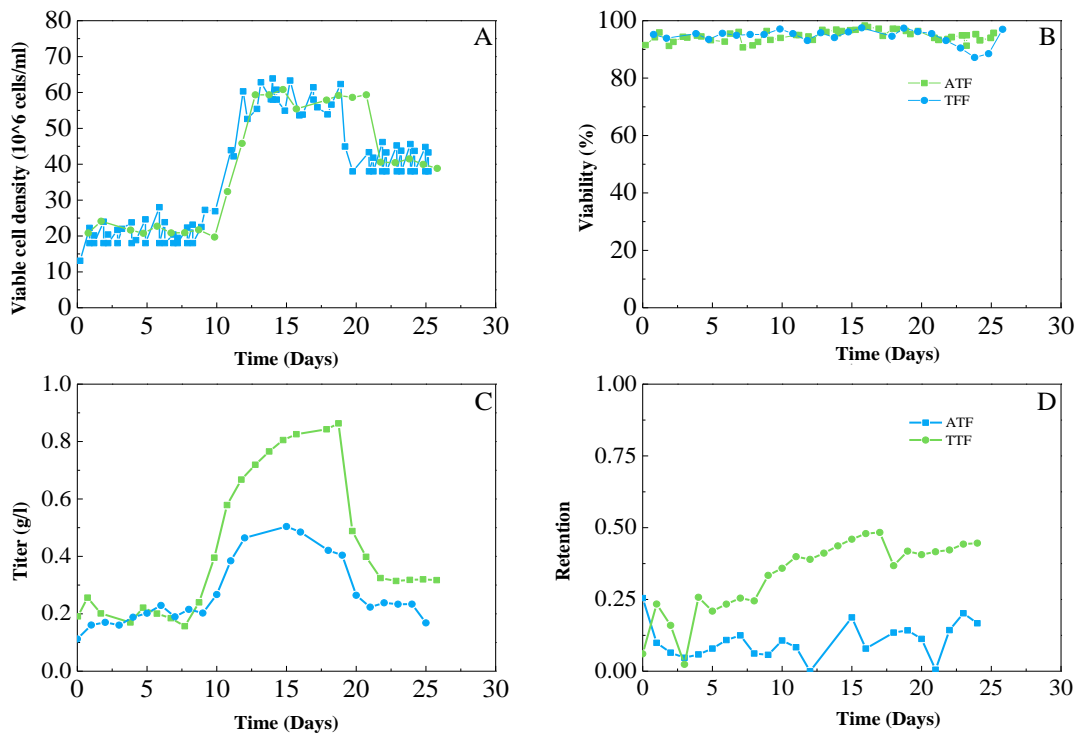


Figure 3 - Viable cell density (A), viability (B), reactor titer (C) and retention (D), as a function of time, in the TFF (green) equipped with the flow sensor and the biomass sensor and in the ATF (blue).

Keywords: continuous cell culture, multiple steady states, bioreactor characterisation, monoclonal antibody.

SOMMARIO

Dalla loro introduzione sul mercato nel 1986, gli anticorpi hanno guadagnato un interesse sempre maggiore fino a rappresentare oggi giorno il 30% del totale della produzione biofarmaceutica. Generalmente le complesse modifiche post-traslazionali necessarie non sono ottenibili con batteri o lieviti, quindi la maggior parte degli anticorpi è prodotta utilizzando cellule di mammifero. Per questo motivo negli ultimi anni l'interesse per le colture cellulari è aumentato. Tradizionalmente gli anticorpi sono prodotti in reattori *fed-batch* in cui uno o più nutrienti sono aggiunti al reattore durante l'esperimento in risposta al loro consumo. Questo tipo di coltura cellulare, durante la quale viene raggiunta una densità massima pari a $20 * 10^6$ cellule/ml, dura circa due settimane al termine delle quali viene estratto il prodotto. Durante gli anni 2000 lo sviluppo di nuovi medium e di nuove linee cellulari ha permesso di raggiungere densità cellulari e concentrazioni di anticorpi sempre maggiori. In seguito a questi progressi le industrie hanno iniziato a spostare il loro interesse verso i sistemi a perfusione. Nei sistemi a perfusione un ambiente costante e favorevole alle cellule è ottenuto mediante una continua aggiunta di nutrienti e rimozione di sottoprodotti. I sistemi a perfusione sono costituiti da un dispositivo di ritenzione che permette di trattenere le cellule nel bioreattore estraendo il prodotto durante l'esperimento. I dispositivi di ritenzione possono separare il prodotto sfruttando la differenza in densità, ad esempio *gravity settler*, centrifughe o *acoustic settler*, oppure in base alle dimensioni come gli *spin filters* o le *hollow fibers*. Rispetto al sistema *fed-batch* la perfusione consente sia di aumentare la durata della coltura sia di ottenere densità cellulari maggiori. Inoltre, l'aggiunta continua di nutrienti e la contemporanea rimozione di sottoprodotti permettono di mantenere la densità cellulare costante nel tempo, determinando una produzione costante e una migliore qualità del prodotto. Infine, i sistemi perfusi sono candidati di prima fascia per la produzione di proteine instabili essendo il prodotto estratto durante la coltura cellulare.

In questo progetto due sistemi a perfusione sono stati confrontati: il *Tangential Flow Filter* (TFF) e l'*Alternating Tangential Flow Filter* (ATF) (Figura 1). Entrambi i sistemi utilizzano una cartuccia cilindrica chiamata hollow fiber, costituita da fibre porose cilindriche in cui la sospensione contenente le cellule e il prodotto da separare fluisce

tangenzialmente. Nel TFF il dispositivo di ritenzione cellulare è connesso al bioreattore da una doppia porta e quindi la sospensione cellulare circola all'interno dell'*hollow fiber* in un'unica direzione. Diversamente, nell'ATF l'*hollow fiber* è connessa al reattore da una singola porta e la sospensione viene alternativamente pompata nelle due direzioni da una pompa a diaframma. Secondo il produttore la pompa a diaframma crea uno sforzo di taglio inferiore a quello generato dalla pompa centrifuga utilizzata nel TFF. Inoltre, il flusso bidirezionale all'interno dell'*hollow fiber* dovrebbe prevenire il *fouling* della membrana e il cambiamento della pressione transmembranale durante il ciclo della pompa dovrebbe creare un flusso in grado di pulire i pori delle fibre.

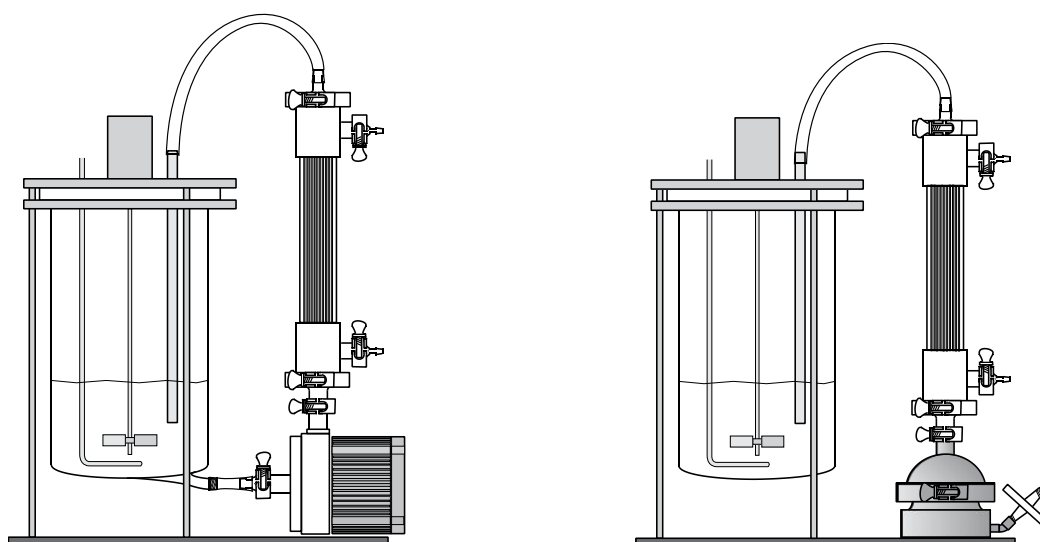


Figura 1 – Rappresentazione schematica dei due sistemi a perfusione, a sinistra il TFF e a destra l' ATF, studiati. Nel TFF una pompa centrifuga crea un flusso monodirezionale all'interno dell' *hollow fiber*, nell'ATF una pompa a diaframma crea un flusso alternato.

Inizialmente i due sistemi sono stati caratterizzati in termini di sforzo di taglio massimo e di velocità di trasferimento dell'ossigeno. La velocità di trasferimento dell'ossigeno è risultata essere indipendente dal *setup* considerato e tale da garantire ossigeno sufficiente alle cellule. Diversamente, lo studio dello sforzo di taglio ha rivelato che la pompa a diaframma produce sforzi di taglio inferiori alla pompa centrifuga (Figura 2). In entrambi i *setups* lo sforzo misurato dipende dal tipo di *hollow fiber* utilizzata. La “long” *hollow*

fiber, 60 cm in lunghezza e area totale pari a 1300 cm², crea sforzi di taglio maggiori della “*short*” *hollow fiber*, caratterizzata da una lunghezza di 25 cm e da un’area totale pari a 1570 cm². In ogni caso, considerando il flusso di gas e la velocità di rotazione del girante utilizzati durante la coltura cellulare, 20 l/h e 400 rpm rispettivamente, in entrambi i sistemi il massimo sforzo di taglio è risultato essere inferiore a uno sforzo pari a 50 Pa avente un effetto negativo sulla vitalità cellulare.

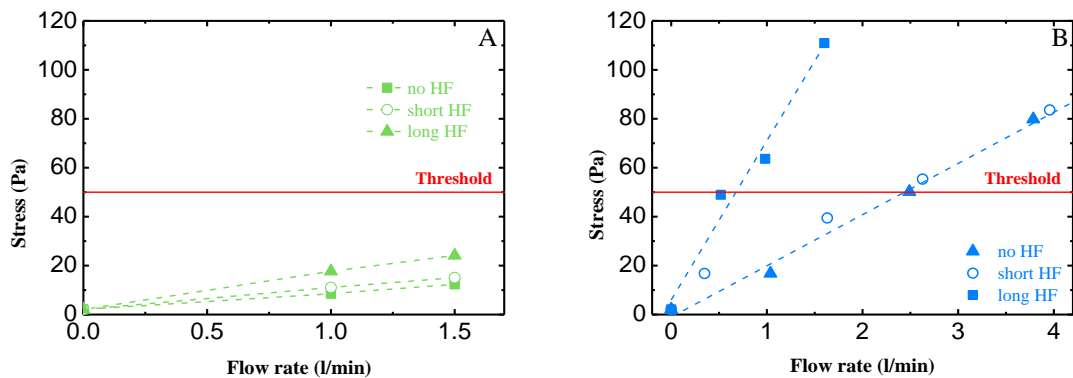


Figura 2 – A) Sforzo di taglio in un sistema equipaggiato con l’ATF, in funzione della portata, determinato senza *hollow fiber* (quadrato verde), con la “*short*” *hollow fiber* (cerchio vuoto) e con la “*long*” *hollow fiber* (triangolo verde). B) Sforzo di taglio nel sistema equipaggiato con la TTF, in funzione della portata, determinato senza *hollow fiber* (triangolo blu), con la “*short*” *hollow fiber* (cerchio vuoto) e con la “*long*” *hollow fiber* (quadrato blu).

Prima della coltura cellulare due esperimenti sono stati condotti in *spin tubes*. Il duplice scopo è stato quello di valutare quale fosse l’effetto del *bleeding* e quale composizione del medium dovesse essere utilizzata per mantenere costante una data densità cellulare. Gli esperimenti hanno mostrato che è necessario adattare il *bleeding* durante l’esperimento e che con più di $25 \cdot 10^6$ cellule/ml il medium normalmente utilizzato non è sufficiente ma *feed* e glucosio devono essere aggiunti. In seguito, i due sistemi a perfusione sono stati confrontati in due colture cellulari. Tre densità cellulari sono state mantenute costanti per una settimana con una vitalità per la maggior parte dell’esperimento superiore al 90% (figura 3B). I *set points* sono stati raggiunti cambiando la composizione del medium e sono stati mantenuti costanti aggiustando il *bleeding*. Nella prima coltura cellulare si è utilizzato un *bleeding* manuale quindi, dopo aver misurato la densità cellulare, è stato estratto dal bioreattore un volume tale da ottenere una densità cellulare di $2 \cdot 10^6$ cellule/ml inferiore al

set point. Nell'ATF tutte e tre le densità cellulari sono state raggiunte e mantenute mentre nella TFF, a causa dell'interruzione del flusso nel *loop* esterno, non è stato possibile mantenere $60 * 10^6$ cellule/ml. Per questo motivo nel secondo esperimento un sensore di flusso è stato connesso al TFF in modo da monitorare online il flusso nel *loop* esterno e mantenerlo costante modificando la velocità di rotazione della pompa centrifuga. Inoltre, al fine di automatizzare il processo, un sensore di biomassa è stato aggiunto a entrambi i bioreattori in modo che il *bleeding* fosse controllato dalla densità cellulare misurata *online* dal sensore. L'utilizzo del sensore di flusso ha evitato il blocco dell' *hollow fiber* facendo sì che anche nel TFF fossero raggiunti e mantenuti tutti e tre gli stati stazionari (Figura 3A). Inoltre, con il sensore di biomassa il *bleeding* è stato effettuato automaticamente ogni qualvolta la densità cellulare superasse il target, premettendo in questo modo di ottenere densità cellulari più vicine ai *set points*. L'analisi della concentrazione del prodotto ha mostrato che una densità cellulare costante determina anche una produzione costante (Figura 3C). Nessuna differenza è stata riscontrata in termini di qualità del prodotto tra i due sistemi mostrando che questa non viene influenzata dal *setup* utilizzato. Diversamente, la ritenzione all'interno della TFF si è mostrata essere significativamente maggiore di quella nel reattore equipaggiato con l'ATF (Figure 3D). Di conseguenza, la dinamica dell'ATF caratterizzata da un flusso alternato, diminuisce il *fouling*. In conclusione, entrambi i sistemi hanno permesso di raggiungere e mantenere costanti le tre densità cellulari prefissate. Ciò nonostante, a causa della ritenzione minore, l'ATF dovrebbe essere preferita per la produzione di anticorpi.

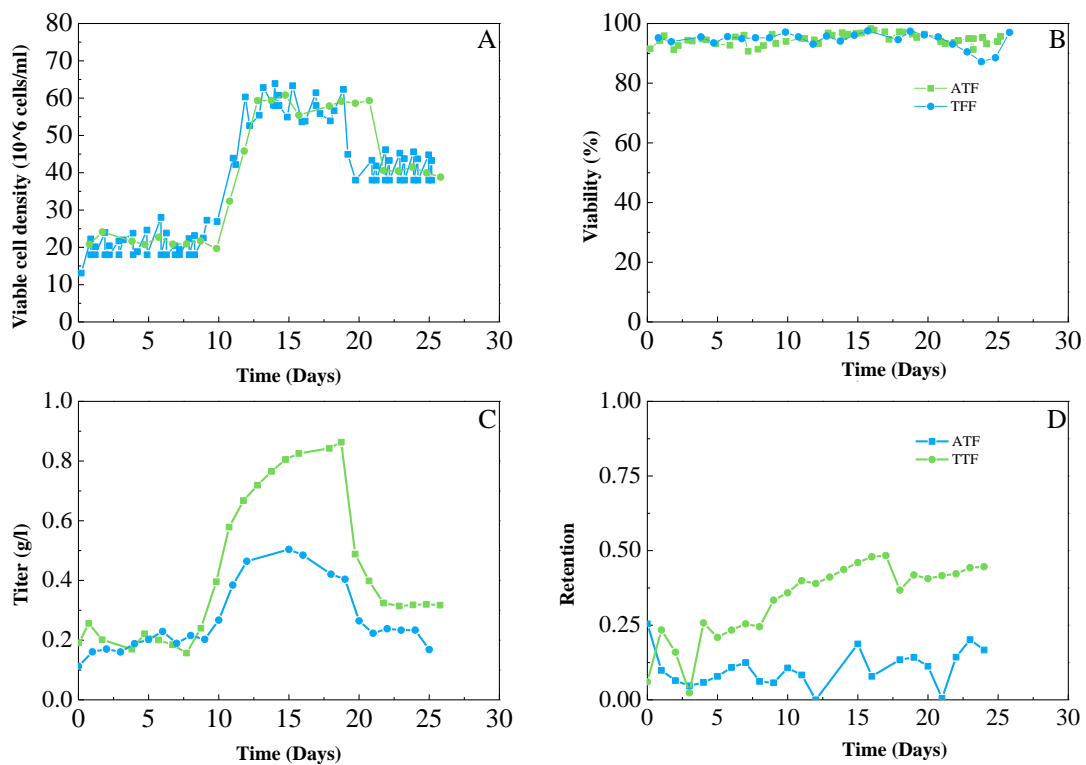


Figura 3 - Densità cellulare (A) ,vitalità (B), concentrazione del prodotto nel reattore (C) e ritenzione (D) ,in funzione del tempo, nel TFF con il sensore di flusso e di biomassa (verde) e nella ATF (blu).

Parole chiave: coltura cellulare continua, caratterizzazione del bioreattore, stati stazionari multipli, anticorpi monoclonali.

CHAPTER 1

INTRODUCTION

Antibody drugs, first introduced to the pharmaceutical market in 1986, nowadays represent 30% of the total biopharmaceutical production [1]. The antibody (Ab), or immunoglobulin (Ig), is a protein produced by plasma cells to protect the body from foreign pathogens. It is able to recognise and link to a specific part of the pathogen called antigen. The antibody-antigen binding can either directly inactivate the foreign agent or can activate the immune system, neutralizing the target [2]. Due to their high binding specificity, immunoglobulins are used in several therapies against cancer, rheumatoid arthritis or Crohn's disease. However, only glycosylated antibodies are not autoimmune and are therefore able to inactivate the foreign agents. These complex post-translational modifications are generally not achievable with bacteria, yeast or insect cells [3]. So, the majority of antibodies are produced by mammalian cells such as Chinese Hamster Ovary (CHO) and myeloma (SP2/0, NS0). In particular CHO cells produce 70% of all recombinant therapeutic proteins because it has been demonstrated that they are a safe host and so the approval of new products by the Food and Drug Administration (FDA) is simplifying [4]. Moreover they can be modified using gene amplification system in order to increase the titer.

In general, therapies based on antibodies require high doses and have to be applied for a long period. So, in order to meet the market, a large scale - high productivity process is needed. In the 1980s, at the beginning of the modern biotechnology, the production cell lines were not fully developed and the product expression was small. The cell concentrations achievable were only a few million per milliliter resulting in rather low titers (i.e. from a few micrograms to a few hundred milligrams per litre). To bypass the low production and concentration typical of batch as well as fed-batch cultures, the industries started focusing on perfusion systems. They increased cell concentration of an order of magnitude but resulting in a new problem: the scalability. In the early days of perfusion cultures, internal spin filters were used as retention device. As the volume of the bioreactor scales with the cube of the radius, the filtration surface of the perfusion device

only scaled by the square of the radius, taking up a significant portion of the production space inside the bioreactor. Therefore, during the 1990s, the industry decided to move away from perfusion and to refocus in the well-understood batch and fed-batch systems. In these systems the scale up was simply performed moving to bigger vessels and the typical low production was bypassed thanks to the improvement both in the media and in the cell lines. However, during the 2000s, the interest in perfusion cultures renewed as a suitable manufacturing method. Further advances in development of cell lines, expression systems and media formulation resulted in an impressive ability to grow cells to very high concentration reaching titers of 10 g/l previously inconceivable. These incredible progresses and the concomitant development of new cell retention devices, allow obtaining high cell density - scalable perfusion processes [5, 6]. In particular in a perfusion reactor the operating conditions are constant and can be precisely controlled. The cell retention device permits to take out the product during the cell culture run increasing the quality of the product. For this reason the perfusion systems are suitable for the production of unstable proteins such as FVIII, Simulect, Rebif. Finally, compared to the fed-batch, a high volumetric productivity can be obtained using smaller vessels [6].

1.1 CELL CULTURE

Mammalian cell cultures are commonly performed in stirred tank bioreactors. There are three different basic modes in operation.

1.1.1 Batch

The batch mode is a closed system in which all the nutrients required are supplied at the beginning of the culture (Figure 4). After inoculation the cells consume the available nutrients and produce waste and by-products accumulate in the bioreactor.

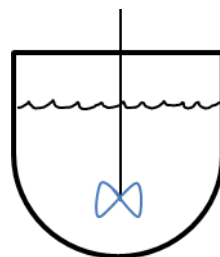


Figure 4 - Batch stirred bioreactor.

This results in a typical cell density profile, consisting of four different phases: the lag phase in which the cells adapt to the new environment, the exponential phase characterised by a rapid increase of the cell density, the stationary phase in which the cells divide and die at the same rate and a final death phase where the rate of death is higher than the rate of cell division and the cell density decreases (Figure 5). In batch cultures cell densities of approximately 5×10^6 cells/ml can be reached and all segregated product is removed at the end of the run [7]

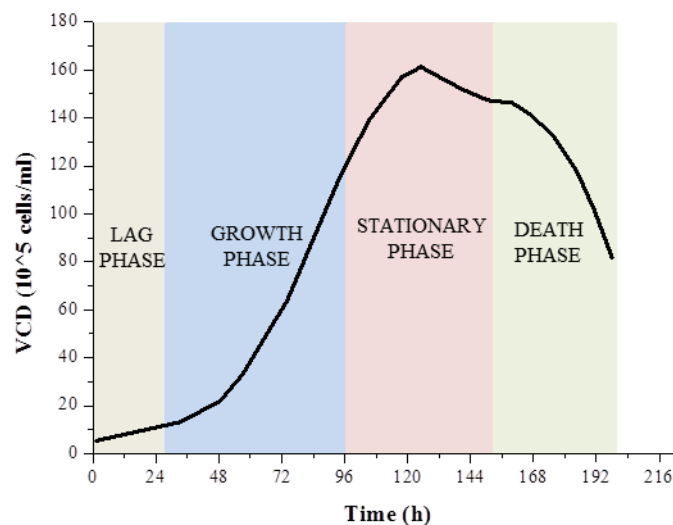


Figure 5 - Mammalian cell growth in a batch reactor as a function of time.

1.1.2 Fed-batch

In the fed-batch mode one or more nutrients are fed during the cultivation in response to their depletion (Figure 6). Like in the batch culture, it is possible to distinguish the characteristic four phases in the cell density profile [7]. However, the culture can be maintained up to three weeks with an increase in cell density (20×10^6 cells/ml) and in concentration of the product (up to 10 g/l) [5]. The fed-batch system is the typical operation mode applied in the production of monoclonal antibodies at industrial scale because of its simplicity and well - understood process.

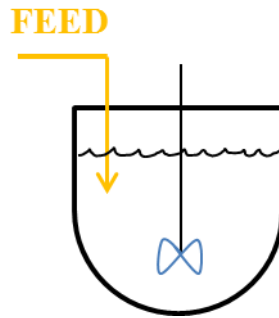


Figure 6 - Fed batch stirred bioreactor characterised by an inlet stream that permits to feed one or more nutrients during the culture.

1.1.3 Continuous culture

In the continuous culture a constant favourable environment is obtained through a continuous addition of nutrients and removal of by-product. Chemostat and perfusion reactors are examples of continuous culture. The chemostat is mainly used in microbial cultures allowing controlling the rate of bacteria growth by the rate of addition of the fresh medium and the rate of removal of bacterial cells and spent medium [8]. Since the cell growth is slower, it is needed to retain the cells in the reactor. For this reason the perfusion system is mainly used in the cell culture.

The perfused reactor is equipped with one or more inlet streams, permitting the continuous feed of fresh medium and additives. The segregated proteins as well as waste products are steadily removed during the cell culture in the harvest stream. In order to keep the cell density constant, a cell retention device is mounted inside or outside of the bioreactor. The cell suspension flows into the cell retention device and the cells are completely or partially separated from the supernatant that contains the desired product. The concentrated cells are recycled back to the bioreactor while the harvest is processed in order to capture the protein product (Figure 7) [9].

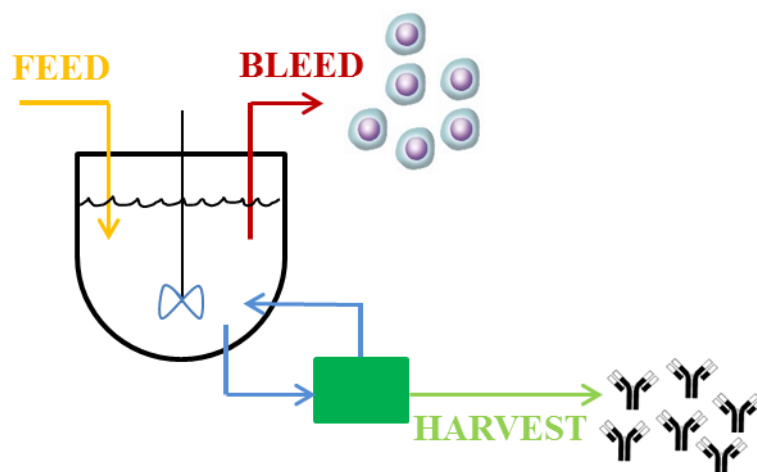


Figure 7 - Perfusion system equipped with a feed line that permits to add continuously nutrients and a bleed line that allows taking out the by products and the death cells. A cell retention device separates the supernatant containing the product from the cell suspension.

The continuous addition of nutrients allows reaching higher cell densities and therefore smaller volumes are needed compared to batch and fed-batch cultures. The perfusion permits a prolonged and steady healthy culture that guarantees a constant and improved quality of the product (Figure 8) [10]. Furthermore, since the product is removed throughout the run, this mode is suitable for the production of unstable proteins. The main concerns regarding the perfusion systems are the more complex process equipment and the control system needed that determine high costs. In general the high costs of investment are balanced by the smaller equipment needed. Moreover, compared to the fed-batch system, the product concentration in the harvest stream is usually lower but, since the cell densities reachable are higher, the productivity is increased. Furthermore, the product can potentially be processed in an integrated continuous manner [11] directly connecting a downstream capture and purification train.

Nowadays, the perfusion systems are used for the creation of high density-large volume cell banks and as both seed as well as production bioreactors [5]. They have also been applied in the large scale production of viruses for vaccines [12].

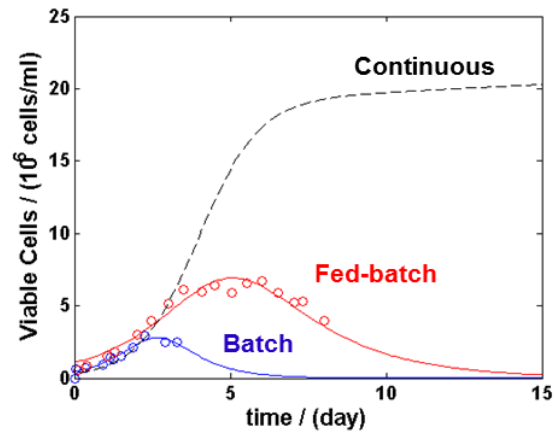


Figure 8 - Typical viable cell densities, as a function of time, obtainable in a batch (blue), fed-batch (red) and perfusion (black) cell culture.

1.1.4 Process parameters

During a cell culture several parameters have to be optimized to enhance the cell growth rate, the productivity and the product quality. The parameters are usually classified in physical and chemical. Physical parameters include the temperature, the gas flow rate and the stirring speed while chemical parameters consist of pH, osmolality and dissolved oxygen (DO) as well as carbon dioxide (CO₂) concentration. The temperature is usually kept to physiological levels at 37 °C. During the process it is important to provide enough oxygen to the cells to ensure a working metabolism. For this reason the dissolved oxygen (DO) is ideally maintained between 20% and 50%, compromising between a low level of DO, that could lead to an increase in the production of lactate, and a high one that could be cytotoxic [13]. Levels of DO lower than 10% can even affect the product quality causing a decrease of glycosylation. The DO can be kept to the set point controlling the gas flow rate, its composition or the impeller speed. Both the impeller speed and the gas flow rate also influence the removal dissolved CO₂. In particular the pCO₂ can accumulate during the time, at increased cell densities, reaching values higher than 120 mmHg that have been proved to inhibit the growth and affect the product quality [13]. The effect of the pH on the growth rate and on the production has been investigated by Ivarsson et al. [14] who observed lower growth rates at pH values lower than 6.8 and higher than 8. Usually in the growth phase a pH > 7.0 is preferred because this phase is usually accompanied by lactate production. Instead, in the steady phase, the production of lactate is lower and the pH has

to be decreased by CO₂ sparging [13]. Another chemical parameter that influences the growth rate and the product quality is the osmolality. In general cell culture media is designed to have an osmolality in the range of 270-330 mOsm/kg, potentially changing during the cell culture, for instance with base addition. Zhu et al. [15] reported that the cell growth rate decreases linearly with the osmolality. They particularly observed a drop in viable cell density at osmolality levels exceeding 400 mOsm/kg.

1.2 MAMMALIAN CELL PERFUSION CULTURE

1.2.1 Kinetics of perfusion cultures

In addition to maintain physical and chemical parameters in a desired range, in a perfusion culture the in and outgoing streams have to be controlled precisely. The harvest flow rate is usually set to a desired value and the feed rate is consequently adjusting to keep the reactor volume constant. Several methods can be used to adjust the perfusion rate during the cell culture, such as adapting the perfusion according to the cell density measured or according to the consumption of oxygen or the concentration of metabolites [16]. Ozturk et al. [16] introduced the concept of cell specific perfusion rate (CSPR). The CSPR is defined as the volume of medium renewed per cell per day. The main idea is that if a suitable CSPR can be defined for a moderate cell density, the same CSPR should be applied for higher cell densities, assuming that the cell activity doesn't change with time and cell density [16]. Moreover, the proper choice of the bleed rate is of central importance in a perfusion system. The bleeding is performed to remove death cells and by-product. However simultaneous removal of viable cells, results in a decrease in viable cell density. Dalm et al. [17] studied the effect of the perfusion and bleed rate on different parameters such as the cell density, the viability, glucose and lactate. They reported that with low feed and bleed rates the viable cell density is a function of the feed rate, meaning that depletion in nutrients is determining the maximum cell density. For example fixing the bleed rate to 0.05 day⁻¹, 42 * 10⁶ cell/ml were measured with a feed rate of 1 day⁻¹ and 22 * 10⁶ cell/ml with a feed rate of 0.5 day⁻¹. Instead, considering high feed and high bleed rates the viable cell density is independent of the feed rate, decreasing with higher bleed rates.

1.2.2 Cell retention device

As mentioned above, cell retention devices are employed in perfusion cultures to concentrate the cells inside the bioreactor, allowing the perfusion operation. Therefore the ideal system should be able to retain 100% of viable cells, in order to achieve high cell density, and at the same time permitting the passage of cell debris and of nonviable cells. In the best case no effect on cellular growth and viability is present. Moreover, ensuring the device functionality throughout the entire culture process it is essential to avoid contamination that could occur during the replacement of the device [9]. There are several cell retention devices available which are based on two separation principles, using either difference in particle sizes or densities. The absence of a physical barrier is the main advantage of devices that utilize the difference in density between cells and culture medium, as the risk of clotting is avoided, prolonging the culture runtime. However, given the small difference in density between cells and medium, sedimentation is very slow, limiting the maximum harvest flow rate and making a complete retention difficult. A low flow rate is undesirable since it increases the time that cells spend outside the bioreactor in unfavourable conditions [16]. Sedimentation devices include gravity settlers, centrifuges and acoustic settlers. In a vertical gravity settler, the cells sediment in a vertical settling chamber. The cell free liquid is taken out from the device while the settled cells are returned to the bioreactor. In order to have an efficient separation, the liquid velocity should be lower than the settling velocity of the viable cells [16]. Inclined settlers have been used to increase the efficiency of the separation. The suspension is forced to flow up between a pair of inclined plates. The cells settle between the two plates and return back to the bioreactor while the harvest is taken out. The distance between the inclined plates is small and so dead cells and debris do not settle. The retention efficiency of the viable cells is greater 99%. Moreover, the reduced time of the vertical sedimentation allows using higher perfusion rates [16]. Alternatively, the velocity of sedimentation can be increased by applying a centrifugal force. The use of continuous cell centrifuges permits the total retention of cells. But the effect of shear stress on cell viability is still not clear, as the cells are compressed in a pallet, lacking nutrients and oxygen [16]. The settling velocity can also be augmented increasing the particles diameter. The ultrasonic cell retention device uses the aggregation of cells in a standing wave, occurring due to the difference in density and compressibility between cells and medium. Once the standing wave is removed, the

aggregates quickly sediment and can be separated from the supernatant. This device is not susceptible to fouling, as there is no physical barrier, and no effect on cell viability has been reported [3].

The retention devices based on filtration are employing a physical barrier that allows the separation of cells with respect to size. They can be mounted either inside or outside of the bioreactor. Main problem is the fouling and final clogging of the filter, occurring during the culture. Moreover the retention of high molecular weight products inside the bioreactor is possible [3]. The first cell retention devices based on filtration have been spin filters. They are built of a cylindrical membrane or stainless steel mesh with defined pore size and are attached to the impeller of the bioreactor. The harvest passes through the filter and is pumped out, while the cells are retained in the bioreactor. Since the device is inside the bioreactor, it is not possible to replace it during the culture, limiting the runtime to the degree of fouling which is mainly a function of pore size, membrane material and rotation speed. Large pores can prolong the life of the filter but at the same time decrease the retention efficiency [16]. The main concern of internal spin filters, lacking the ability to replace it, is bypassed using external filters. In particular, cross flow filters, in which the suspension is forced to flow tangentially to the membrane, are considered most suitable. The induced shear stress limits the deposition of material on the surface prolonging the lifetime of the device [9]. Cross-flow filtration is performed using hollow fiber modules, cylindrical cartridges constituted by multiple cylindrical porous fibers in which the suspension flows. In the tangential flow mode (TFF) the cartridge is connected to the bioreactor by two ports. At the inlet or outlet of the hollow fiber usually a peristaltic or centrifugal pump is connected allowing the flow of the concentrated stream back to the bioreactor. The trans-membrane pressure, created by a peristaltic pump on the permeate side, permits the flow through the porous of the membrane and the consequent harvest of the supernatant (Figure 9). The trans-membrane pressure gradient at the inlet is higher than the one at the outlet of the hollow fiber, resulting in a non-uniform permeate flux across the hollow fiber [3].

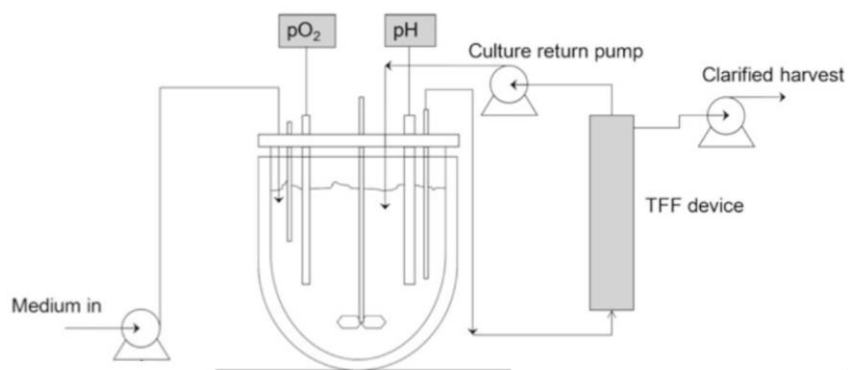


Figure 9 - Schematic representation of a perfused bioreactor equipped with a tangential flow hollow fiber. A pump returns the concentrated stream to the reactor and one creates a trans-membrane pressure that allows the removal of supernatant from the hollow fiber.

Several parameters, such as membrane material, pore size, number of fiber, surface area and flow rate have to be optimized in order to maximize the lifetime of the filter and at the same time obtain a healthy culture. The pores usually have a diameter between 0.2 and 0.65 μm , to efficiently retain the cells of approximately 10 μm . Although small pores are more prone to clogging the retention efficiency of big pores decreases significantly (i.e. lower than 70% with a diameter of 60 μm) [16]. In order to reduce the accumulation of debris and cells on the surface of the filter, a high linear velocity in the fiber is desired, but it is bound by the related shear stress damaging the cells [16]. Even if the tangential flow can limit the deposition of materials on the membrane surface, the fouling of the pores remains the main problem.

Recently a novel retention system, called Alternating Tangential Flow (ATF) system has become available. The ATF is composed of an external hollow fiber module connected to the bioreactor by a single port. A diaphragm pump alternately pumps the cell suspension in the hollow fiber and back to the bioreactor (Figure 10). The pump is made of a silicone membrane cyclically deflated by a vacuum pump and inflated by compressed air. Therefore a positive or negative pressure gradient across the hollow fiber is created [4].

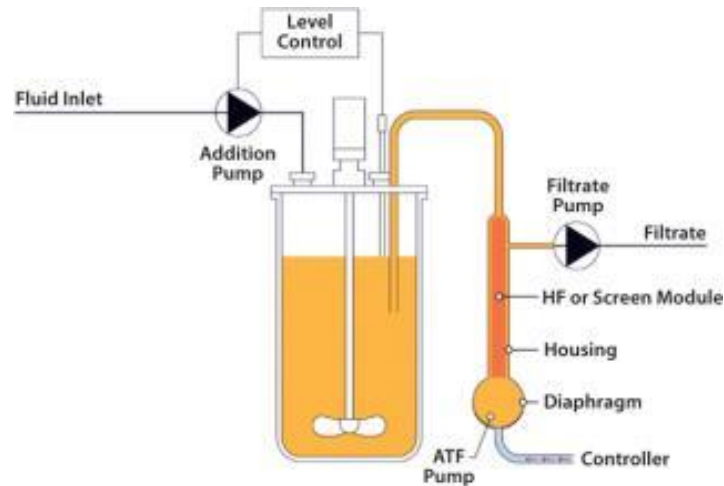


Figure 10 - Perfused bioreactor equipped with an alternative tangential filter. A diaphragm pump controlled by a vacuum creates a two ways flow inside the cartridge.

According to the vendor, the diaphragm pump is thought to induce lower shear stress compared to the generally applied peristaltic or centrifugal pumps. Moreover, the hydrodynamics of the ATF system could help to prevent the fouling of the hollow fiber. First, the periodic reversal of the flow in the device inhibits the attachment of cells and their debris on the membrane. Second, the reversal of the trans-membrane pressure during the pump cycle creates a back flush from the permeate side, cleaning the pores of the fibers [18].

1.2.3 Objectives in a perfusion culture

Considering the continuous harvest of cell free product, the direct integration with a downstream processing stream is evident. This was first shown by Warikoo et al. [18] connecting a perfusion bioreactor to a protein capture process. Keeping the final integration in mind, a robust and stable culture has to be obtained to promote a constant production with a stable product quality. However, since the volumetric productivity scales with the viable cell density, it would be desired to reach the very high cell density as fast as possible. The acceleration of the initial growth phase is of major importance, as it usually demands a significant time of the entire process. The decoupling of the growth and production phase can be obtained using a “seed” bioreactor enabling the separation and

optimization of both sections. Moreover, when the desired cell concentration is achieved in the seed bioreactor, the production bioreactor is able to start immediately from the cell density set point, suitable for the production of antibodies. From an economical point of view it would be desired to achieve the targeted production cell density at a lowest possible perfusion rate; reducing the liquid throughput while increasing the harvest titer and therefore enhancing the productivity of the entire process. Moreover liquid handling and media costs are still major concerns in the biotech industry and even more in a laboratory environment. Although productivity might be increased compared to batch and fed-batch processes, the amount of medium needed to produce a defined amount of product in perfusion is significantly higher.

1.3 CHARACTERISATION AND OPERATING CONDITIONS OF A PERFUSION CELL CULTURE

1.3.1 Shear stress

Cell lysis causes the release of intracellular components to the culture media which can reduce cellular growth and negatively impact the product quality. Moreover, cell debris can cumulate in the hollow fiber causing retention of the product inside the bioreactor and final clogging of the pores of used cell retention system [19]. Several factors influence the integrity of cell membrane such as shear stress, the deformation of the cells into filter pores exposed to transmembrane pressure (TMP), the turbulent flow in the circulating loop as well as the pump circulating the culture broth [20]. Therefore the determination of optimal operating conditions is essential.

The effect of the shear stress, in selected filter modules including hollow fibers, on mammalian cell viability has been investigated by Maiorella et al. [20]. After 20 passes through the filter, cells are not damaged at average wall shear rates lower than 3000 s^{-1} while they are proportionally damaged at higher shear rates. The TMP must be maintained below a critical value to avoid cell lysis due to deformation of the membrane in the pores. Available data for erythrocytes, being characterized by a more fragile inner structure

compared to other cell types allows the indication of a critical TMP threshold (Figure 11). For instance, at a shear rate of 2000 s^{-1} and with a pore diameter of $0.2 \text{ }\mu\text{m}$, the TMP should be lower than 1.24 bar to prevent cells from damage.

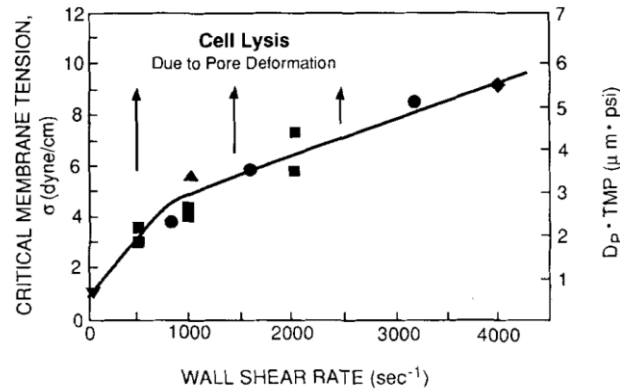


Figure 11- Cell lysis due to the deformation into the membrane pores of diameter D_p induced by the transmembrane pressure (TMP) [20].

Blaschczok et al. [21] investigated the mechanical stress caused to CHO (Chinese hamster ovary) by three centrifugal pumps from Levitronix which differ in pump head geometry and scale. The correlation between the viability and the rotation speed of the pumps showed that the higher the pump speeds are, the higher the cell death is. A further CFD analysis showed that the turbulence inside the pump increases with the speed of the pump.

1.3.2 Fouling

The fouling of the hollow fiber could cause clogging of the hollow fibers and results in retention of the product inside the bioreactor. There are three different ways of fouling, namely, complete blockage of the pores by cells or aggregates of feed molecules, pore constriction and cake formation due to the build-up of a biological matrix on the outer membrane surface [22]. Fouling increases the total resistance by decreasing the available pore area, due to pore blockage, or by thin layer formation on the membrane surface building a filter cake. As consequence, keeping constant the perfusion rate, the transmembrane pressure difference increases leading to a final interruption of the permeate flow.

Keely and Scully [22] investigated the impact of key parameters, such as cell density, viability, flow rate and antifoam, on the fouling rate of an ATF cartridge. When the transmembrane pressure exceeded 1 bar the permeate flow, pulled from the hollow fiber cartridge by a peristaltic pump, could not be maintained at the desired flow rate. The authors claimed this value of pressure as threshold indicating fouling. Moreover it was observed that the fouling rate is influenced by the cell density since it took approximately 320 minutes with a cell density of $37 * 10^6$ cells/ml while 430 minutes with $28 * 10^6$ cells/ml to have a reduction of 17% of the permeate flow. The SEM analysis showed that most of the hollow fiber inner surface was covered with a cake layer. Repeating the experiment with cell free culture medium no fouling was observed while the addition of antifoam created micelles that deposit on the inner membrane. So, in general the fouling of the hollow fiber can be accounted to both cell deposition as well as antifoam [22].

Stressman and Moresoli [23] investigated the effect of pore size, shear rate and harvest time on the fouling of a TFF cartridge. The highest fouling was observed for the smallest pore size (0.2 μm) at the higher shear rate (8000 1/s). A higher initial fouling was detected with the highest shear stress, suggesting that a faster transport of the feed components increases the interaction between the components themselves and the membrane [23]. In the article two types of resistance have been distinguished, a reversible as well as an irreversible fouling resistance. The reversible fouling being easily removed by flushing with water is in contrast to the irreversible fouling, which can only be cleaned using chemicals. The experiments showed that the reverse fouling resistance is influenced by the shear stress while the irreversible fouling resistance is affected by the pore size. However, the membrane fouling is found to be independent of the harvest rate.

1.3.3 Mass transfer

Oxygen is a key nutrient in cellular metabolism. Low concentrations of oxygen impact the growth rate and productivity while high concentrations of oxygen can be cytotoxic. The requirement of oxygen depends on the cell line type but the typical oxygen uptake rate is between $3 * 10^{-10}$ and $2 * 10^{-10}$ mg/cell*h [16]. So, the oxygen transfer is of primary consideration during the built up of a cell culture process. The oxygen transfer rate (OTR) can be calculated as given in the following equation (1):

$$OTR = \frac{dC}{dt} = k_L a (C_L^* - C_L) \quad (1)$$

where $k_L a$ is the oxygen mass transfer coefficient and $(C_L^* - C_L)$ represents the driving force. C_L^* is the oxygen saturation in liquid phase, depending on the partial pressure of oxygen in the inlet, while C_L is the actual measured oxygen concentration in liquid phase [24]. The OTR can be varied both increasing the driving force or the $k_L a$. Since during the process even CO_2 should be sparged to control the pH, usually the OTR is increased by the $k_L a$. Ozbek et al. [25] investigated the relation between the oxygen mass transfer coefficient and several process parameters such as the impeller speed, the gas flow rate, the temperature, the viscosity and the percentage of particles. It was observed that increasing both the rotational speed of the impeller and the gas flow rate results in an increase of $k_L a$ while the viscosity and the presence of biomass particles have a negative impact on the oxygen transfer. In particular a $k_L a$ value equal to 2.76 1/min was obtained at 37 °C in distilled water using an impeller speed 300 rpm and air flow rate 0.3 l/min while adding 50 % of glycerol and 50% of biomass particles the $k_L a$ was equal to 0.450 1/min.

CO_2 is another key parameter in cell culture as it has been shown that high CO_2 levels can be cytotoxic to the cells and influence the product quality [13]. Due to the lower mass transfer coefficient of CO_2 , compared to the oxygen, generally CO_2 can accumulate in the reactor reaching, especially with high cell density. The main parameter to counteract the accumulation of CO_2 is an increase in volumetric gas flow rate. Moreover a headspace aeration should be maintained [16].

1.4 COMPARISON ATF AND TFF

In 2013 Clincke et al. [26] [27] developed a perfusion process for the production of antibodies with CHO cells, using a WAVE BioreactorTM equipped with two different cell retention devices, the classical TFF and the commercial ATF. The process parameters of dissolved oxygen concentration (DO), pH, temperature, and working volume were 35%, 7.0, 37 ° C, and 4 l. The aeration rate was manually tuned between 0.025 and 0.15 vvm. A

constant cell density of 25×10^6 cells/ml was achieved for 10 days using an adaptive bleeding strategy at a perfusion rate of 1.5 RV/day in both setups (Figure 12).

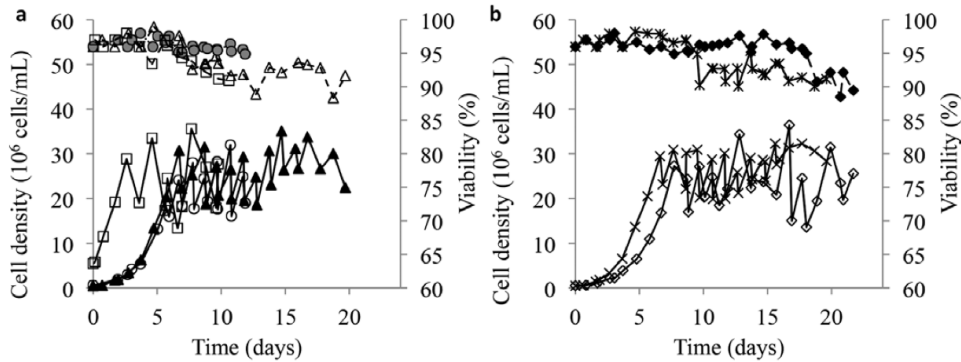


Figure 12 - Cell density and viability, as a function of time, in the ATF system (left) and in the TFF (right) [26].

A maximum viable cell density of 1.32×10^8 cells/ml in the ATF at 6 RV/day adjusting the CSPR was accomplished. At this density the flow in the hollow fiber interrupted resulting from the high viscosity leading to a failure of diaphragm pump. Instead, in the TFF a cell density of 2.14×10^8 cells/ml was reached with a perfusion of 10 RV/day, before the cells stopped growing because of the high level of pCO_2 (232 mmHg). The cell metabolism was independent of the system used. However a decrease of the q_{gln} , q_{lac} and q_{amm} with the increasing cell densities was observed, meaning that metabolism restricted growth is associated with larger cell densities. So, according to this study, the TFF should be favourable for reaching higher cell densities and even more robust against the presence of bubbles. Indeed, in the ATF system the agitation had to be limited in order to avoid the accumulation of bubbles in the tubing, preventing the application of higher agitation speeds to remove the CO_2 and to control the oxygenation. In both setups protein product retention was observed in the hollow fiber module. The production yield, ratio between the accumulated harvested product and the accumulated reactor product, was between 46-56% in the TFF and 54-71% in the ATF. [26].

1.5 AIM OF THE PROJECT

The aim of the project is the characterization and comparison of two perfusion bioreactor setups with different tangential flow filtration devices. The first system is equipped with a tangential flow filtration hollow fiber driven by a centrifugal pump and the second employs the commercially available Alternating Tangential Flow (ATF) technology. Subsequent to a thorough characterization with respect to mass transfer and shear stress, their effects on cell performance will be identified. Moreover the study focuses on the determination of interactions between other key process parameters such as perfusion, harvest and bleed rate, media composition, shear stress, pH and CO₂ concentration.

CHAPTER 2

MATERIALS AND METHODS

2.1 PERFUSION BIOREACTOR DESIGN

2.1.1 Bioreactor

Two equivalent reactor setups were designed for the comparison of the two retention devices, namely ATF and TFF. The design was based on a 3L DASGIP parallel bioreactor system (DASGIP Technology, Eppendorf, Switzerland) equipped with a glass vessel of 26 cm in height and 13 cm in diameter. Two types of hollow fiber filter modules (MiniKros[®] Filter Modules, SpectrumLabs, USA) were used in this study, with similar physical properties relating filtration area, membrane pore size and material. The original hollow fiber supplied in addition to the ATF device, here referred to as the “long HF”, as well as one shorter in length but with increased number of fibers, called “short HF”. Their main characteristics are reported in the table 1.

Table 1 - Main characteristics of the “short” and “long” hollow fiber.

Hollow Fiber Type	Length	Area	Pore Size	Ø Fiber	Number fibers	Material
Short	25 cm	1570 cm ²	0.5 µm	1 mm	276	PES
Long	60 cm	1300 cm ²	0.5 µm	1 mm	76	PES

Depending on the type of hollow fiber, customized conical connectors were used for the linkage to the respective pump. The ATF device (Refine Technology, USA), consisting of a diaphragm pump and a hollow fiber, connected to the reactor by a silicone tubing (ID 8 mm x OD 12 mm) and a metal dip tube (ID = 12 mm) as visualized in figure 13. The diaphragm pump, characterized by a constant displacement volume of 84.4 ml was

controlled by a C-24 Controller (Refine Technology, USA). The silicone membrane was cyclically inflated by compressed air and evacuated by the attached vacuum to create a positive or negative pressure, allowing the flow in both directions. Given the constant displacement volume, the flow rate in the external loop is controlled by the duration of the exhausting and filling cycle.

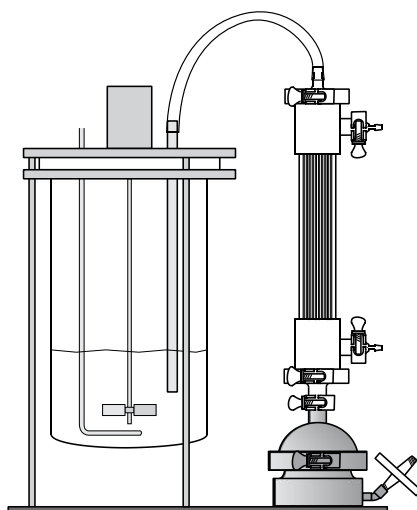


Figure 13 - Sketch of the ATF setup, equipped with the “short” hollow fiber connected to a diaphragm pump that creates an alternating flow in the cartridge.

In the TFF setup, the retention device was connected to the reactor using two ports, enabling a circular flow. Therefore an outlet with an M12 thread was created, modifying the bottom part of the glass vessel. A bearingless centrifugal pump (PuraLev-200, Levitronix, Switzerland) was connected to the reactor using a silicone tubing (ID = 10 mm, OD = 12 mm) or a flexible tubing ADCF C-Flex® 374 (ID= 9.6 mm, OD=1.4) (Integra Companies, USA) allowing the attachment of a flow sensor (LEVIFLOW® LFSC-12, Switzerland). The hollow fiber was vertically mounted on the pump by an adapter. The outlet of the hollow fiber was attached to the reactor with a silicone tubing (ID = 8 mm, OD = 12 mm) (Figure 14).

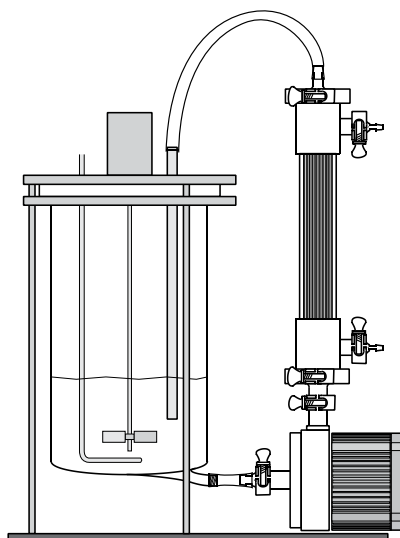


Figure 14 - Sketch of the TTF setup equipped with the “short” hollow fiber connected to a bearingless centrifugal pump creating a one-way flow in the cartridge.

In both setups the supernatant was withdrawn at the upper exit of the hollow fiber using a silicone tubing (ID = 2 mm * OD = 4 mm) while the lower exit was kept close. The stirring was performed with a 6 blade Rushton turbine impeller (OD= 46 mm * ID = 8 mm) pumping the fluid in radial direction. An open pipe sparger, with five wholes of 1 mm size, provided dispersed gas bubbles. Evaporation during the cell culture was minimized using an off-gas condenser.

2.2 CHARACTERISATION

2.2.1 External loop flow rate

In the ATF setup the flow rate in the external loop is controlled by the duration of the exhausting and filling cycle. The diaphragm pump used allows reaching flow rates between 0.2 l/min and 1.5 l/min. In the TFF setup the flow rate cannot be controlled directly by the system but depends on the rotational speed of the pump. A relation between the rpm of the bearingless centrifugal pump and the flow rate was obtained using a Leviflow LSFC-12 flow sensor (Levitronix AG, Switzerland). The sensor is composed by

two piezoelectric transducers that generate and receive an ultrasonic wave. The sensor, clamped on the inlet of the pump, previously connected to the bioreactor with the ADCF C-Flex® 374 tubing, measures the flow rate. The flow rate in the external loop of the TFF setup was measured with both the “short” and the “long” hollow fiber as well as using a silicone tubing (ID = 8 mm, OD = 12 mm) in place of the hollow fiber. The rotational speed of the pump was gradually increased from 500 to 3000 rpm (Table 2). The measurement was repeated three times for each condition.

Table 2 - Rotational speeds of the bearingless centrifugal pump used to study the flow rate with no hollow fiber and with both the “short” as well as the “long”.

Hollow fiber type	RPM					
no HF	50	1100	1500	2000	2500	3000
“short” HF	50	1100	1500	2000	2500	3000
“long” HF	50	1100	1500	2000	2500	3000

2.2.2 Shear stress

The maximum shear stress in both bioreactor setups was determined using a characterisation method based on the aggregation and break up properties of polymethyl methacrylate (PMMA) particles [28]. Initial PMMA aggregates were prepared adding 150 g of PMMA nanoparticles and 0.2 mol/l of sodium chloride (Merck Millipore, USA) to 1.35 l of deionized water in a 2 l beaker. The solution was gently stirred at 50 rpm for 14 h until a steady aggregate size was reached. Then, 25 ml of the suspension were added to the bioreactor, previously filled with 1.5 l of deionized water, 0.5 g/l of Pluronic F-68 (AppliChem PanReac, Germany) and 3 g/l of sodium bicarbonate (Merck Millipore, Switzerland). The dilution of the salt concentration (1M) prohibited further aggregation and assured that breakage is the only mechanism controlling the aggregate size. Villiger et al. [28] showed that the resulting steady state aggregate size depends on the maximum value of the shear stress presents in the system. For analysis, 25 ml of aggregates suspension was gently withdrawn from the bioreactor and the cluster size was measured

by small angle light scattering (SALS) using a Mastersizer 2000 (Malvern Instruments, UK). The cluster size distribution of the aggregates is determined by the angle-dependent intensity of the scattered light. The intensity of scattered light, $I(q)$, under diluted conditions can be expressed as following (2):

$$I(q) = I(0)P(q)S(q) \quad (2)$$

where $I(0)$ denotes the zero-angle intensity, $P(q)$ is the form factor of primary particles and $S(q)$ is the structure factor due to the arrangement of primary particles within the aggregates. The magnitude of the scattering wave vector (q) is evaluated as in equation (3):

$$q = 4\pi \frac{n}{\lambda} \sin(\theta/2) \quad (3)$$

with θ being the scattering angle, n being the refractive index of the dispersing fluid and λ representing the laser wavelength in vacuum. $S(q)$ can be used to evaluate the root-mean-square radius of gyration of the formed aggregates, $\langle R_g^2 \rangle$, according to equation (4):

$$\ln\left(\frac{I(q)}{P(q)I(0)}\right) = \ln(S(q)) = -\frac{q^2}{3} \langle R_g^2 \rangle_{S(q)} \quad (4)$$

In order to characterize the maximum shear stress Villiger et al. [28] first broke the aggregates by a well-defined elongational flow generated in contracting nozzles. In this way, the dependency of the steady aggregates size as a function of known stress was

determined. So, once the size of aggregates in the reactor was measured applying SALS, the maximum shear stress was estimated using the calibration curve.

The different conditions investigated are reported in table 3. Each setup was run for 1 hour assuring steady state aggregate size. If not indicated differently, homogenization within the reactor was achieved applying gentle stirring at 30 rpm. In the first part of the experiment, the shear stress induced only by the centrifugal or the diaphragm pump, was investigated. Therefore in the external loop no hollow fiber module was mounted. In the TFF setup the rotational speed was varied between 1100 rpm and 3000 rpm, whereas the flow rate of the diaphragm pump was changed from 1.0 to 1.5 l/min. Subsequently, the same conditions were applied either attaching the short or long hollow fiber. A batch reactor of similar setting served as reference, changing the stirring speed between 30 and 500 rpm, to investigate the multiphase effect when applying a volumetric gas flow rate of 20 l/h (i.e. 0.22 vvm).

Table 3 - Conditions investigated during the analysis of the maximum shear stress in a reference batch setup and in both TFF and ATF setups without as well as with “short” and “long” hollow fiber.

BATCH		BATCH		TFF NO HF/SHORT HF/LONG HF			ATF NO HF/SHORT HF/LONG HF		
RPM	Gas flow rate [l/min]	RPM	Gas flow rate [l/min]	RPM	Gas flow rate [l/min]	PUMP	RPM	Gas flow rate [l/min]	PUMP
30	0	30	20	110	0	1100	110	0	0.5
170	0	170	20	110	0	1500	110	0	1
250	0	250	20	110	0	2000	110	0	1.5
350	0	350	20	110	0	3000			
500	0								

2.2.3 $k_L a$ measurement

Both reactor setups were filled with 1.5 l of production medium and heated up to 36.5 °C, A stirring speed of 400 rpm was combined with a constant volumetric gas flow rate of 20

l/h. The volumetric mass transfer coefficient for oxygen was measured in the ATF and the TFF system at a circulation flow rate of 1.5 l/min, as well as without the external loop. The $k_{L}a$ measurement was performed applying the dynamic method [24]. Therefore the liquid phase was first purged with pure nitrogen to zero the DO. Subsequently, the gas fraction was switched supplying pure air and the rate of increase of the DO was observed (Figure 15).

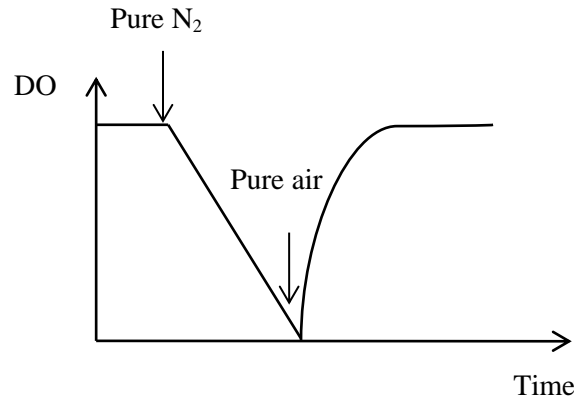


Figure 15 - Sketch of the experimental $k_{L}a$ determination. N_2 is first purged to zero the DO, followed by the subsequent supply of pure air. The change of oxygen concentration is monitored over time.

The mass balance for oxygen in the liquid phase can be expressed using following equation (5):

$$\frac{dC}{dt} = k_L a (C_L^* - C_L) \quad (5)$$

where $k_L a$ is the volumetric mass transfer coefficient and $(C_L^* - C_L)$ the driving force. C_L^* denotes the oxygen saturation concentration in the liquid phase, while C_L represents the oxygen concentration in the liquid phase at any time. After integration and applying the natural logarithm results in equation (6):

$$\ln \left(\frac{C_L^* - C_L^0}{C_L^* - C_L} \right) = k_L a (t_2 - t_1) \quad (6)$$

where C_L^0 is the concentration at t_0 and C_L^* the saturation concentration. Hence, the $k_L a$ can be expressed as the slope of the logarithmic term in the time interval between t_1 and t_2 .

2.3 CELL CULTURE

2.3.1 Cell line

Chinese Hamster Ovary (CHO) cells producing a monoclonal antibody (IgG1) were used in subsequently described experiments. The cell line was kindly provided by an industrial partner.

2.3.2 Medium and feed

The chemically defined and animal component free culture media was prepared from basic powder mixtures provided by the industry partner. Three media compositions can be differentiated depending on the cell culture stage: the expansion medium, used for the cell expansion, the production medium, used during the cell culture, and the feed medium, a high concentrated version of the production medium. After the preparation, the feeds and the media were filtered with Sartobran 300 Sterile Capsule filters (Sartorius AG, Germany) in 50 l sterile bags (HyClone BioProcess ContainerTM, Thermo Fisher, U.S.) and stored in a fridge at a temperature of 4°C. The pH of the media was adjusted to 7.1 – 7.2 using 1M sodium hydroxide (NaOH, Fisher Chemical, Switzerland). Depending on the experiment, supplements were added to the feed media to avoid depletion or to effect product quality.

2.3.3 Expansion

CHO cells, stored in liquid nitrogen at a concentration of 5×10^6 cells/ml (media + DMSO (7.5%)), were thawed in a waterbath at 37°C and suspended in 19 ml of chemical defined and animal component free expansion medium (MS-CHO-M01). Cell density was measured and the residual volume was centrifuged at 300 rpm for 3 minutes in order to remove the freezing mixture. The supernatant was discarded and the cells were resuspended in fresh expansion media at an initial cell density of 0.3×10^6 cells/ml using a 50 ml spin tube (TPP, Switzerland). The CHO cells were kept in a shaking incubator, applying a rotational speed of 320 rpm, at 36.5 °C, 90% humidity and 5% pCO₂. On day three cells were diluted in fresh expansion medium to a final cell density of 0.3×10^6 cells/ml. Subsequently, the dilution step was repeated every two days until inoculation of the bioreactor or of the spin tubes. Upon increase of the cell culture volume above 100 ml, cells were transferred to roller bottles reducing the rotational speed of the shaking incubator to 120 rpm. A scheme of the expansion procedure is showed below (Figure 16).

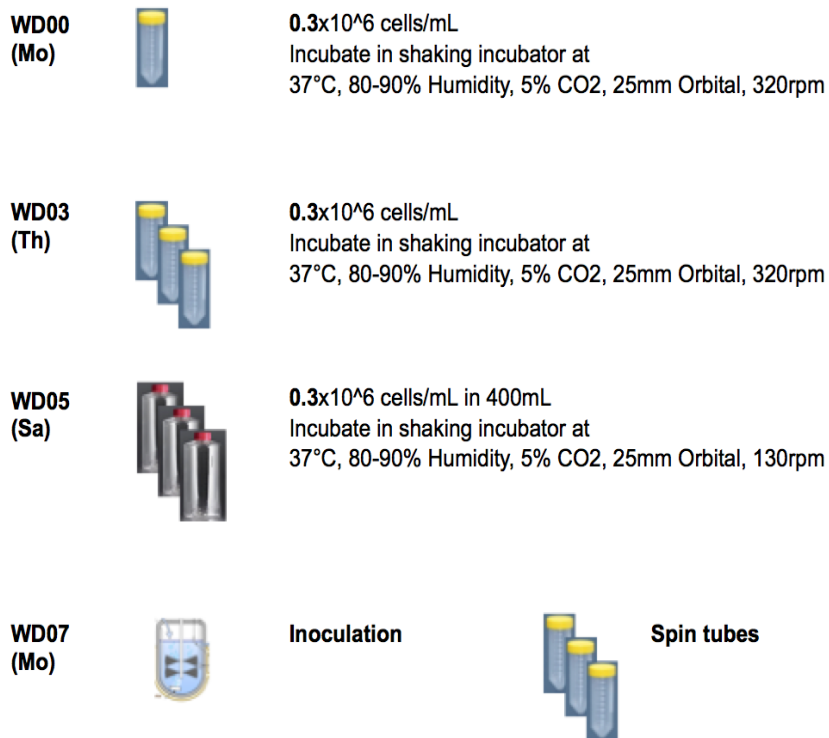


Figure 16 - Expansion procedure from thawing (WD00) to inoculation (WD07). The containers in which cells were suspended and the respective cell densities and incubator settings are reported.

2.4 SPIN TUBE EXPERIMENTS

Prior to the bioreactor runs, spin tubes experiments were conducted. The aim of these preliminary experiments was to understand the effect of the bleed rate on the perfusion culture, aiming to achieve a constant cell density profile. Moreover different media compositions were tested to guarantee the supply of required nutrition, depending on the cell density. For this purpose two types of spin tube experiments were performed. The experiments were carried out in 50 ml Tube Spin Bioreactors (TPP, Switzerland) in a shaking incubator at 320 rpm 37°C, 5% CO₂ and 90% humidity.

2.4.1 Setting a constant harvest/bleed ratio

In a first experiment, five different ratios of harvest and bleed at a constant perfusion rate of 1 RV/day were investigated for 14 days. The experimental design is listed in the following table 4:

Table 4 - Fraction of the perfusion, harvest and bleeding used in the 6 spin tubes.

	PERFUSION [RV/day]	HARVEST [RV/day]	BLEEDING [RV/day]
ST1 (BATCH)	1	0	0
ST2	1	0,95	0,05
ST3	1	0,9	0,1
ST4	1	0,75	0,25
ST5	1	0,5	0,5

The spin tubes were inoculated at an initial cell density of $0.3 * 10^6$ cells/ml in base media with a final working volume of 30 ml. The perfusion was initiated after 3 days of batch culture. A perfusion rate of 1 RV/day was achieved by exchanging the spin tube volume once a day with fresh medium after spinning down the cells. The bleeding was performed by removing different volumes of cell suspension prior to centrifugation depending on the harvest to bleed ratio (ST1 = 0 ml, ST2 = 1.4 ml, ST3 = 2.8 ml, ST4 = 7 ml and ST5 = 14

ml). Centrifugation was performed at 100 rpm for 3 minutes and extended to one more minute in case not all cells settled. Cell density was measured twice a day and 1 ml supernatant was removed and sterile filtered (Spartan 13/0.2 RC, WhatmanTM, Chromatographic Specialties Inc., Canada) in an Eppendorf tube to be stored at -20 °C for later titer analysis. A schematic of the experimental procedure is shown in figure 17.

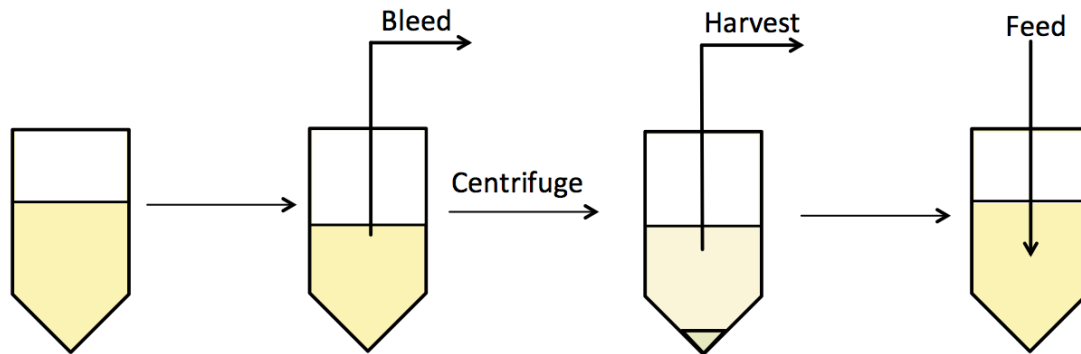


Figure 17 - Sketch of the experimental procedure: subsequently to the bleeding, the cells are spun down and the supernatant is removed (harvest). Finally the cells are resuspended in fresh media (feed).

2.4.2 Different cell densities and percentage of feed

The aim of the second spin tube experiment was to achieve different constant cell density set points and to determine which medium composition was required. A Design of Experiment (DoE) with two parameters was performed. The two parameters controlled were the cell density (30, 50 and 70 * 10⁶ cells/ml) on one hand and the percentage of feed added to the base medium (5, 15 and 25% feed) on the other hand. Six conditions were investigated in the DoE, namely the four points at the vertexes (30 * 10⁶ cells/ml – 5%, 30 * 10⁶ cells/ml – 25%, 70 * 10⁶ cells/ml – 5%, 70 * 10⁶ cells/ml – 25%), the central point (50 * 10⁶ cells/ml – 15%) as well as one additional point at the base in order to have two spin tubes for each cell density considered (50 * 10⁶ cells/ml – 5%) (Figure 18).

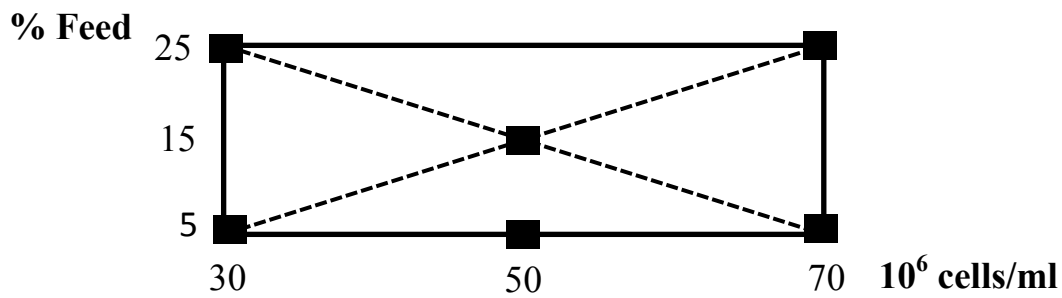


Figure 18 - DoE of viable cell density and feed fraction in the base medium. Six conditions were investigated: 30×10^6 cells/ml – 5%, 30×10^6 cells/ml – 25%, 70×10^6 cells/ml – 5%, 70×10^6 cells/ml – 25%, 50×10^6 cells/ml – 5% and 50×10^6 cells/ml – 15%.

The spin tubes were inoculated with an initial cell concentration which was 5×10^6 cells/ml lower than the desired set point (25, 45 and 65×10^6 cells/ml) using 30 ml of medium. In order to obtain a constant cell density an adaptive bleeding was performed. Meaning, based on the standard VCD measurement, the respective volume of cell suspension was removed resulting in concentrations of 25, 45 or 65×10^6 cells/ml (Figure 19).

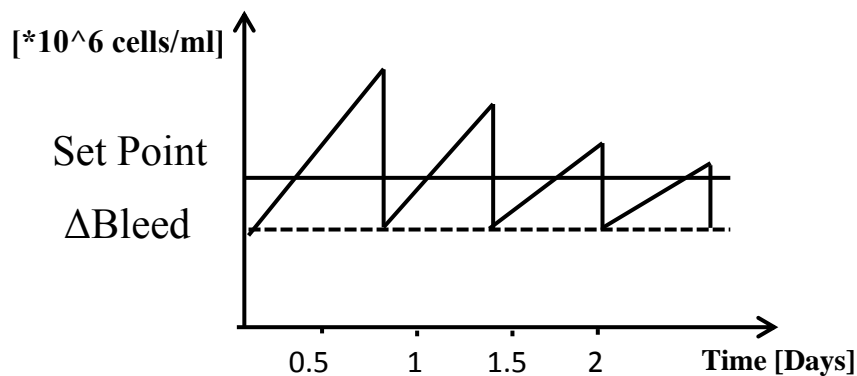


Figure 19 - Sketch representing the adaptive bleeding strategy. Twice a day, the viable cell density was measured and the respective amount of cell suspension to bleed 5×10^6 cells/ml below the set point was withdrawn.

Similar to the first experiment, the perfusion rate was kept constant at 1 RV/ day by exchanging half of the medium twice a day. The cell free harvest was discarded subsequent

to the bleeding step and the centrifugation at 300 rpm for 3 min. Adding bleed and harvest, a total volume of 15 ml was extracted.

2.5 BIOREACTOR RUNS

2.5.1 Bioreactor preparation

A precise procedure was followed for the setting up of the reactors. Following an exemplary schedule of a standard bioreactor preparation procedure.

- Wednesday: built up of the bioreactor
- Thursday:
 - Two point calibration of the pH probe using two buffer solutions with a pH of 7.0 and 4.01 (Technical buffer solution, Mettler Toledo, Switzerland)
 - Reactor sterilization (45 minutes of sterilisation at a temperature of 121 °C)
 - Calibration of the peristaltic pumps for harvest, feed and bleed with silicone tubing (ID = 2mm, L = 4m) using a flow rate of 62 ml/h, except for the bleed pump, being calibrated with a flow rate of 15,6 ml/h
 - Overnight polarization of the DO-probe
- Friday:
 - One point calibration of the DO-probe using a flow rate of 5 l/h, with a gas composition of 21% O₂ and 0% CO₂
 - Media filling (1 l)
- Monday:
 - CO₂-probe calibration performed with a flow rate of 20 l/h, using a gas composition of 21% O₂ and 10% CO₂
 - Setting of process parameters (T=36.5 °C, agitation speed=400 rpm, gas flow rate=20 l/h, external loop flow rate = 1.5 l/min)
 - Cell seeding
 - Media filling to final working volume (1.5 l)
 - Connection of harvest and bleed.

- Start of perfusion
- Connection antifoam bottle

2.5.2 Seed reactor

A seed bioreactor was used to inoculate the production bioreactors, equipped with ATF or TFF, to start the culture directly from the stationary phase decoupling the production from the growth phase. After one week of expansion, cells were seeded to a Labfors (Infors HT, Switzerland) 3.5 l double jacketed glass bioreactor equipped with an external loop employing a hollow fiber in tangential flow mode driven by a bearingless centrifugal pump (BPS-200, Levitronix, Switzerland). The hollow fiber (SN 3273918-08/14-003, MiniKros[®] Filter Modules, SpectrumLabs, USA) used for cell retention was 25 cm in length, had an area of 1570 mm² and a porous diameter of 0.5 μm. The bioreactor was inoculated from roller bottles at an initial cell density of roughly 0.5×10^6 cells/ml with resulting working volume of 2 l. The temperature of the bioreactor was set to 36.5 °C, controlling the temperature of the water in the jacketed glass. An elephant ear impeller (ID 7 mm) allowed good mixing at a stirring speed of 250 rpm. A gas flow rate of 0.33 l/min was applied to maintain a DO set point of 50%, controlling the fractional composition of O₂, air and N₂. The pH was kept constant at 7.10 by pulsed sparging of CO₂. The flow rate in the external loop was set to 1.5 l/min. Based on previous calibration a consistent rotational speed of 1500 rpm in the centrifugal pump was employed, while in later runs it was adjusted during the culture according to the clamp-on flow sensor measurement (Leviflow LSFC-12.S, Switzerland) attached to the outlet of the pump. While the bleed removal as well as feed and anti-foam addition were performed using peristaltic on/off controlled pumps mounted on the bioreactor system, the harvest flow rate was set by an external peristaltic pump (BPS-200 LPP-200.1) from Levitronix (Zurich, Switzerland). Daily checks of the harvest flow rate were carried out, weighting the attached 5 l harvest bottle. The feed rate was feedback-controlled by the bioreactor weight, since the entire system was placed on a balance. Using a simple if-condition the feed pump was initiated as soon as the weight of the reactor fall below the set point. The bleeding was performed manually according to the respective off-line cell density measurement. 2 g/l of antifoam were added on demand once the foam level approached the top of the bioreactor. Silicon tubings of different diameter and length were used for all in and outlet streams of the bioreactor. Feed, bleed, harvest

and antifoam lines were 2 mm in diameter and approximately 4 m in length. Sterile connections to media bags as well as harvest and bleed bottles were created using a sterile tubing welder (Terumo Medical Corporation, USA). On day 7, when reaching 40×10^6 cells/ml, cells were inoculated to the production bioreactors.

2.5.3 Comparison ATF and TFF

Subsequent to the cell expansion in the seed bioreactor, cells were transferred to the production bioreactor systems. As described above, two similar perfusion culture setups, employing either ATF or TFF, were built. The reactors were equipped with a pH-sensor (05-DPAS-SC-K85 pH Probe, Mettler Toledo, Switzerland), a DO sensor (InPro 6820, Mettler Toledo, Switzerland), a CO₂-sensor (Autoclavable CO₂ sensor, PreSens Sensing GmbH, Germany) and a temperature-sensor to control the pH, DO, CO₂ and temperature. Process parameters were chosen according to previous physical characterization. Sufficient mixing was ensured fixing the rotational speed of the Rushton turbine impeller to 400 rpm. 50% of DO was sustained using a gas flow rate of 20 l/h (0.22 vvm), varying the mixture of air, O₂ and N₂. pH was controlled at 7.10, adjusting the CO₂ fraction in the inlet gas. To avoid CO₂ accumulation in the liquid phase, headspace aeration was implemented at a volumetric gas flow rate of 50 l/h using pure air, for later runs. The temperature was kept at 36.5 °C cooling or heating the reactor with the heating blanket. The flow rate in the external loop was set to 1.5 l/min, maintained by a diaphragm pump in the ATF and a bearingless centrifugal pump in the TFF setup. The diaphragm pump allowed the direct control of the flow rate, automatically adjusting the duration of the filling and exhausting cycle. Instead, in the centrifugal pump the flow rate can only be controlled changing the rotational speed of the pump. Using previous calibration, the centrifugal pump was run at 1100 rpm throughout the first culture, corresponding to 1.5 l/min. In later experiments, the rotational speed was adjusted according to flow sensor clamped on the inlet with the ADCF C-Flex® 374 tubing (ID = 9.5 mm, OD = 14.3 mm). Daily checks of the flow rate allowed the tuning of the pump rpm monitoring an offset from the set point.

The cells were cultured in a constant volume of 1.5 l at a perfusion rate of 1 RV/day. Both reactor systems were each placed on a balance (X3200L, Mettler Toledo GmbH,

Switzerland) to keep the 1.5 l working volume constant. The peristaltic pumps of the media feeds were controlled by a PID controller implemented in the DASGIP control software. The harvest rate was fixed to 1 RV/day using a pre-calibrated peristaltic pump on the permeate side of the respective “short” hollow fiber (SN 3273918-08/14-003, MiniKros® Filter Modules, SpectrumLabs, USA) (Figure 20). The flow rate was monitored on a daily basis, weighting the attached harvest bottle and if necessary adjusting the pump speed when an offset more than 2% was detected.

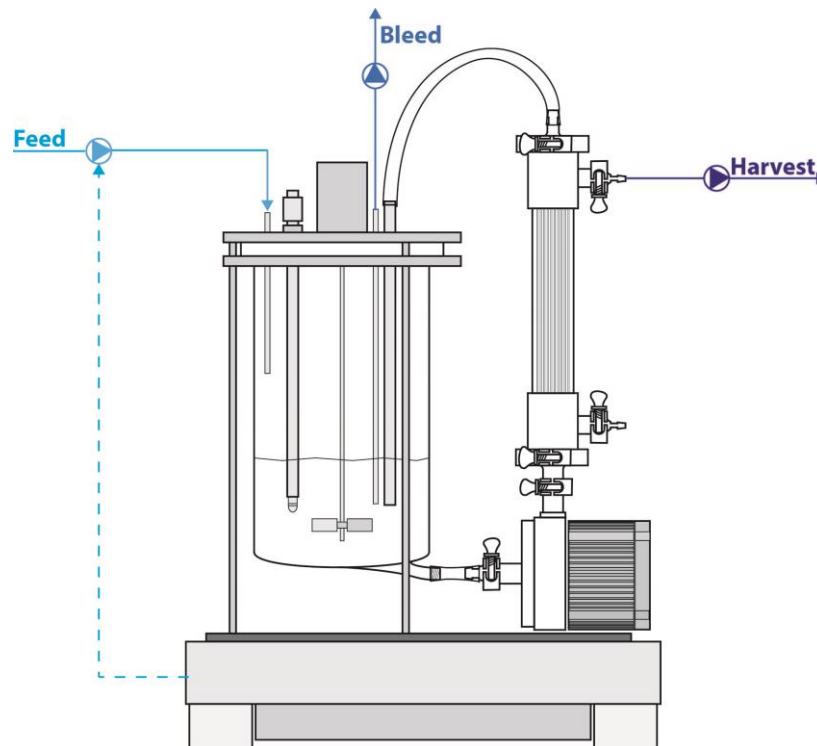


Figure 20 - Control system used in the bioreactor to keep constant the working volume. The harvest flow rate is set to 1 RV/day and the bleeding is performed manually or automatically according to the cell density.

The feed pump is controlled by the weight of the balance.

To compare the two retention systems, CHO cells were cultured at three different consecutive viable cell density set points. Starting at 20×10^6 cells/ml, cells were grown to 60×10^6 cells/ml, followed by a set point of 40×10^6 cells/ml. To reach a steady state environment, each set point was kept for one week. The different cell densities were achieved changing the media composition. Two bags, one containing the pure base medium and the other one filled with base medium but supplemented with 10% of feed

medium as well as additives, were connected to the reactor with silicone tubings (ID = 2 mm, OD = 4 mm, length = 4 m). In particular 12 g/l of glucose (D(+)-Glucose, Acros Organics, U.S.), 7.5 mM of Asparagine (L-asparagine monohydrate, AppliChem PanReac, Germany) as well as Cysteine (L-Cysteine, Merck, Switzerland) and Tyrosine (L-Tyrosine 2Na salt, Sigma, Switzerland), in an amount equal to the 0.0375 (v/v) % of the feed, were added to the feed bag to avoid depletion. Each feed line was controlled by an independent peristaltic pump allowing the change of media composition by adjusting the fraction between both bags during the cell culture according to the viable cell density. At 20×10^6 cells/ml cells were supplied with base medium only, however at 60×10^6 cells/ml a ratio of 30% base to 70% feed medium was set. Bleeding to 40×10^6 cells/ml the ratio changed to 65% base and 35% feed media (Figure 21).

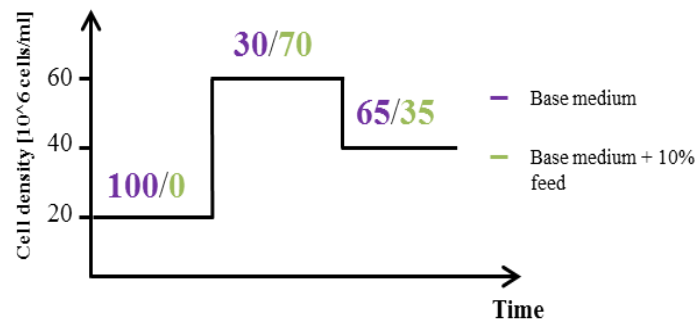


Figure 21 - Fraction of production medium (purple) and production medium supplemented with 10% of feed (green) used with 20 , 40 and 60×10^6 cells/ml.

The cell density was kept constant applying a bleeding of culture broth. In the first experiment a manual adaptive bleeding strategy was chosen. Therefore, the cell density was measured twice a day and the corresponding cell suspension volume to bleed 2×10^6 cells/ml below the current set point (18×10^6 cells/ml, 58×10^6 cells/ml and 38×10^6 cells/ml) was withdrawn from the bioreactor using a peristaltic pump. The amount of suspension to bleed was calculated applying following formula (7):

$$V_{bleed} = \frac{(X_{real} - X_{setpoint}) * V_{reactor}}{X_{real}} \quad (7)$$

with $X_{real} = \frac{(V_{reactor}-V_{sample}) * X_{measure}}{V_{reactor}}$; $X_{measure}$,cell density measured; $X_{setpoint}$, cell density set point; $V_{reactor}$, working volume; V_{sample} , sample volume.

In later experiments both reactors were equipped with an online biomass sensor (Aber Instruments Ltd, UK) based on radio frequency impedance, to achieve an automated bleed. As the capacitance is strongly related to the presence of viable cells with an intact membrane, it is a direct measure of the viable cell density in the culture. Therefore, a simple on/off control was implemented in the DASGIP control software automatically activating the peristaltic pump when the measured online VCD exceeded the set point. The online measurement was compared to the offline measurement on a daily basis and was adjusted if the two values were off more than 10^6 cells/ml. In particular, the correction consisted of changing the Biomass CPM Factor which correlates the capacitance value to the viable cell density. Every six hours, an automated cleaning pulse was applied to the biomass sensor in order to remove cells and debris attached or accumulated on the electrodes. Prior to the inoculation the biomass sensor was zeroed in fresh base media.

2.6 OFFLINE MEASUREMENTS AND ANALYTICS

In order to monitor cellular growth and productivity, as well as product quality, reactor samples were withdrawn at least once per day. Therefore, 20 ml of fresh cell suspension was collected with a syringe, after flushing the sample port from residual culture broth. The cell suspension was collected in a 50 ml falcon tube (50 ml TPP Centrifuge Tube, Switzerland) and ready for further analysis.

- **Cell count**

The cell number was determined by applying the trypan blue exclusion method using a CedeX cell counter (Roche, Switzerland). 50 μ l of the cell suspension were mixed with 50 μ l of Trypan Blue solution (10% in H₂O, Sigma Aldrich, Switzerland). Subsequent, 10 μ l of the mixture were pipetted into the measurement slide. The viable cell density was determined by the staining of the cells. While viable cells appear white under the microscope, dead cells became dark as their membrane is permeable to the trypan blue dye.

The viability was obtained by the ratio between the viable cells and the total number of cells counted. The Cedex cell counter also displays information on cell diameter, the average compactness and the aggregation rate of cells. In order to obtain a valuable measurement the total cell count should not exceed 800 cells and a maximum aggregation of 20% is recommended. Therefore depending on the cell count, the cell suspension was diluted with PBS (Gibco, Life Technology, USA) accordingly. To obtain an aggregation lower than 20%, 5x Trypsin (Trypsin-EDTA Solution (10x), Sigma-Aldrich, Switzerland) was used for dilution. The Trypsin was heated to 37 °C and mixed with the respective volume of cell suspension. After 3 minutes incubation, the mixture was thoroughly pipetted up and down in order to break the aggregates by shear.

- **Glucose and lactate**

1 ml of the cell suspension was centrifuged for 3 minutes at 300 rpm. The supernatant was removed using a 1 ml syringe and filtered (Spartan 13/0.2 RC, WhatmanTM, Chromatographic Specialties Inc., Canada). 10 µl of the filtered solution were added to 0.5 ml of the buffer solution (BSL, System Gluk/Lak/HB, Hitado, Germany). The glucose and lactate concentrations were measured using the electrochemical measuring device Hitado Super GL compact (Hitado, Germany) based on glucose and lactate oxidase. Daily calibration was performed using a standard supplied by the vendor (Glucocapil, Hitado, Germany), containing 12 mmol/l glucose and 10 mmol/l lactate.

- **Offline pH measurement**

The offline pH measurement was performed using a FE20 – FiveEasyTM pH probe (Mettler Toledo, Switzerland). 3 ml of the cell suspension in a 15 ml falcon tube were used to measure the pH immediately after the extraction from the bioreactor, to prevent CO₂ degassing. Finally, the offline value was compared to the online measurement. If an offset exceeding 0.05 was present, the calibration of the pH probe in the bioreactor was adjusted by half of the measured difference.

- **Reactor sample**

15 ml of the cell suspension were spun down for 3 minutes at 300 rpm. The supernatant was removed using a 20 ml syringe and filtered through a 0.2µm Filtropur Syringe Filter (Sarstedt, Germany) in six Eppendorf tubes which were stored at -20°C for later analysis of amino acids, glycosylation, titer and ammonia.

- **Harvest sample**

To flush the sample line, 4 ml of supernatant was extracted and discarded from the harvest bottle. Subsequently, 6 ml were withdrawn using a 20 ml syringe and divided in six Eppendorf tubes, subsequently frozen at -20° for further analysis of titer.

- **Titer**

Titer analysis was performed on an Agilent 1200 HPLC system (Agilent Technologies, USA) using a Protein A affinity column model 2-1001-00 (Applied Biosystems, USA) that specifically binds human IgG antibodies. The reactor and harvest samples, stored during the offline measurement, were thawed and loaded in the column using a buffer near physiological pH and ionic strength (150 mM NaCl, 10 mM sodium phosphate, pH=7.5). Then, the column was washed to remove the low affinity particles. The elution process of the bound product was performed using a strong buffer (150 mM NaCl, pH 2.0). Finally, after each sample, the column was cleaned with 10 mM HCl. The evaluation of the data was performed with the Agilent ChemStation software (Agilent Technologies, USA). The peak of interest was detected by a UV lamp at 280 nm and the antibody concentration was calculated using the following equation (8) :

$$C_{titer} = \frac{AQ}{kV_{injection}} \quad (8)$$

where A is the area under the peak, Q the flow rate through the column, $V_{injection}$ the injection volume of the sample and k the calibration constant.

- **Amino acids**

Amino acids were determined by reversed-phase chromatography using a C18 analytical column (Agilent Zorbax Eclipse Plus). Pre-column OPA/FMOC derivatization was used while the separation was carried out by applying a gradient of mobile phase A (10 mM Na₂HPO₄ : 10 mM Na₂B₄O₇) and mobile phase B (acetonitrile : methanol : water 45 : 45 : 10, v : v : v) from 2 to 57 % of buffer B over 20 minutes. Concentrations of the amino acids were obtained by interpolating from a standard curve. Prior to analysis each sample was filtered using Vivaspin 500 (5000 Da) centrifugation filters (Sartorius Stedim Biotech, Germany) at 4000 g (4 °C).

- **Ammonia**

Ammonia concentration was evaluated using the Ammonia (Rapid) Assay kit (Megazyme, Ireland) on a 96 well plate (TPP, Switzerland). 10 µl of sample solution were pipetted into wells, followed by the addition of 200 µl Millipore water, 30 µl of supplied Buffer 1 (pH 8.0), 20 µl of supplied concentrated NADPH solution and 2 µl of glutamate dehydrogenase (GIDH) solution. Absorbances at 340 nm were read using an EnSpire 2300 Multilabel Reader (Perkin Elmer, USA) before and after enzyme addition, so with NADPH and NADP⁺. Ammonia concentrations were obtained by interpolating from a standard curve. To get an estimated level of ammonia below 0.4 g/l, as suggested by the manufacturer, the samples were previous diluted with Milipore water.

- **Glyco**

MAbs were purified from the supernatant using Vivapure miniprepA purification kit (Sartorius Stedim Biotech, Germany) according to the manufacturer's protocol. The purified mAbs were incubated in the supplied denaturation buffer at 37 °C for 10 min. So, N-linked glycans were enzymatically detached from the peptide backbones by incubating for 14 h at 37 °C after the addition of 2 µl of PNGase F (New England Biolabs, USA). Released N-glycans were isolated using Superclean ENVI-Carb column tubes (Sigma Aldrich, Switzerland) loading the samples in 2% acetonitrile / 0.1 M ammonium acetate solution and eluting with 50% v/v acetonitrile in H₂O. Eluted fractions were collected and

dried overnight under vacuum in a Vacufuge[®] plus (Eppendorf, Germany). Further, in order to be fluorescently labelled the N-linked oligosaccharides were dissolved in 20 µl of 70% DMSO 30% acetic acid, 1 M sodium cyanoborohydride solution containing 0.35 M 2-Anthralamide (2-AA) (Sigma Aldrich, Switzerland), according to Bigge et al. [29], and incubated in the same solution at 65 °C for 2 h. Subsequently the mixture was cooled to room temperature and diluted with 380 µl acetonitrile. To remove the excess of unreacted dye, all samples were loaded to 3 Whatman 3MM filter paper disks placed on Ultrafree[®] MC (0.5 ml) centrifugal filter units (PTFE membrane, 0.45 µm pore size) (Millipore, USA) as described by Merry et al.[30]. The system was washed 3 times with 95% acetonitrile and oligosaccharides were eluted 3 times using 50 µl of Millipore water (Millipore, USA). After drying, samples were dissolved in 30 µl Millipore water and 70 µl acetonitrile.

Finally chromatographic separation was carried out to determine the relative quantity of each glycoform. Single peaks were finally resolved by means of Time-Of-Flight Mass-Spectroscopy (MALDI-TOF). Different N-glycan structures were first separated by hydrophilic interaction chromatography (HILIC) using a GlycoSep N-Plus column (4.6 mm x 150 mm, Prozyme, USA) equipped on an Agilent 1200 HPLC system (Agilent Technologies, USA). The analysis was carried out at 30 °C using 10 mM formic acid, 80% w/w acetonitrile (pH 4.4) and 30 mM formic acid, 40% acetonitrile (pH 4.4) as mobile phase A and B respectively. The gradient started from 70% and was reduced to 35% mobile phase A over 90 min at 0.6 ml/min. After the gradient, the column was washed for 10 min with 0.5 % formic acid and re-equilibrated at 30% mobile phase B before next analysis. For each sample the injection volume was set to 90 µl. Fluorescence-labeled N-glycans were detected with an excitation wavelength of 250 nm and an emission wavelength of 410 nm. Fractions containing separated oligosaccharides were collected every minute using a FC 203B (Gilson, Switzerland) fraction collector. Each sample was completely dried in a Vacufuge[®] plus (Eppendorf, Germany), resuspended in 10 µl of Millipore water and stored at -20 °C prior to mass spectroscopy analysis.

2.7 SPECIFIC CALCULATION

- Cell specific rate of apparent growth (9)

$$\mu = \frac{1}{\bar{X}_v} \frac{dX_v}{dt} + B \quad (9)$$

- Cell specific consumption of glucose (10)

$$q_{GLC} = \frac{dGLC}{dt} \frac{1}{\bar{X}_v} + \frac{(H+B)(GLC_{IN} - GLC_{OUT})}{\bar{X}_v} \quad (10)$$

- Cell specific production of lactate (11)

$$q_{LAC} = \frac{dLAC}{dt} \frac{1}{\bar{X}_v} + \frac{(H+B)LAC_{OUT}}{\bar{X}_v} \quad (11)$$

- Cell specific production of antibodies (12)

$$q_{mAb} = \frac{dmAb}{dt} \frac{1}{\bar{X}_v} + \frac{(H+B)mAb}{\bar{X}_v} \quad (12)$$

with H , harvest rate; B , bleed rate; \bar{X}_v , viable cell concentration; $\bar{X}_v = \frac{(X_v(t_1) + X_v(t_2))}{2}$; GLC , glucose concentration; LAC , lactate concentration; mAb , titer concentration.

CHAPTER 3

RESULTS AND DISCUSSION

3.1 CHARACTERISATION

The cell cultures were preceded by a characterisation of the ATF and TFF setups in terms of flow rate, sheat stress and gas-liquid mass transfer. The characterisation was applied to estimate suitable operating conditions to be used during the cell culture.

3.1.1 External loop flow rate

Since the flow rate in the external hollow fiber module of the TFF setup could not be directly set, a relation between the rotational speed of the bearingless centrifugal pump and the flow rate was investigated. In figure 22A a typical profile obtained clamping the flow sensor at the inlet of the bearingless centrifugal pump is given. Each step, corresponding to a gradually increase of the rotational speed of the pump from 500 rpm to 3000 rpm, causes an increase of the flow rate. The analysis was carried out mounting either the “long”, the “short” or no hollow fiber module in the external loop. As can be seen in figure 22B, the relation depends on the type of hollow fiber used. In particular, running the pump at the same rotational speed, the lowest flow rate was measured with the “long” hollow fiber. The flow rate is a function of the pressure drop so, because of the greater length and the smaller cross sectional area (i.e. lower number of fibers), the head-loss is higher in the “long” hollow fiber and consequently the flow rate is lower. Moreover, since the hollow fibers are vertically mounted, the “long” hollow fiber is even the one characterised by the highest hydrostatic pressure.

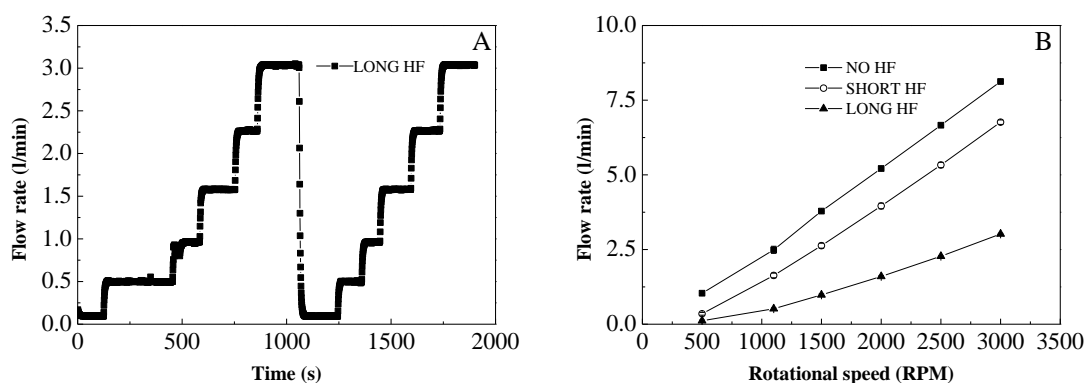


Figure 22 - A) Liquid flow measured with the “long” hollow fiber in the TFF setup, running the centrifugal pump at 50, 1100, 1500, 2000, 2500 and 3000 rpm. B) Flow rate, as function of the rotational speed, measured without (black square), with the “short” (open circle) and the “long” (black triangle) hollow fiber module attached.

3.1.2 Shear stress

The maximum shear stress was evaluated using a shear sensitive PMMA particulate system developed by Villiger et al. [28]. Initial PMMA aggregates are formed by uniform nanoparticles. Since the PMMA nanoparticles are stabilised by electrostatic repulsive forces, aggregation is enabled by salt addition above the critical coagulation concentration (CCC). The clusters grow until the shear stress applied exceeds the strength of the clusters. The fragments can undergo reaggregation until a dynamic equilibrium between aggregation and breakage is reached, leading to a steady state aggregate size. Steady state aggregate size of about 30 μm with a fractal dimension of 2.6 was reached after 14 h stirred at 50 rpm in 5 l beaker. The initial aggregates were then used in the determination of maximum shear stress in both, the ATF and TFF reactor systems. The size of the particles can be analysed by light scattering and correlated to stress values. As shown in figure 23A, the particle dimensions changed during time but since the change could be due to both the breakage caused by the shear stress or the rearrangement of the internal structure, the structural factor $S(q)$ was plotted as a function of the scattering amplitude (q) normalized for the radius of gyration (R_g). The slope of the curve subsequent to the bending represents the fractal dimension (d_f), being a measure for the compactness of the clusters. Since the fractal dimension, displayed in figure 23B for a reference batch experiment at different stirring speeds, was found to be constant, the changes of particle dimension can

be entirely accounted to the breakage of aggregates. Similar findings were observed in both ATF and TFF setup.

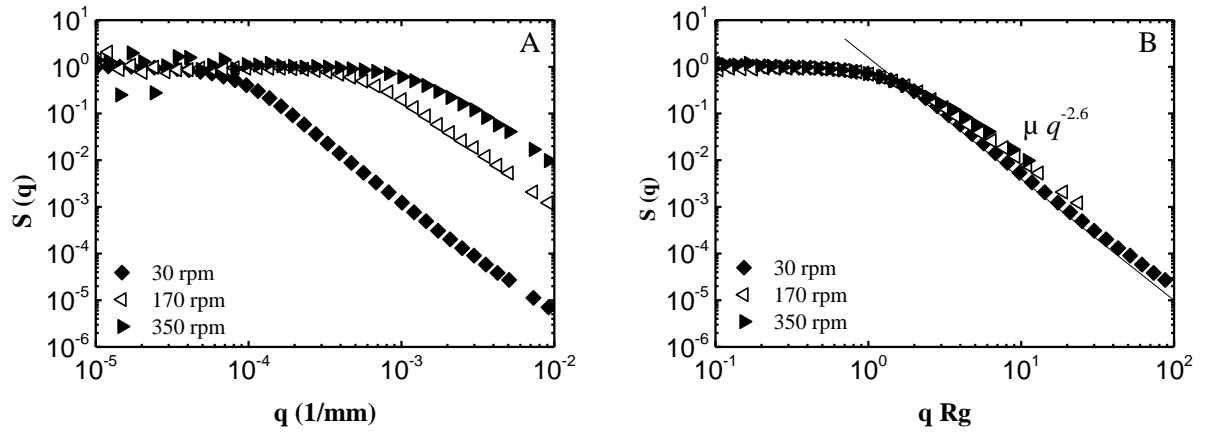


Figure 23 - A) Structural factor ($S(q)$), as a function of the scattering multiple (q), measured in a batch culture at 30 rpm (closed square), 170 rpm (opened left triangle) and 350 rpm (closed right triangle). B) Evaluation of the fractal dimension (d_f) from the power law of $S(q)$ plotted as a function of $q Rg$ measured in a batch culture at 30 rpm (closed square), 170 rpm (opened left triangle) and 350 rpm (closed right triangle).

The time needed to reach the steady size state was evaluated studying the time resolved aggregate size in the ATF system without the hollow fiber module in the external loop. As visible in figure 24, after one hour the stress measured was constant, indicating the achievement of steady aggregate size.

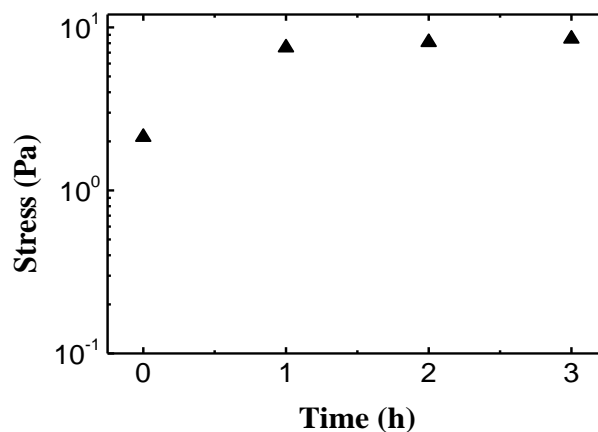


Figure 24 – Evolving shear stress, as a function of time, measured with the PMMA method in the ATF system without the hollow fiber module in the external loop.

The threshold stress for the used cell line was evaluated in a previous study of Neunstöcklin et al [31]. In particular, a fed-batch system, equipped with contracting nozzles of defined stress in an external loop, was used to expose cells to increasing shear levels during the culture. A drop in maximum viable cell density was observed when the shear stress exceeded 50 Pa. Given this threshold value, a feasible operating range can be deflected for the two retention systems.

The maximum shear stress measured in the ATF system is displayed in figure 25A. The shear stress increases with the flow rate from 0 to 1.5 l/min remaining below the threshold during all the experiment. The trends of the stress without hollow fiber and with the “short” one attached are very similar, meaning that the impact of the “short” hollow fiber is negligible. Contrary, the mounting of the longer hollow fiber module showed increased stress values because of the length and the smaller cross sectional area that leads to higher velocities.

The velocities and the Reynolds numbers calculated with the “short” hollow fiber, as well as the “long” one, are reported in table 5. The velocities in the “long” hollow fiber are higher but, in both set ups, the Reynolds numbers are well below 2100 meaning that the flow is laminar.

Table 5 – Velocities and Reynolds numbers calculated in the “short” and “long” hollow fiber setting a flow rate equal to 0.5 l/min, 1 l/min and 1.5 l/min.

Flow rate [l/min]	Velocity [cm/s]		Reynolds number	
	Short HF	Long HF	Short HF	Long HF
0.5	3.84	13.97	38.46	139.68
1	7.69	27.93	76.92	279.36
1.5	11.54	41.90	115.38	419.04

Similarly, the shear stress in the TFF increases with the flow rate applied in the external loop, calculated from the rotational speed of the pump using the before mentioned correlation. Again the “long” hollow fiber was found to induce the highest stress while the “short” shows values similar to the setup without hollow fiber (Figure 25B). However

compared to the ATF, the shear stresses are significantly higher. In the case of “long” hollow fiber the threshold is exceeded for rotational speeds higher than 1500 rpm while in the case of the short hollow fiber the threshold is exceeded for rotation speed higher than 2000 rpm.

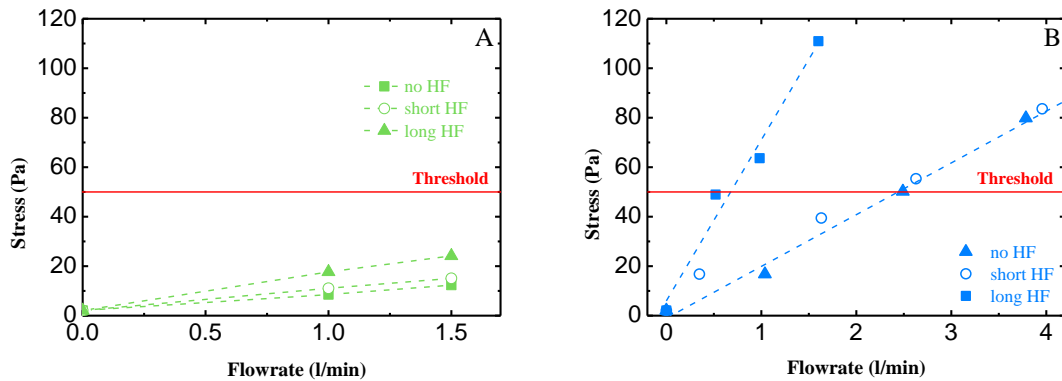


Figure 25 – A) Shear stress in the ATF system, as a function of the flow rate, calculated without (green square), with the “short” (empty circle) and with the “long” (green triangle) hollow fiber module attached. B) Shear stress in the TFF system, as a function of the flow rate, calculated without (blue triangle), with the “short” (empty circle) and with the “long” (bleu square) hollow fiber attached.

In summary, the shear sensitive particulate system indicates a higher maximum shear stress using the TFF with respect to the ATF, confirming that the diaphragm pump produces less shear than the bearingless centrifugal pump. However both systems can run in regions in which the shear produced by the pumps are lower than the threshold.

The impact of stirring and the sparging on the shear stress level was studied in a reference batch system. As shown in figure 26, at low rotational speeds of up to 30 rpm, corresponding to impeller Reynold number of 1.5×10^3 , the shear stress induced by sparging at 0.22 vvm is higher than the one measured applying only agitation. Instead, at higher rotational speeds the stresses induced by the impeller become higher (Figure 26). When comparing the obtained values with previously determined threshold value it was found that applying the rotational speeds higher than 500 rpm create shear stresses which can cause cell damage and therefore has to be avoided during the cell culture.

The steady state cluster size is controlled by two mechanisms: the turbulence generated by the impeller and the stress resulting from the presence of bubbles [28]. The results of the

shear stress study are in agreement with the trends obtained by Villinger et al. that reported that at low Reynolds impeller the cluster size is dominated by the bubbles, while increasing the Reynolds impeller, the turbulence generated by the impeller takes over and the measured cluster size is similar to that measured for single phase [28].

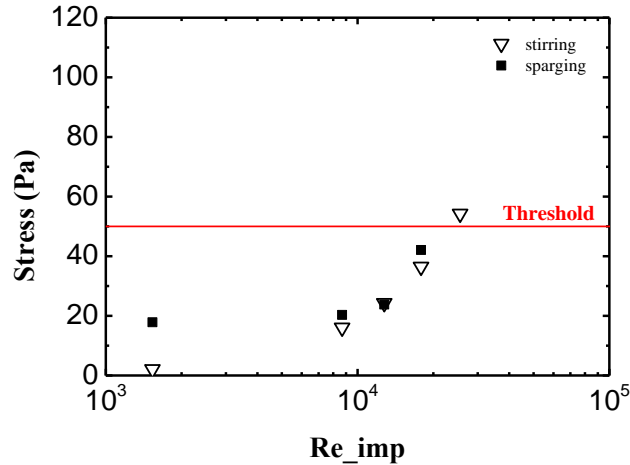


Figure 26 - Shear stress, as a function of the Reynolds impeller, calculated in a batch system stirring and stirring and sparging constantly at 20 l/min.

Based on the obtained results, the stirring speed was set to 400 rpm for the later cell culture experiments. The flow rate in the external loop was fixed at 1.5 l/min with the short hollow fiber module attached to the respective pump. Since the method evaluates the maximum stress induced in the system, the chosen parameter values should enable a viable long term culture.

3.1.3 $k_L a$ characterisation

Generally, during cell culture it is important to ensure the adequate supply of oxygen to the cells. This is even more crucial in perfusion cultures, where cell densities of 10^7 cells/ml are realistic. Therefore the gas-liquid mass transfer in the ATF and TFF bioreactor setup has been quantified. The $k_L a$ was studied at the operating condition (i.e. $T = 36.5$ °C, 400 rpm, gas flow rate = 20 l/h), without the external loop employed, as well as with the “short” hollow fiber attached to see the impact of the cell retention device on the transfer.

In figure 27A a real DO profile, obtained in the TFF system using the dynamic method described in the section 2.2.3, is displayed. The k_La , calculated by the slope of the plot, as shown in figure 27B, are given in the table 6. It can be observed that both the external loop and bioreactor setups do not influence significantly the oxygen transfer as in both setups it is higher than the threshold fixed to 5 1/h [32].

Table 6 - k_La values calculated with the dynamic method in the TFF system and in the ATF without the external loop and with the “short” hollow fiber.

	TTF no loop	TTF loop	ATF no loop	ATF loop
k_La [1/h]	18.72	20.16	18.36	18

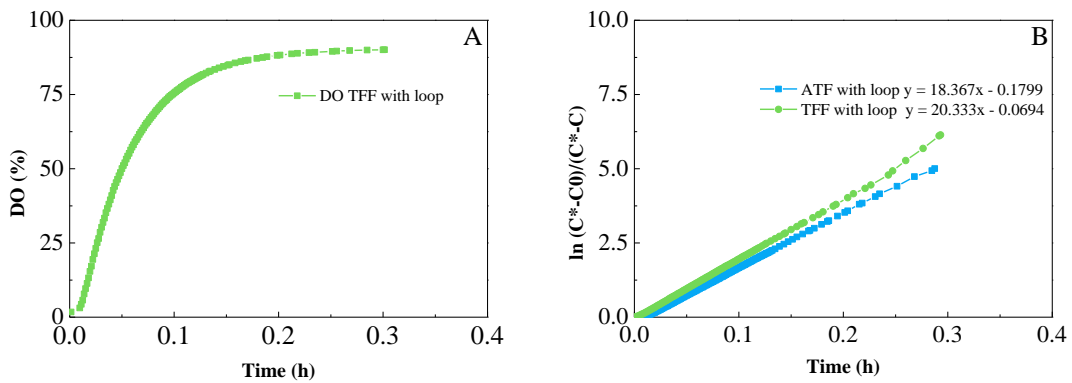


Figure 27 - A) DO_t , as a function of time, measured in the TFF system equipped with the “short” hollow fiber. B) $\ln \frac{C_L^* - C_L^0}{C_L^* - C_L}$, as a function of time, measured in the ATF and TFF setups with the external loop.

The slope represents the k_La given in 1/h.

3.2 EXPANSION

Starting from the thawing solution, one week of expansion was performed prior to the inoculation of the spin tubes or the seed reactor. In the figure 28A and 28B the viable cell density and the volume in which the cells were suspended are given. At each step the cells were resuspended in fresh production medium to a concentration of $0.3 \cdot 10^6$ cells/ml increasing the total volume every time. So, starting from a cell density of $0.3 \cdot 10^6$ cells/ml in 20 ml of expansion media, after 7 days a cell density of $1.4 \cdot 10^6$ cells/ml was measured in 930.6 ml.

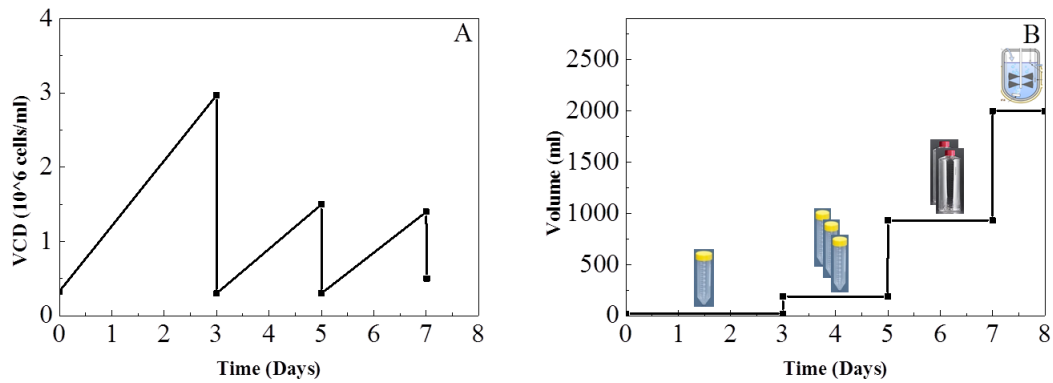


Figure 28 - A) Viable cell density profile during the expansion procedure from day 0 (thawing) until day 7 (inoculation). B) Amount of volume in which the cells are suspended and respective containers in which they are stored (1 spin tubes, 3 spin tubes, 2 roller bottles and 1 reactor).

3.3 SPIN TUBE EXPERIMENTS

Prior to the reactor cell cultures, preliminary experiments were conducted to understand the effect of the bleed rate on the perfusion culture, aiming to achieve a constant cell density profile, and to test the media compositions required depending on the cell density. To minimize media consumption and time of analysis all experiments were performed at the small scale (i.e. 50 ml spin tubes).

3.3.1 Constant harvest/bleed ratio

Five different ratios of harvest and bleed at an overall perfusion rate of 1 RV/day were studied in the first spin tube experiment starting from a initial cell density of 0.2×10^6 cells/ml. Figure 29A displays the viable cell density profiles as a function of time.

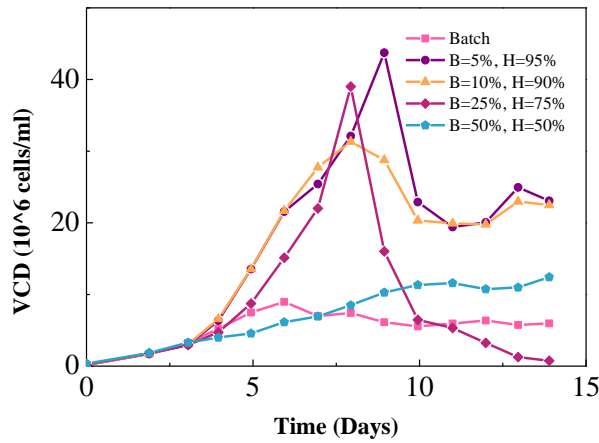


Figure 29 - Viable cell density, as a function of time, in the five spin tubes investigated: batch (pink), 5% bleed (purple), 10% bleed (orange), 25% bleed (red) and 50% bleed (blue).

A reference spin tube in batch mode was carried out to outline the effect of the perfusion. The batch spin tube described the typical viable cell density profile starting from a lag phase to an exponential growth phase and followed by a decrease in the cell density (Figure 29). Glucose, being the main energy source, is entirely consumed on day seven (Figure 30A), resulting in the acquisition of an alternative carbon source, lactate, which has been previously produced (Figure 30B). Since all nutrients are depleted, on working day eight, cells stop growing and a drop in viability to 70% is observed (Figure 31).

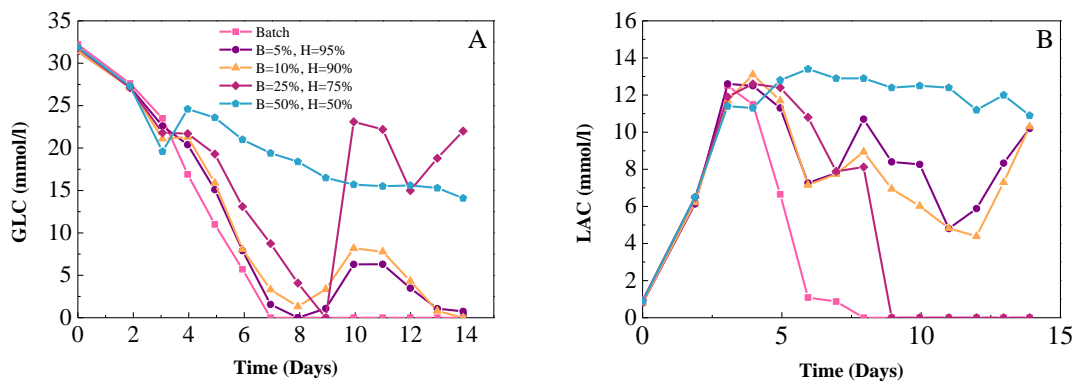


Figure 30 - Glucose (A) and lactate (B) concentration, as a function of time, in the five spin tubes investigated: batch (pink), 5% bleed (purple), 10% bleed (orange), 25% bleed (red) and 50% bleed (blue).

The spin tubes with a daily bleed of 5% and 10% show similar trends (Figure 29). The initial growth phase is extended and a maximum viable cell density of 30×10^6 cells/ml is achieved on day eight. Since glucose is depleted at that point, the maximum corresponds to an overgrowth leading to a subsequent decrease of the cell number, stabilizing above 20×10^6 cells/ml. Therefore, the production medium is generally not sufficient to keep cell densities higher than 30×10^6 cells/ml. To reach higher cell densities at a constant perfusion rate, an increase of medium depth by supplementing feed and further glucose is necessary. On the other hand, the experiment proves that it is possible to keep a steady state at 25×10^6 cells/ml by using base medium only. Compared to the batch standard, the cell viability maintains above 90% during most of the experiment (Figure 31).

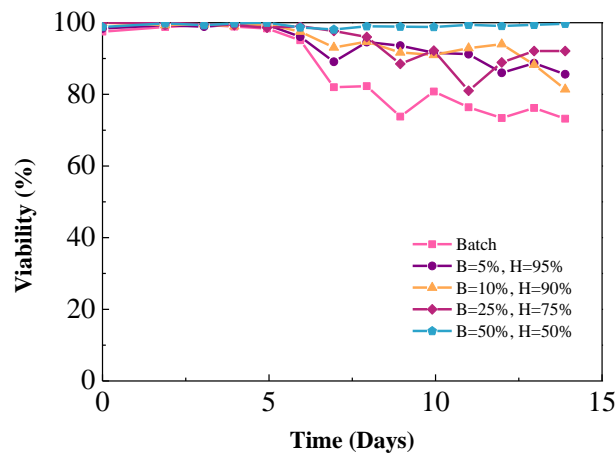


Figure 31 – Viability, as a function of time, in the five spin tubes investigated: batch (pink), 5% bleed (purple), 10% bleed (orange), 25% bleed (red) and 50% bleed (blue).

The cell culture applying 25% bleed crashed on day nine after reaching 40×10^6 cells/ml due to the synergic effect of glucose and lactate depletion in the spin tube; the cells did not recover and stopped growing (Figure 29 and 30). The spin tube with 50% bleed is characterized by a slow incline of viable cell density achieving a steady state at 11×10^6 cells/ml from day ten on. Although the cell density is significantly lower than in the other perfused spin tubes, the viability is constantly above 98% and no glucose depletion is present (Figure 30 and 31). The low cell density can be accounted to the high ratio of bleeding, as each day half of the cell suspension volume is withdrawn from the spin tube. However the specific growth rate is the highest of all spin tubes (Figure 32), showing that

the cells keep growing throughout the entire experiment. In detail, all conditions show a maximum in specific growth rate immediately after inoculation and decreasing with culture time, being zero when depletion of glucose is observed.

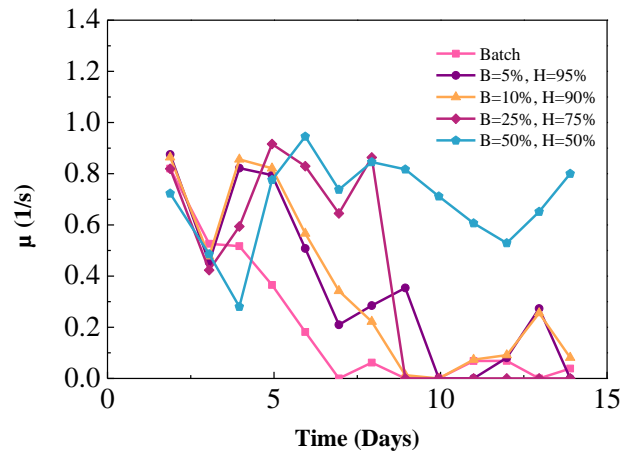


Figure 32 - Specific growth rate, as a function of time, in the five spin tubes investigated: batch (pink), 5% bleed (purple), 10% bleed (orange), 25% bleed (red) and 50% bleed (blue).

The titer depends on the viable cell density as well as on the bleed fraction, removing both cells and product. For this reason, the lowest titer is present in the spin tube with a bleed of 50%. The titer in the spin tubes with 5 and 10% of bleeding average between 0.20 – 0.25 g/l at the constant viable cell in the end of the culture (Figure 33A). So, the constant cell densities lead to a constant production. Despite the low cell concentration, the batch spin tube shows the highest product concentration, as the product is not removed during cell culture. Indeed, the lowest specific productivity is in the batch culture and is almost equal to zero after day 9, when the cells stop growing (Figure 33B).

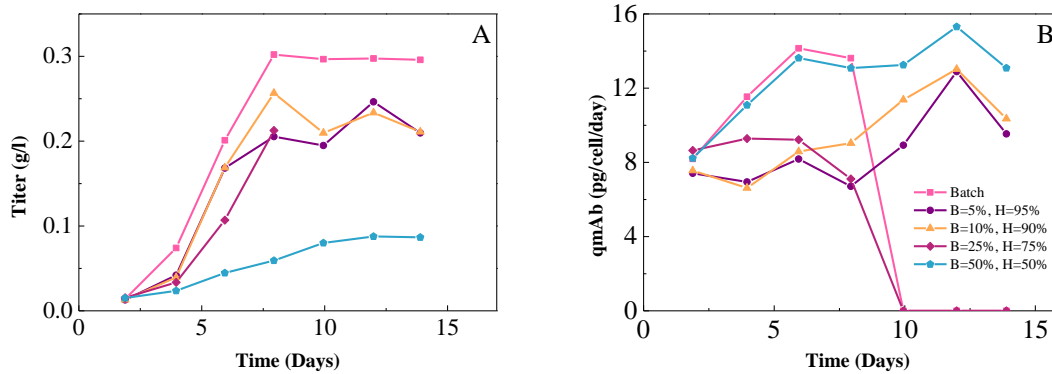


Figure 33 – Tite (A) and specific productivity (B), as a function of time, in the five spin tubes investigated: batch (pink), 5% bleed (purple), 10% bleed (orange), 25% bleed (red) and 50% bleed (blue).

In conclusion, the first spin tube experiment showed that the constant bleeding is not the right strategy to keep the density constant. An adaptive bleeding should be preferred withdrawing an amount of volume according to the cell density measured. Moreover, although for cell densities lower than 25×10^6 cells/ml the base medium is sufficient, it has to be supplemented with feed and glucose when aiming at higher densities.

3.3.2 Different cell density and percentage of feed

In the second spin tube experiment different cell densities were kept constant using an adaptive bleeding. Moreover, different media compositions were investigated to determine a suitable supplementation of base media with concentrated feed according to the cell density. For this reason a DoE was performed controlling the viable cell density and the percentage of feed added to the base medium. Because the previous experiment showed that with high densities the glucose contained in the base medium is not enough, 12 g/l of glucose and two amino acids, cysteine and tyrosine, were added to the feed medium. The spin tubes were inoculated close to the set point cell density (i.e. 30×10^6 cells/ml, 50×10^6 cells/ml and 70×10^6 cells/ml) and, immediately after the inoculation a high growth was observed (Figure 34A).

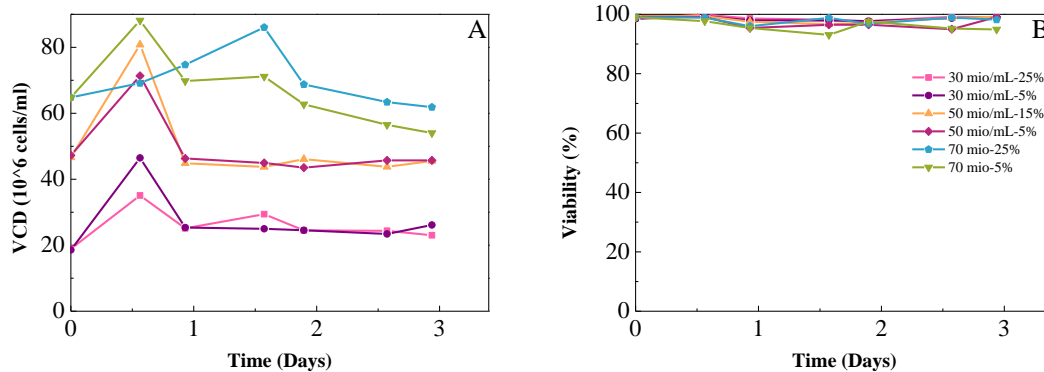


Figure 34 - Viable cell density (A) and viability (B), as a function of time, in the six spin tubes: 30×10^6 cells and 5% of feed (pink circle), 30×10^6 cells and 25% of feed (purple circle), 50×10^6 cells and 15% of feed (orange triangle), 50×10^6 cells and 5% of feed (red square), 70×10^6 cells and 25% of feed (blue circle), 70×10^6 cells and 5% of feed (green triangle).

In all the spin tubes the viability was higher than 90% (Figure 34B) and, as shown in figure 35A, the addition of glucose permitted to avoid depletion.

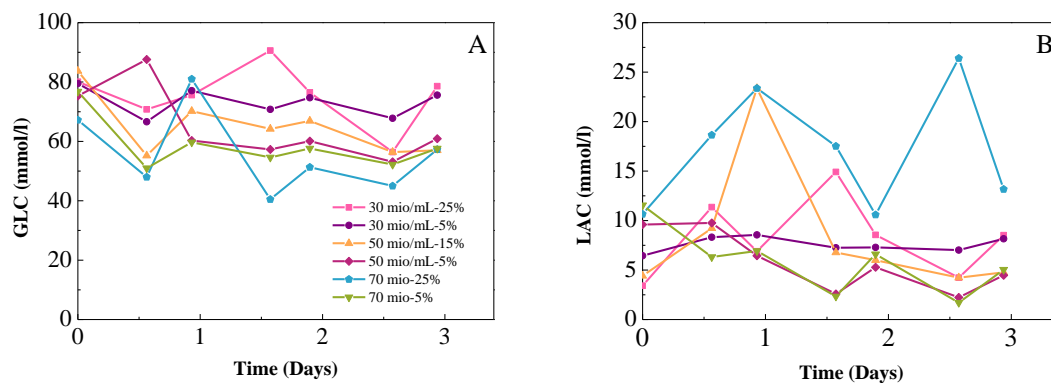


Figure 35 – Glucose (A) and lactate (B) concentration, as a function of time, in the six spin tubes: 30×10^6 cells and 5% of feed (pink circle), 30×10^6 cells and 25% of feed (purple circle), 50×10^6 cells and 15% of feed (orange triangle), 50×10^6 cells and 5% of feed (red square), 70×10^6 cells and 25% of feed (blue circle), 70×10^6 cells and 5% of feed (green triangle).

Even if after the inoculation the cells started growing in all the spin tubes, the rate was quite different according to the cell density and the percentage of feed added (Figure 36). The highest specific growth rate was observed in the spin tube with the lowest target cell density and feed fraction (i.e. 30×10^6 cells/ml and 5%). On day one the adaptive bleeding strategy was initiated and the cell density was adjusted to the respective set point. Subsequent the conditions with 30 and 50×10^6 cells/ml reached a constant cell density

while in the spin tubes with 70×10^6 cells/ml the cell density started slightly decreasing (Figure 34A). In any case, the analysis of the specific growth rate shows that the steady states reached are not dynamic but static, since the cell density was constant because the cells were not growing anymore. Instead, a preferential steady state would be characterized by a slow growth and high production, while the cell density is kept constant by bleeding, beneficial to maintain the viability of the culture.

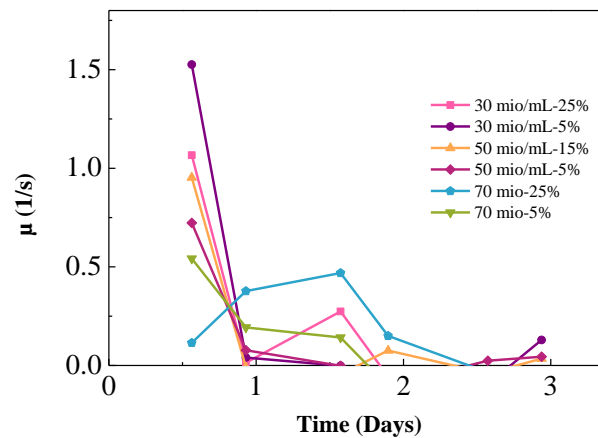


Figure 36 – Growth rate, as a function of time, in the six spin tubes: 30×10^6 cells and 5% of feed (pink circle), 30×10^6 cells and 25% of feed (purple circle), 50×10^6 cells and 15% of feed (orange triangle), 50×10^6 cells and 5% of feed (red square), 70×10^6 cells and 25% of feed (blue circle), 70×10^6 cells and 5% of feed (green triangle).

The main important difference between the bioreactor and the spin tubes is that in the bioreactor the perfusion is performed during all the day while in the spin tubes it is achieved changing the medium at discrete times. In this experiment the perfusion was set to 1 RV/day and the medium was exchanged twice a day to first prevent the removal of all metabolites and second to limit the increase in osmolality. In any case, even changing the medium twice a day, the osmolality in the spin tubes was high (Table 7). In literature osmolality values above 400 mOsm/kg are reported to inhibit growth and act cytotoxic [13].

Table 7 – Osmolality of the medium with 5%, 15% and 25% fraction of feed.

Osmolality [mOsm/kg]	Feed fraction		
	5%	15%	25%
	415	494	573

Moreover, given the poor control of operating parameters in the shaking incubator, negative effects on culture performance can arise from insufficient oxygen supply, suboptimal pH or CO₂ accumulation.

The evolution of the product concentration in time scales with the cell density and depends on of the percentage of feed added (Figure 37A). Precisely, in the spin tubes with a target density of 30×10^6 cells/ml, an increased titer is observed at lower percentages of feed added. Contrary in the other spin tubes a higher percentage of feed leads to higher mAb concentration. The surface in figure 37B shows the titer as a function of the feed fraction and viable cell density. The highest titers are obtained with the highest cell densities and lowest feed fractions. Instead, low cell densities combined with high feed fractions should be avoided because they lead to low production.

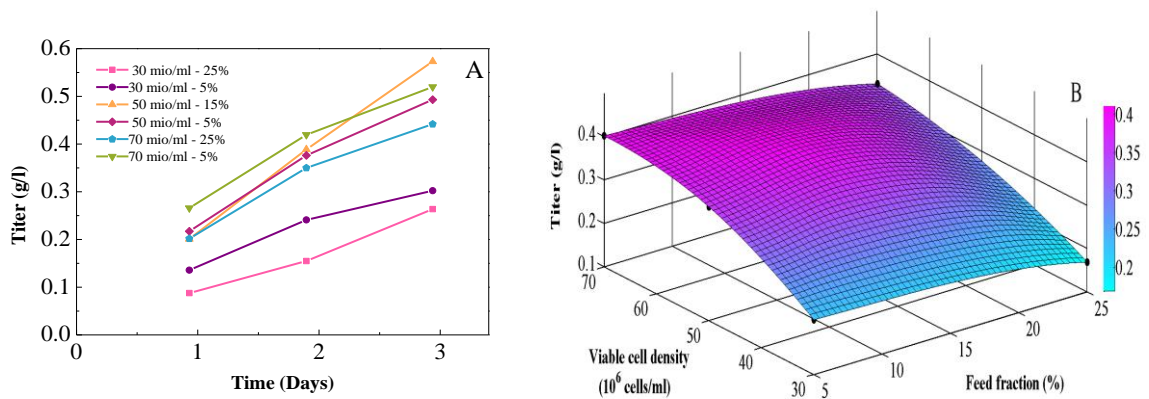


Figure 37 – A) Titer, as a function of time, in the six spin tubes: 30×10^6 cells and 5% of feed (pink circle), 30×10^6 cells and 25% of feed (purple circle), 50×10^6 cells and 15% of feed (orange triangle), 50×10^6 cells and 5% of feed (red square), 70×10^6 cells and 25% of feed (blue circle), 70×10^6 cells and 5% of feed (green triangle). B) Titer as a function of the feed fraction and viable cell density.

The spin tube experiments showed that an adaptive bleeding strategy is suitable to maintain a constant viable cell density set point, avoiding overgrowth. A high concentrated

feed has to be used to supply enough nutrients to the cells. The fraction of feed used should be chosen properly not to exceed harmful osmolality levels in the reactor that can inhibit the growth. Last, the achievement of high cell densities is dependent on the further addition of glucose.

3.4 BIOREACTOR RUNS

3.4.1 Preliminary run: media composition

Before the comparison of the designed ATF and TFF bioreactor set ups, the perfusion was developed in a preliminary run performed in the seed bioreactor to test the setup and the medium composition. The experimental setting was similar to the one described in section 2.5.2. The figure 38A shows the viable cell density as a function of time.

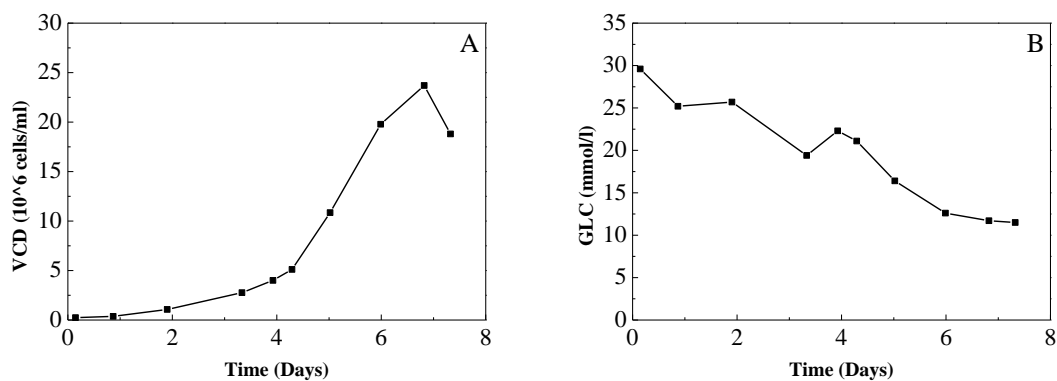


Figure 38 - Viable cell density (A) and glucose concentration (B) as a function of time.

The reactor was inoculated at a cell density of 0.2×10^6 cells/ml and constantly perfused at 1 RV/day using basic production media. The observed initial growth mimics the spin tube experiment performed with 5 and 10% of bleed. The exponential growth phase results in a maximum cell density of roughly 25×10^6 cells/ml, not facing any depletion in glucose (Figure 38B). The analysis of the amino acids showed low levels of cysteine and asparagine in the reactor on day four (Figure 39). Moreover tyrosine concentration, which

has a high deviation in the fluorescence HPLC analysis, is comparably low. To avoid depletion, being even more severe at higher cell densities, in the further experiments 7.5 mM of asparagine as well as cysteine and tyrosine were added. In particular the media strategy of the standard fed-batch run, being the initial subject for the optimization of the media composition, suggests the addition of cysteine and tyrosine in an amount equal to 0.0375 % with respect to the feed.

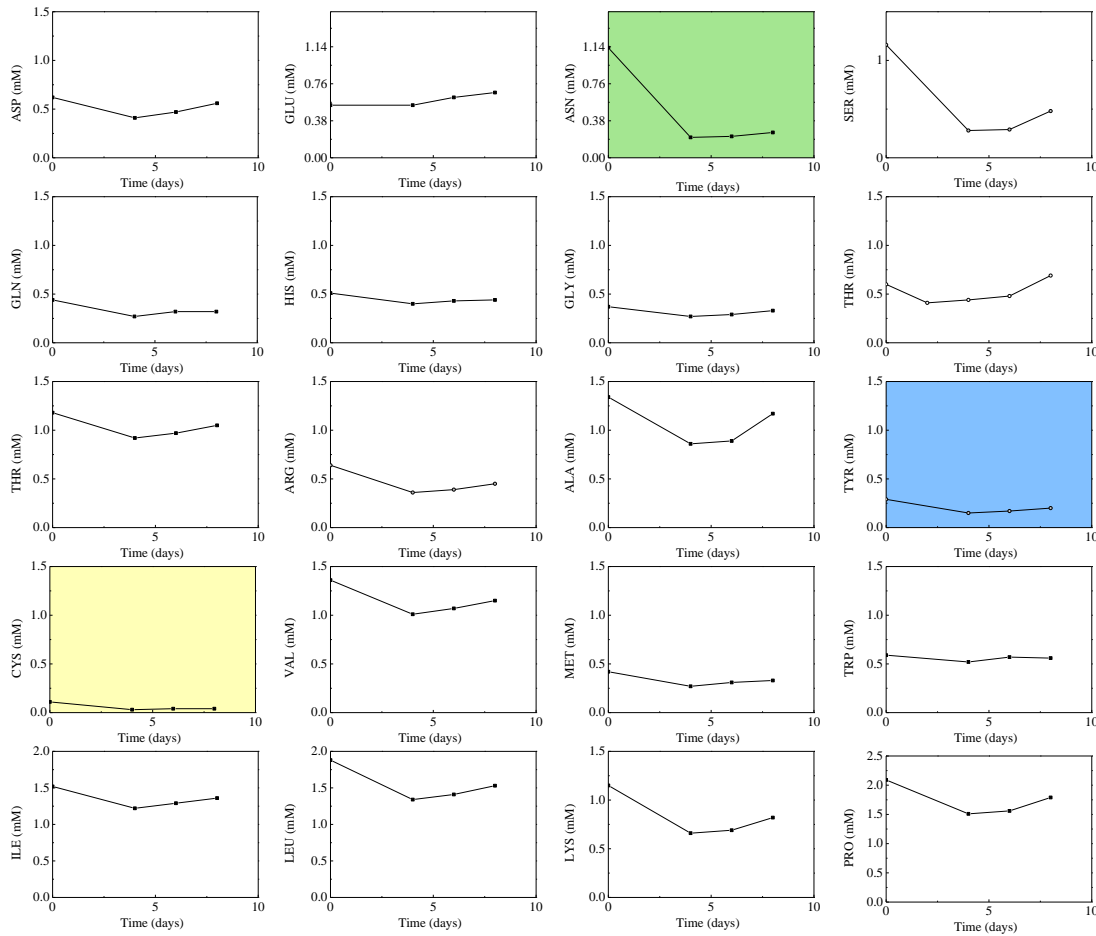


Figure 39 - Amino acids concentrations as a function of time. Highlighted in green the asparagine, in blue the tyrosine and in yellow the cysteine.

3.4.2 Seed reactor

One of the main problems of a perfusion culture performed with a cell retention device based on filtration is the fouling of the filter module limiting the possible run time. Moreover, since the titer scales with the viable cell density, a steady state at high cell

densities is suitable for the production of antibodies. The use of a seed bioreactor permits the decoupling of both the growth and production phase, optimizing them separately. Considering the mentioned objectives, the initial growth phase was carried out in a seed bioreactor enabling the inoculation of multiple production bioreactors close to their desired initial cell density. So, the expansion was extended from the roller bottles to a seed bioreactor inoculated at an initial cell density of roughly 0.5×10^6 cells/ml with resulting working volume of 2 l. The seed reactor was equipped with the “short” hollow fiber and a gas flow rate of 0.33 l/h as well as a stirring speed of 250 rpm were set. A perfusion rate of 1 RV/day was started immediately after the inoculation. The typical exponential growth, characterised by a doubling of the density is given in figure 40A. After having reached a cell density of 10×10^6 cells/ml, the perfusion rate was switched to 2 RV/day to supply sufficient nutrition, as the maximum cell density in the previous spin tube experiments and preliminary run was limited to 30×10^6 cells/ml at 1 RV/day perfusing only production media (Figure 40B).

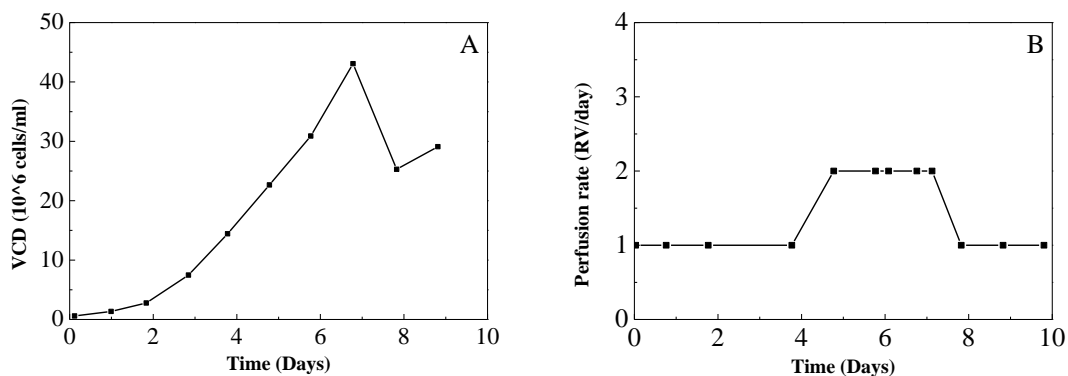


Figure 40 – Viable cell density (A) and perfusion rate (B), as a function of time.

The increase of the perfusion rate lead to a higher growth rate, quickly reaching the target cell density of 40×10^6 cells/ml necessary to inoculate the production bioreactors close to their first set point at 20×10^6 cells/ml. The maximum cell density was achieved on working day seven with a viability higher than 90%. As can be seen in figure 41 the perfusion rate set to 2 RV/day permits depletion in glucose during the culture. After the inoculation, the seed reactor can be reused to prepare a further inoculation or it can proceed as normal production reactor.

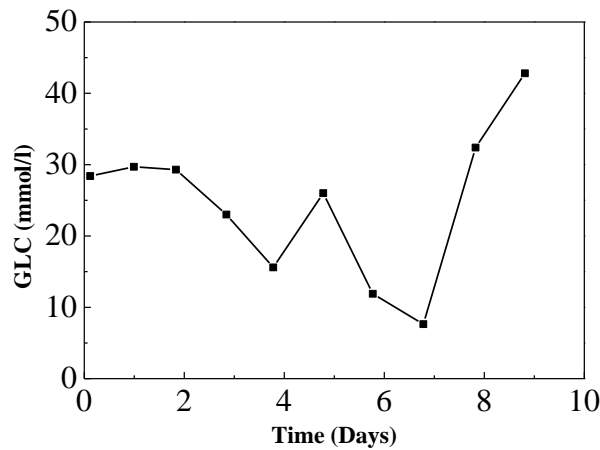


Figure 41 – Glucose concentration in the seed bioreactor as a function of time.

3.4.3 Comparison of ATF and TFF applying manual bleed

A perfusion process was developed to compare the ATF and the TFF cell retention devices. The operating condition were chosen with respect to previous cold characterization. The rotation speed of the impeller was fixed to 400 rpm while the rotation speed of the centrifugal pump was set to 1100 rpm corresponding to a flow rate in the external loop equal to 1.5 l/min. Both reactors were equipped with the “short” hollow fiber that minimizes the effect of the shear stress. Since the first viable cell density set point was fixed to 20×10^6 cells/ml, both reactors were inoculated with the respective amount of cell suspension from the seed bioreactor, allowing the achievement of the first steady state within one day. In both reactors the first set point was kept for eight days using an adaptive bleeding and perfusing with basic production medium (Figure 42). The oscillation in the cell density profiles are due to the adaptive bleeding performed. Twice a day, after the measurement of the viable cell density, a volume to bleed to 18×10^6 cells/ml was withdrawn causing the zigzag profile. In day nine to reach the second steady state the bleed was released and the cells started growing. The medium composition was gradually adjusted by adding feed medium to supply sufficient nutrition. The final fraction to maintain 60×10^6 cells/ml composition was chosen, consisting of 30% production medium and 70% feed medium. At this cell density the two systems deviate in their behaviour. While the reactor equipped with the ATF was able to keep the set point throughout the

entire period of eight days, the TFF failed due to the blockage of the external loop (Figure 42A).

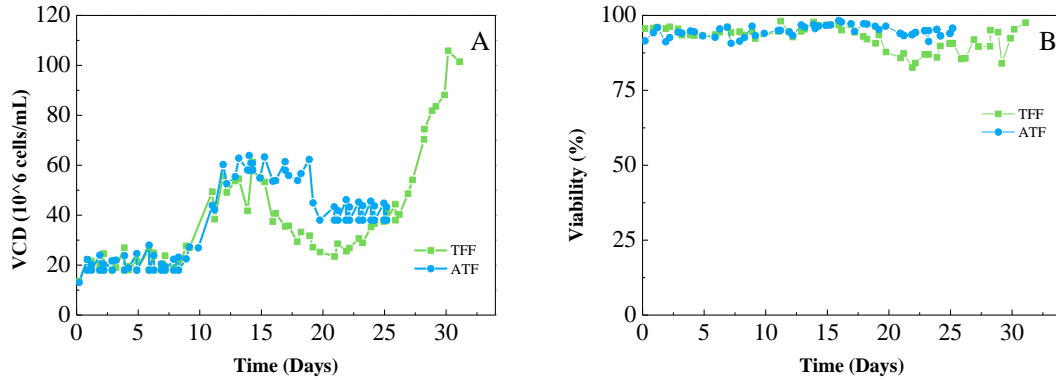


Figure 42 - Viable cell density (A) and viability (B) as a function of time in the TFF (green square) and ATF (blue circle) reactors.

At 60×10^6 cells/ml the cellular growth was lower and more cells died. The increase of the debris in the culture determines a significant fouling of the hollow fiber of the TFF system. Fixing the rpm at constant value, the pump was not able anymore to overcome the pressure drop, leading to a drop in flow rate and the final blockage of the hollow fiber (Figure 43A). Since the perfusion rate was controlled by the permeate flux, the dilution stopped. The flow was restarted on the next morning and the rotational speed of the pump was increased to 1500 rpm. After the blockage of the hollow the cells took six days to restart growth reaching the third steady state at 40×10^6 cells/ml. In the TFF this steady state was kept for 3 days adjusting the media composition to 65% base media and 35% feed media. The rest of the time was dedicated to investigate the maximum cell density reachable with a perfusion rate of 1 RV/ day. The bleeding was stopped and the feed fraction was further increased, leading to a maximum cell density of 105.82×10^6 cells/ml, finally only using feed medium. Instead, the last set point of the ATF setup at 40×10^6 cells/ml was achieved by heavy bleeding and then kept for one week (Figure 42A). To prevent the growth inhibiting effect of high osmolality base media solely replaced the amount bleed.

The perfusion, harvest and bleed rates applied during the cultures are given in figure 43. The bleeding depends on the cell density measured and was found to be a function of the steady state. Since the growth rate was found to be higher at 20×10^6 cells/ml, more cell

suspension had to be withdrawn in order to maintain the set point compared to 60×10^6 cells/ml. The variation in bleed rate, given the fixed harvest rate of 1 RV/day, resulted in a change of the overall perfusion rate.

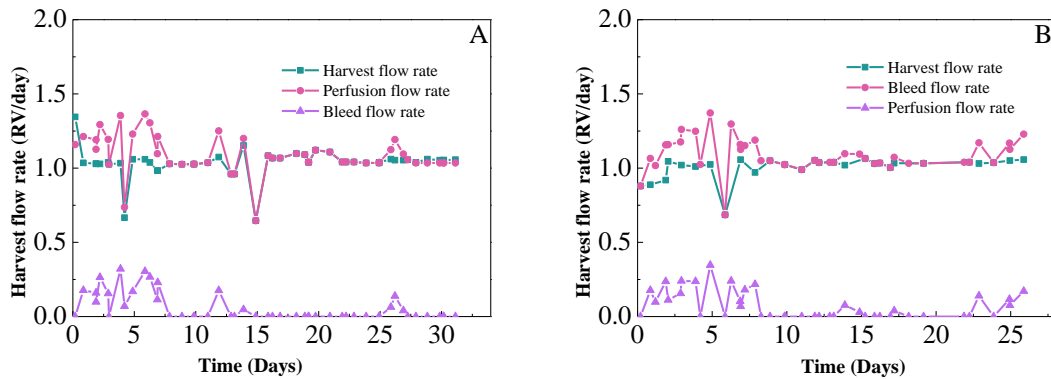


Figure 43 – Harvest (blue), bleed (pink) and perfusion (purple) rate, as a function of time, in the TFF (A) and ATF (B) reactors.

In figure 44A the glucose concentration is reported as a function of time. The glucose concentration in the feed media is given as function of the viable cell density set point. No depletion was observed, meaning the amount of glucose added in the feed medium (12 g/l) and the fractions used at the different set points were chosen properly. The steady states observed in the cell density profile are also recognizable in the glucose and lactate profile of the ATF (Figure 44). Taking in account the amount of glucose being fed in each steady state, the concentration at each set point can be considered constant, meaning that not only the number of cells was constant but also the consumption of glucose. The concentration of glucose depends on the cell growth so in the TFF, it started increasing subsequent to the blockage of the hollow fiber revealing the stop in cell growth.

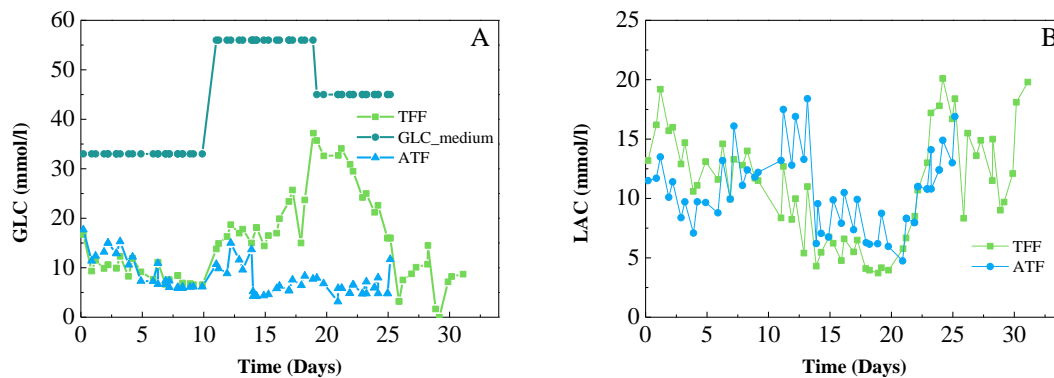


Figure 44 – A) Glucose concentration, as a function of time, in the feed (dark green) and in TFF (green) and ATF (bleu) reactors. B) Lactate concentration, as a function of time, in TFF (green) and ATF (bleu) reactors.

The concentrations of mAbs produced in both reactors are given in figures 45A and 45B. The titer scales with the viable cell density mimicking the cell density profile. The product concentration in the reactor equipped with the ATF retention device was constant within each of the three set points. The difference between the titer in the reactor and the harvest is a measure for product retention in the hollow fiber. In the ideal case, where no retention occurs, the concentration in both segments is the same resulting in an overlap of the two curves. In the ATF setup the product retention is low throughout the entire culture especially during the first steady state at 20×10^6 cells/ml (Figure 45C). Instead the product retention in the TTF setup is significantly higher increasing during the experiment above 65% (Figure 45D). The retention is related to the fouling of the hollow fiber and the pore diameter so, since the same hollow fiber was used in both systems, it can be concluded that the ATF is less subjected to the fouling. So, as asserted by the vendor, the dynamic of the ATF determines a lower fouling. In particular, the periodic reversal of the flow inhibits the attachment of cells and debris on the membrane while the backflush cleans the membrane pores.

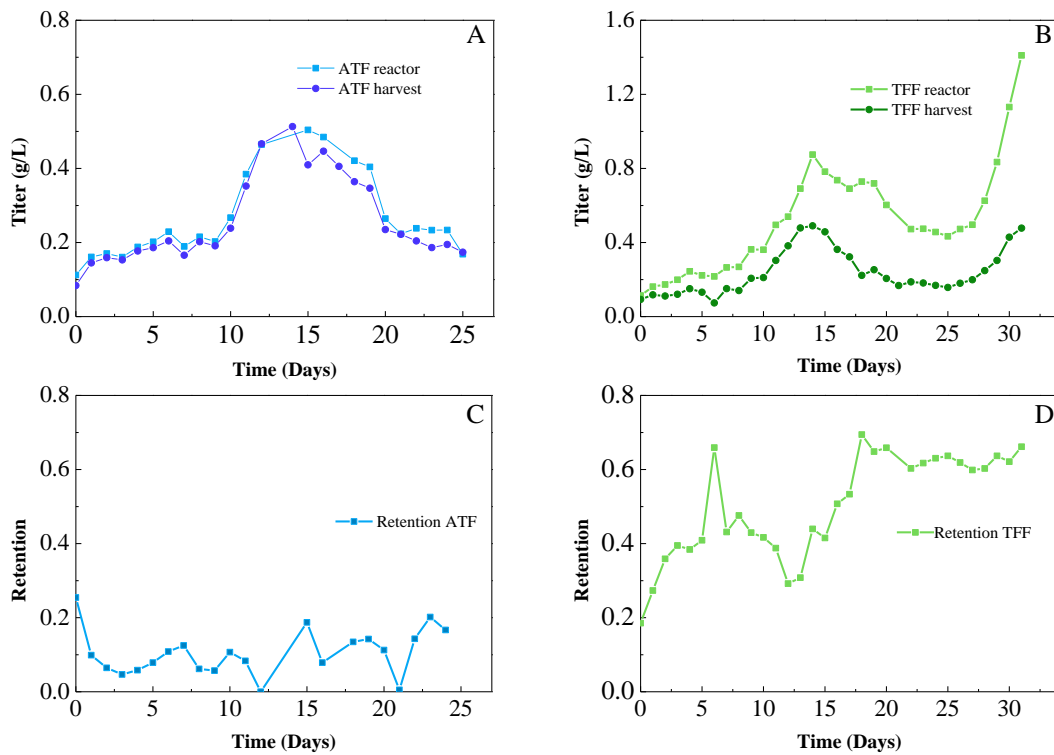


Figure 45 – A) Titer in the ATF reactor (blue circle) and in the harvest (light blue square) as a function of time. B) Titer in the TFF reactor (light green square) and in the harvest (green circle) as a function of time. C). Retention of the product in the ATF setup. D) Retention of the product in the TFF setup.

Similar results in term of fouling were obtained by Clinké et al. with a production yield, ratio between the accumulated harvested product and the accumulated reactor product, between 46-56% and 54-71% with the ATF and the TFF respectively. So, the authors obtained higher retention in the system equipped with the TFF but they had also a significant retention with the ATF. Since the retention is a function of the pore diameter, the higher retention could be due to the smaller diameter of the pores of the hollow fiber used [26].

3.4.4 Comparison of TFF and TFF applying manual bleed

In the second run an online biomass sensor was added to each reactor aiming at the automation of the bleeding operation. Moreover in the TFF setup a clamp-on flow sensor was attached, measuring the flow rate and adjusting the rotational speed of the pump in the

external loop to prevent the blockage of the hollow fiber module. As in the previous experiment, the first viable cell density at 20×10^6 cells/ml was maintained in both reactors (Figure 46A).

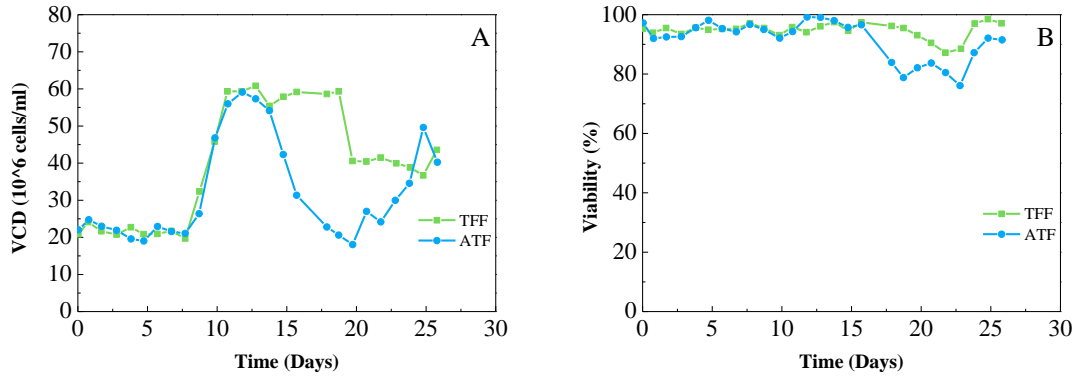


Figure 46 - Viable cell density (A) and viability (B), as a function of time, in the TFF (green square) and ATF (bleu circle) reactors.

Compared to the previous run, the biomass sensor allowed the flattening of the cell density profile since cell suspension was removed in a continuous manner. On working day nine, approaching the second VCD set point at 60×10^6 cells/ml, the composition was switched to 35% production media and 65%. A lower feed fraction was used compared to the previous experiment to test the robustness of the process to a different feed fraction. Since this time the blockage of the external loop was prevented, the steady state at 60×10^6 cells/ml was kept constant in the TFF. To maintain a flow rate of 1.5 l/min, the rotational speed of the pump was increased from 1000 to 1200 at this point. Comparing it to the rotational speed used in the previous run, 1100 rpm have not been sufficient to keep 1.5 l/min. However in the reactor equipped with the ATF it was not possible to maintain a cell density of 60×10^6 cells/ml. Similar to the failure of the TFF in the previous run, it took one week before the reconstitution of the cell growth (Figure 46A). The pCO₂ measured in the reactor was found to exceed 120 mmHg, being on a level potentially inhibiting cellular growth according to the literature data [13]. A second hypothesis relates to the linkage of the perfusion rate to the bleed rate. In essence the perfusion rate was not fixed to a constant value but controlled by the extend of the bleed rate. In the experiment the perfusion rate was aimed to be 1 RV/day in order to limit the costs and enhance the productivity of the process. So, since permeate flux was set to 1 RV/day and the perfusion rate was controlled

by the weight of the reactor, the perfusion rate was equal to 1 RV/day, when no bleed was applied, but increased when bleeding was necessary. In the ATF from day 12 the bleeding was not performed anymore because the cell density was lower than the set point causing a perfusion rate of exactly 1 RV/day. In the TFF instead 145 ml were extracted leading to a perfusion rate of 1.1 RV/day (Figure 47). Hence the crash of the ATF could be caused by the comparably low perfusion rate of 1 RV/day when no bleed is present, not providing enough nutrients to keep $60 * 10^6$ cells/ml. Moreover, the bleed rate plays an important role in the removal of dead cells and their lysed toxic debris that can inhibit the growth. During the transition between the two steady states from 20 to $60 * 10^6$ cells/ml no bleed was performed for three days leading to an accumulation of by-products. Therefore it is essential for later experiments to maintain a certain bleed fraction at all times in the culture.

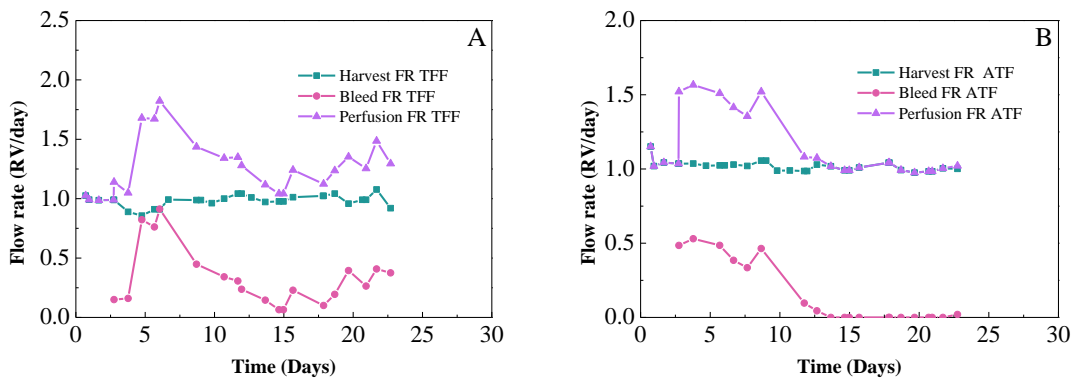


Figure 47 – Harvest (bleu), bleed (pink) and perfusion (purple) rate, as a function of time, in the TFF (A) and ATF (B) reactors.

The glucose profiles are given in figure 48 and reflect the status of the cell culture. In the TFF it is possible to distinguish the three steady states, while in the ATF an increase in the glucose concentration is visible in conjunction with the system crash. At $60 * 10^6$ cells/ml the ratio of production medium to feed medium resulted in lower levels of glucose in the culture compared to the previous experiment but depletion was avoided.

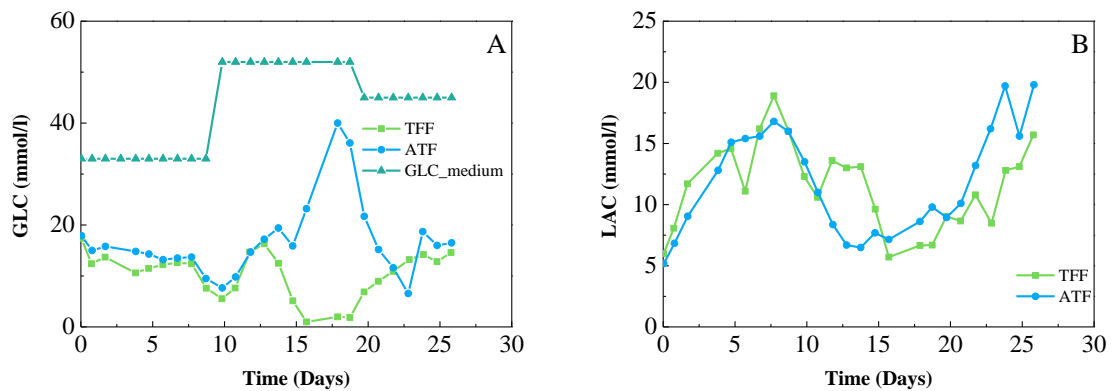


Figure 48 - A) Glucose concentration, as a function of time, in the feed (dark green) and in TFF (green) and ATF (bleu) reactors. B) Lactate concentration, as a function of time, in TFF (green) and ATF (bleu) reactors.

Figure 49A and 49B shows the product concentration in the two reactor setups. As visible in the plots, the reactor titer is similar to the product concentration measured in the harvest for the first set point in case of the ATF. However retention increases to 20% when reaching 60×10^6 cells/ml corresponding to an accumulation of cellular debris caused by the interruption in the bleed. After the recovery of the cell culture the retention got negligible again meaning that the fouling was reversible and it was eliminated successfully by the backflush through the pores (Figure 49C). Again in the TFF it is possible to observed retention of the product from the first day of culture. However the maximum retention observed was 55%, being lower than the maximum one in the previous run thanks to the constant flow rate in the hollow fiber (Figure 49D).

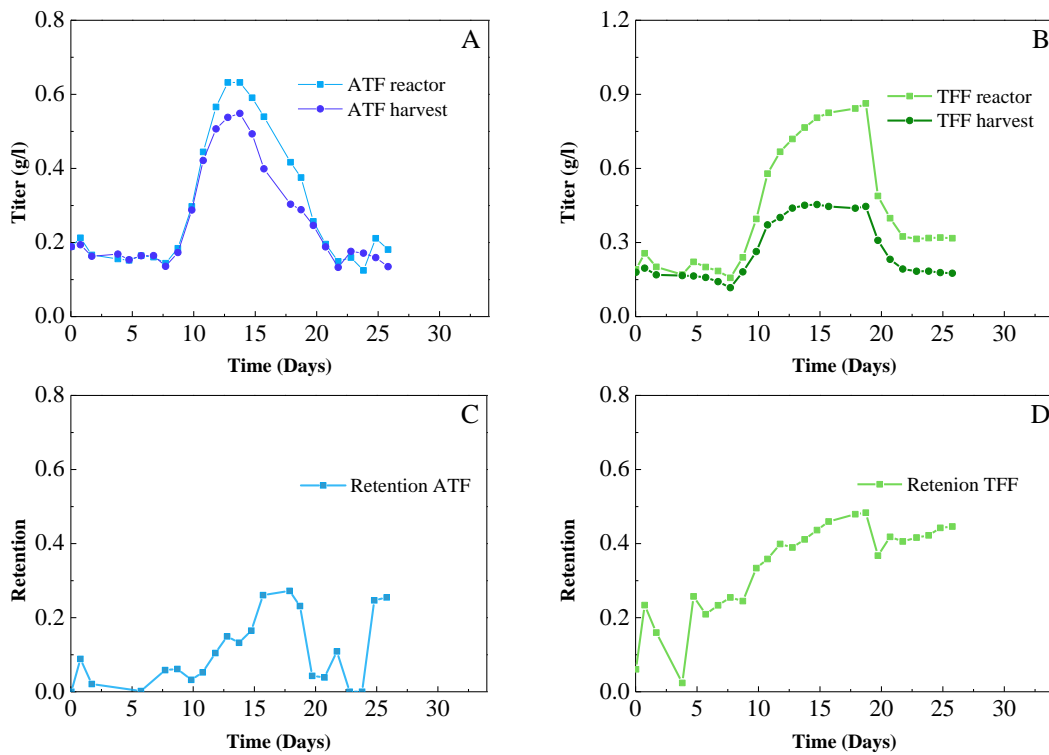


Figure 49 – A) Titer in the ATF reactor equipped with an online biomass sensor (light blue square) and in the harvest (blue circle) as a function of time. B) Titer in the TFF reactor equipped with an online biomass sensor (light green square) and in the harvest (green circle) as a function of time. C) Retention of the product in the ATF setup. D) Retention of the product in the TFF setup equipped with the biomass sensor.

Table 8 and 9 give compared the two experiments in which the three following steady states were reached (i.e. the ATF without the biomass sensor and the TFF with the flow sensor). The adaptive bleeding used in the TFF determined a viable cell density nearer to the set point. Moreover, the volume withdrawn at each steady state was higher in the TFF leading to a higher perfusion rate (Table 8). The ammonia concentration in both experiments was lower than 8 mM, the critical value that can inhibit the cellular growth [33].

Table 8 – Mean viable cell density (VCD), perfusion and bleed rate, reactor and harvest titer, ammonia concentration measured in the ATF without biomass sensor and TFF with biomass sensor at $20 \cdot 10^6$ cells/ml, $40 \cdot 10^6$ cells/ml and $60 \cdot 10^6$ cells/ml.

Retention System	VCD Setpoint [mio/ml]	VCD [mio/ml]	Perfusion rate [RV/day]	Bleed rate [RV/day]	Titer reactor [g/l]	Titer harvest [g/l]	NH4 [mmol/l]
TFF	20	21.47 ± 1.29	1.31 ± 0.23	0.44 ± 0.36	0.22 ± 0.07	0.17 ± 0.04	1.15 ± 0.12
	40	40.22 ± 2.13	1.26 ± 0.2	0.35 ± 0.08	0.33 ± 0.03	0.19 ± 0.02	4.98 ± 1.25
	60	58.74 ± 1.57	1.13 ± 0.13	0.17 ± 0.1	0.73 ± 0.13	0.42 ± 0.05	3.23 ± 0.22
ATF	20	21.8 ± 3.15	1.26 ± 0.26	0.29 ± 0.19	0.18 ± 0.03	0.16 ± 0.04	0.71 ± 0.18
	40	44.17 ± 1.27	1.22 ± 0.11	0.17 ± 0.06	0.22 ± 0.03	0.2 ± 0.02	7.29 ± 1.68
	60	58.11 ± 5.98	1.07 ± 0.15	0.05 ± 0.15	0.4 ± 0.03	0.38 ± 0.1	3.01 ± 0.82

The cell specific growth rate, the cell specific consumption of glucose and production of lactate and the cell specific productivity were calculated using the formulas stated in the section 2.7. Increasing the viable density decreases the specific growth rate and the specific consumption of glucose and production of lactate (Table 7). So, during the culture the metabolism changes and in particular it is slower at the higher cell densities, as found even by Clinker et al [26], meaning that with higher cell densities the cells grow more slowly.

Table 9 – Mean specific growth rate (μ), mean specific consumption of glucose (qGLC), mean specific production of lactate (qLAC), mean specific production of antibodies (qmAb) in the ATF without biomass sensor and TFF with biomass sensor at $20 \cdot 10^6$ cells/ml, $40 \cdot 10^6$ cells/ml and $60 \cdot 10^6$ cells/ml.

Retention System	VCD Setpoint [mio/ml]	μ [1/s]	qGLC [pmol/cell/day]	qLAC [pmol/cell/day]	qmAb [pg/cell/day]
TFF	20	0.41 ± 0.19	1.41 ± 0.18	0.98 ± 0.23	10.5 ± 2.89
	40	0.18 ± 0.14	1.05 ± 0.09	0.35 ± 0.1	5.47 ± 1.68
	60	0.16 ± 0.16	0.85 ± 0.7	0.18 ± 0.07	10 ± 1.33
ATF	20	0.30 ± 0.2	1.26 ± 0.55	1.31 ± 2.32	10.17 ± 1.84
	40	0.27 ± 0.12	1.12 ± 0.20	0.30 ± 0.16	4.66 ± 0.95
	60	0.15 ± 0.23	0.9 ± 0.25	0.24 ± 0.23	7.85 ± 3.74

Concerning the product quality, the glycosylation can be affected by the media composition, the ammonia which is correlated to the viable cell density, and the operating parameters [34]. In figure 50 the glycoforms measured in the TFF and ATF without the biomass sensor as well as with the biomass sensor are given. As can be observed, the differences in glycosylation, calculated at the same day (i.e. same media composition and level of ammonia), are well below the experimental errors. It can be concluded that the system set up doesn't influence the quality of the antibodies.

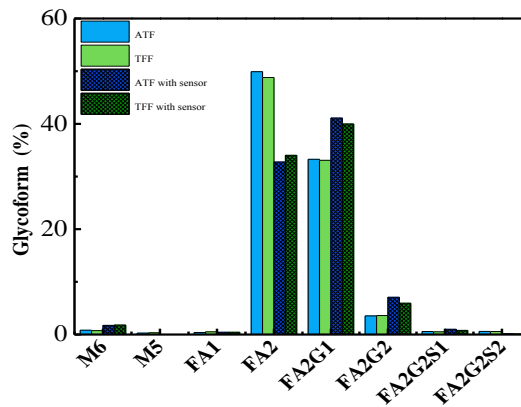


Figure 50 – Glycoforms measured in the two experiments at the same day with the ATF as well as with the TFF.

In figure 51 the glycoforms measured during the same steady state at 20×10^6 cells/ml in the ATF setup equipped with the biomass sensor are given. The glycoforms are very similar meaning that the steady state culture allows reaching a constant product quality.

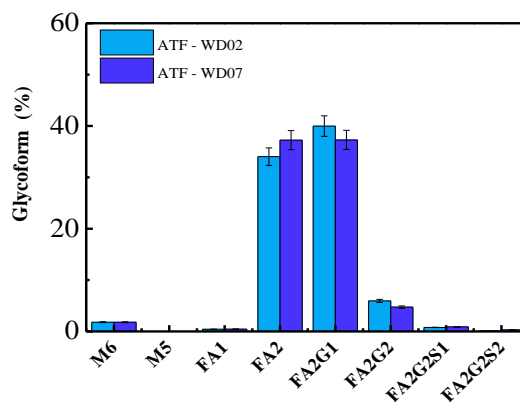


Figure 51 – Glycoforms in the ATF setup equipped with the biomass sensor at working day 2 and 7.

3.4.5 Online measurements

Several parameters including pH, pCO₂, reactor weight, gas composition and the online measurement of the cell density have been monitored during the process. Their development as a function of time is displayed in figure 52. The oxygen fraction is adjusted to maintain a constant set point of 50% dissolve oxygen in the reactor. As visible in figure 52A the oxygen fraction of the first run mimics the cell culture profile and can therefore be related to the number of cells. Being constant during the first viable cell density set point in both reactors, the fraction of oxygen increases towards 60×10^6 cells/ml, whereas in the ATF system it stayed almost constant again. Contrary in the TFF the fraction dropped in conjunction with the crashing of the reactor and the consequent decrease of the cell density (Figure 52A). CO₂ addition is used to keep the pH of the slightly basic medium at the set point of 7.10. However, the amount added depends strongly on that produced by cells as final product of the respiration. Therefore the partial pressure of CO₂ in the cell suspension can be explained by the cell growth and density. At low cell densities (e.g. first set point) cellular growth results in lactate production decreasing the need of CO₂ to maintain the pH set point. However as visible in figure 52B, representing the profile of the ATF in the second run, the CO₂ level increases with higher cell concentrations as more cells produce CO₂. Moreover depending on the operating conditions the removal of CO₂ can be limited resulting in accumulation. Values of CO₂ rose above 120 mmHg at 60×10^6 cells/ml in the ATF and can inhibit growth [13]. The pH was kept constant at the set point of 7.10 during almost the entire run, only slightly deviation at the end of the run. However in the TFF, at cell densities above 60×10^6 cells/ml a high production of lactate caused decrease drop in pH to 6.88 (Figure 52C). An important parameter monitored online was the bioreactor weight (Figure 52D). The weight of the reactor, and consequently the working volume, was kept constant maintaining the feed flow equal to the outlet flows (i.e. harvest and bleed).

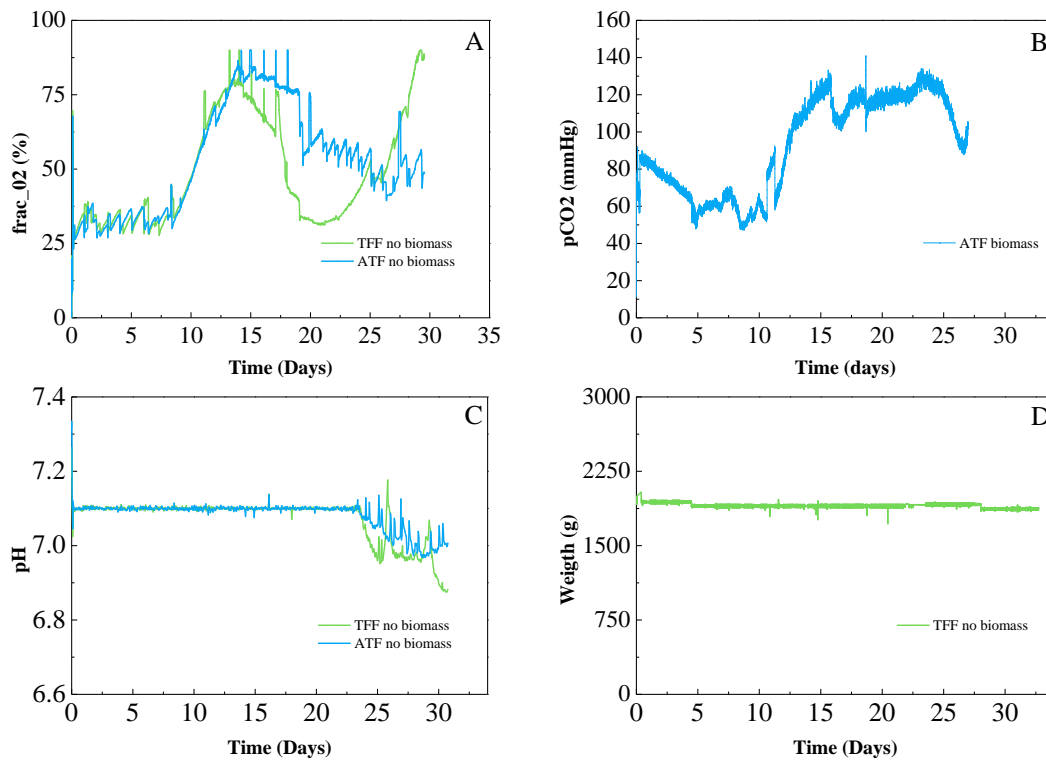


Figure 52 - A) Fraction of oxygen sparged in the ATF (bleu) and TFF (green), without biomass sensor, as a function of time. B) pCO₂ measured in the ATF reactor equipped with the biomass sensor. C) pH measured in the ATF (bleu) and TFF (green) without biomass sensor as a function of time. D) Weight of the TFF reactor without biomass sensor during the experiment.

In figure 53 the biomass sensor profile obtained with the TFF reactor is given. The online measurement of the cell density was used to control the bleeding during the experiment. As can be seen from figure 53 all three steady states are well captured by the online measurement confirming its applicability for the developed perfusion system. The viable cell density was daily compared to the offline measurement and when the two values were off more than 10^6 cells/ml the biomass factor was adjusted. For example the correction was needed switching to the second steady state because of the change in the background.

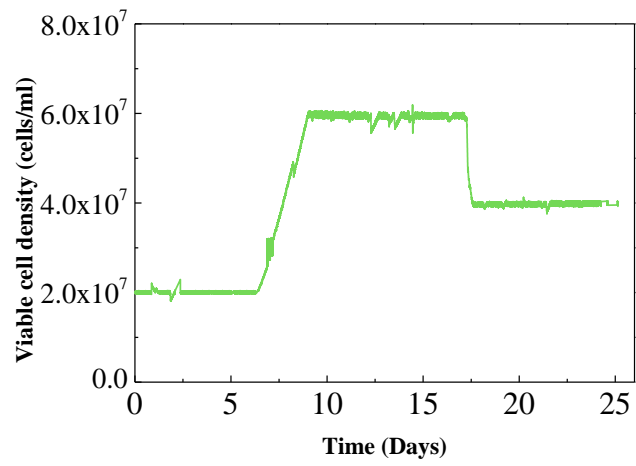


Figure 53 – Viable cell density, as function of time, measured using the online biomass sensor in the TFF setup.

CHAPTER 4

CONCLUSIONS AND OUTLOOKS

The project aimed at the comparison of two perfusion reactor setups employing external filtration for cell retention. One system was equipped with a TFF device whereas the other one had the commercially available ATF system attached. First a thorough characterization was carried out in order to estimate suitable operating conditions. The extend of shear stress in both systems was evaluated and showed a lower level in the diaphragm pump of the ATF setup in contrast to the bearingless centrifugal pump used in the TFF setup. Moreover higher shear stress was observed applying the “long” hollow fiber compared to the alternative “short” hollow fiber module. Based on the previously determined threshold of 50 Pa, causing lysis of the used CHO cells, a flow rate of 1.5 l/min using the “short” hollow fiber was identified to be most suitable for the following cell cultures. Agitation using a Rushton turbine impeller at 400 rpm and a volumetric gas flow rate of 0.22 vvm were found to not induce critical stress values and maintain a sufficient gas-liquid mass transfer. Concerning the oxygen transfer, the analysis shows that the setup doesn't influence the transfer of oxygen since for the systems the k_{La} was equal to 20.16 1/h in the TFF and 18 1/h in the ATF. Small scale experiments in spin tube bioreactors allowed the investigation of critical culture parameters such as perfusion and bleed rate as well as media composition. The spin tubes showed the ability to keep $20 \cdot 10^6$ cells/ml, $40 \cdot 10^6$ cells/ml and $60 \cdot 10^6$ cells/ml using a perfusion rate of 1 RV/day, however adjusting the feed fraction in the media composition. Using adaptive bleeding, meaning the withdrawal of culture broth according to the measured cell density, the number of viable cells was kept constant. The use of a seed reactor permitted to inoculated the production reactors already close to the first viable cell density set point of $20 \cdot 10^6$ cells/ml, saving one week of culture. In a first reactor run, applying previously determined operating conditions and using adaptive bleeding, $20 \cdot 10^6$, $40 \cdot 10^6$ and $60 \cdot 10^6$ cells/ml at viabilities above 90% were achieved and kept constant for one week at a perfusion rate of 1 RV/day in the ATF. In the TFF blockage of the hollow fiber module at $60 \cdot 10^6$ cells/ml prevented a successful culture. An improvement of the setup was achieved adding an online biomass sensor to automatically control the bleed and a clamp-on flow sensor to counteract the descending

flow rate in the external loop. In the subsequent second experiment, the three steady states were also achieved in the TFF. In addition the automation of the bleed lead to less variation cell density profile, representing improved stability of the process. Comparing the two setups in terms of protein production, constant titers were obtained at the respective steady states. However a substantially higher retention of the product inside the TFF setup reaching values of up to 65% was observed. The periodic reversal of the flow induces a change in transmembrane pressure, creating a back flush through the membrane pores, that prevent fouling in the ATF. Following, no significant retention of the mAbs was present. Further, the product quality was not influenced by the setup. In summary the negligible retention and lower shear stress suggest the ATF as preferred retention device for the production of antibodies.

Future efforts should be directed towards the development of a specific medium for perfusion systems, which is not available today. Improvements in the medium composition could lead to a further increase in the productivity of the perfusion culture, minimizing the liquid throughput and at the same time achieving even higher cell densities. Although the adaptive bleeding was found to be the method of choice maintaining a certain viable cell density set point, a defined bleed rate is required to ensure a viable culture at low growth rates. Finally, the retention of the TFF setup could be decreased running the system with a two ways flow, periodically changing the pumping direction or introducing an artificial backflush. Concerning the product quality, the actual benefit of the perfusion systems, the higher quality of the products compared to the fed-batch, could be enhancing in the production of unstable protein since the lower residence time. Finally, the continuous removal of the product during the culture and the possibility to have a stable culture, with a constant cell density and product quality, could permit the directly integration with the downstream resulting in a continuous production of antibodies.

CHAPTER 5

REFERENCES

1. Hecht V, Duvar S, Ziehr H, Burg J, Jockwer A. Efficiency improvement of an antibody production process by increasing the inoculum density. *Biotechnol Progr.* 2014 May-Jun;30(3):607-15.
2. www.britannica.com.
3. Woodside SM, Bowen BD, Piret JM. Mammalian cell retention devices for stirred perfusion bioreactors. *Cytotechnology.* 1998;28(1-3):163-75.
4. Kim JY, Kim YG, Lee GM. CHO cells in biotechnology for production of recombinant proteins: current state and further potential. *Appl Microbiol Biot.* 2012 Feb;93(3):917-30.
5. John Bonham-Carter and Jerry Shevitz, "A Brief History of Perfusion Biomanufacturing"
6. www.cmcbio.com.
7. Weichang Zhou and Anne Kantardjieff, "Mammalian Cell Cultures for Biologics Manufacturing"
8. <http://textbookofbacteriology.net>
9. Voisard D, Meuwly F, Ruffieux PA, Baer G, Kadouri A. Potential of cell retention techniques for large-scale high-density perfusion culture of suspended mammalian cells. *Biotechnol Bioeng.* 2003 Jun 30;82(7):751-65.
10. Furey J. Scale-up of a cell culture perfusion process - A low-shear filtration system that inhibits filter-membrane fouling. *Genet Eng News.* 2002 Apr 1;22(7):62-.
11. www.biopharma.com.
12. www.cellculturedish.com.
13. Li F, Vijayasankaran N, Shen A, Kiss R, Amanullah A. Cell culture processes for monoclonal antibody production. *Mabs-Austin.* 2010 Sep-Oct;2(5):466-79.
14. Ivarsson, Dissertation ETH 22069, " Impact of Process Parameters on Cell Growth, Metabolism and Antibody Glycosylation".

15. Zhu MM, Goyal A, Rank DL, Gupta SK, Vanden Boom T, Lee SS. Effects of elevated pCO₂ and osmolality on growth of CHO cells and production of antibody-fusion protein B1: a case study. *Biotechnol Prog.* 2005 Jan-Feb;21(1):70-7.
16. Ozturk SS. *Cell culture technology for pharmaceutical and cell-based therapies.* New York: Taylor & Francis; 2006.
17. Dalm MCF, Cuijten SMR, van Grunsven WMJ, Tramper J, Martens DE. Effect of feed and bleed rate on hybridoma cells in an acoustic perfusion bioreactor: Part I. Cell density, viability, and cell-cycle distribution. *Biotechnol Bioeng.* 2004 Dec 5;88(5):547-57.
18. V. Warikoo et al., *Biotechnology and bioengineering* 109, 3018–29 (2012).
19. Dittler I, Kaiser SC, Blaschczok K, Loffelholz C, Bosch P, Dornfeld W, et al. A cost-effective and reliable method to predict mechanical stress in single-use and standard pumps. *Eng Life Sci.* 2014 May;14(3):311-7.
20. Maiorella B, Dorin G, Carion A, Harano D. Cross-Flow Microfiltration of Animal-Cells. *Biotechnol Bioeng.* 1991 Jan 20;37(2):121-6.
21. Blaschczok K, Kaiser SC, Loffelholz C, Imseng N, Burkart J, Bosch P, et al. Investigations on Mechanical Stress Caused to CHO Suspension Cells by Standard and Single-Use Pumps. *Chem-Ing-Tech.* 2013 Feb;85(1-2):144-52.
22. Kelly W, Scully J, Zhang D, Feng G, Lavengood M, Condon J, et al. Understanding and modeling alternating tangential flow filtration for perfusion cell culture. *Biotechnol Prog.* 2014 Jul 30.
23. Stressmann M, Moresoli C. Effect of pore size, shear rate, and harvest time during the constant permeate flux microfiltration of CHO cell culture supernatant. *Biotechnol Progr.* 2008 Jul-Aug;24(4):890-7.
24. Bellucci JJ, Hamaker KH. Evaluation of Oxygen Transfer Rates in Stirred-Tank Bioreactors for Clinical Manufacturing. *Biotechnol Progr.* 2011 Mar-Apr;27(2):368-76.
25. Ozbek B, Gayik S. The studies on the oxygen mass transfer coefficient in a bioreactor. *Process Biochem.* 2001 Mar;36(8-9):729-41.
26. Clincke MF, Molleryd C, Zhang Y, Lindskog E, Walsh K, Chotteau V. Very high density of CHO cells in perfusion by ATF or TFF in WAVE bioreactor. Part I. Effect of the cell density on the process. *Biotechnol Progr.* 2013 May-Jun;29(3):754-67.

27. Clincke MF, Molleryd C, Samani PK, Lindskog E, Faldt E, Walsh K, et al. Very high density of Chinese hamster ovary cells in perfusion by alternating tangential flow or tangential flow filtration in WAVE Bioreactor-part II: Applications for antibody production and cryopreservation. *Biotechnol Prog.* 2013 May-Jun;29(3):768-77.
28. Villinger M, Soos. Experimental Determination of Maximum Hydrodynamic Stress in Multiphase Flow Using a Shear Sensitive Particulate System.
29. Bigge JC, Patel TP, Bruce JA, Goulding PN, Charles SM, Parekh RB. Nonselective and Efficient Fluorescent Labeling of Glycans Using 2-Amino Benzamide and Anthranilic Acid. *Anal Biochem.* 1995 Sep 20;230(2):229-38.
30. Merry AH, Neville DCA, Royle L, Matthews B, Harvey DJ, Dwek RA, et al. Recovery of intact 2-aminobenzamide-labeled O-glycans released from glycoproteins by hydrazinolysis. *Anal Biochem.* 2002 May 1;304(1):91-9.
31. Neunstoecklin, "Criteria for scale-up and scale-down of bioreactors for cultivation of mammalian cells".
32. http://infoscience.epfl.ch/record/166942/files/EPFL_TH5135.pdf.
33. Hansen HA, Emborg C. Influence of Ammonium on Growth, Metabolism, and Productivity of a Continuous Suspension Chinese-Hamster Ovary Cell-Culture. *Biotechnol Progr.* 1994 Jan-Feb;10(1):121-4.
34. Grainger RK, James DC. CHO Cell Line Specific Prediction and Control of Recombinant Monoclonal Antibody N-Glycosylation. *Biotechnol Bioeng.* 2013 Nov;110(11):2970-83.